



Master Program  
Global Change Ecology

## Master Thesis

**Field measurements of the cooling effect  
of *Tilia cordata* and *Robinia pseudoacacia*  
in Bayreuth, Germany using  
low-cost-devices**

1<sup>st</sup> examiner: Prof. Dr. C. Samimi

2<sup>nd</sup> examiner: PD Dr. T. Rötzer

Author: Julia Mack

Student-ID: 1214345

September 30<sup>th</sup> 20

# Table of contents

List of tables.....	VII
Summary.....	VIII
1. Introduction and research objectives .....	1
2. Current state of knowledge.....	2
2.1 Climate Change.....	2
2.2 Climatic conditions in Bayreuth, Germany.....	3
2.3 Urbanization .....	5
2.4 City Climate.....	6
2.4.1 Radiation.....	7
2.4.2 Moisture .....	7
2.4.3 Aerodynamics .....	8
2.4.4 Temperature - Urban Heat Island effect .....	8
2.5 Greens – One solution approach.....	12
2.5.1 Urban Green Spaces .....	12
2.5.2 Urban trees.....	13
2.5.3 Species differences.....	15
2.5.4 Previous studies in Munich and Würzburg.....	16
3. Materials and Methods .....	17
3.1 Underlying conditions .....	17
3.1.1 Climatic conditions in Bayreuth during the study period.....	17
3.1.2 Selected tree species.....	18
3.1.3 Selected tree individuals .....	21
3.1.4 Study sites.....	23
3.2 Main measurements .....	27
3.2.1 Components for measuring devices.....	28
3.2.2 Data analysis.....	31
4. Results .....	33
4.1 Underlying conditions .....	33
4.1.1 Climatic conditions in Bayreuth during the study period.....	33
4.1.2 Selected tree individuals .....	35
4.1.3 Microclimate of the urban site.....	36
4.2 Main measurements .....	40
4.2.1 Urban climate .....	40
4.2.1.1 Temperature.....	40

4.2.1.2 Radiation.....	43
4.2.1.3 Moisture .....	44
4.2.1.4 Ground temperature .....	47
4.2.1.5 Aerodynamics.....	48
4.2.2 Effects of urban trees .....	49
4.2.2.1 Cooling effect of urban trees.....	49
4.2.2.2 Transpiration .....	53
4.2.2.3 Ground temperature .....	55
4.2.2.4 Aerodynamics.....	57
4.2.3 Species differences.....	58
4.2.4 Age differences.....	64
5. Discussion .....	68
5.1 Underlying conditions .....	68
5.1.1 Climatic conditions in Bayreuth.....	68
5.1.2 Selected Tree individuals.....	68
5.1.3 Microclimate of the urban site.....	69
5.2 Main measurements .....	72
5.2.1 Urban climate .....	72
5.2.1.1 Temperature.....	72
5.2.1.2 Radiation.....	74
5.2.1.3 Moisture .....	75
5.2.1.4 Ground temperature .....	77
5.2.1.5 Aerodynamics.....	78
5.2.2 Effects of urban trees .....	79
5.2.2.1 Cooling effect.....	79
5.2.2.2 Transpiration .....	81
5.2.2.3 Ground temperature .....	83
5.2.2.4 Aerodynamics.....	84
5.2.3 Species differences.....	85
5.2.4 Age differences.....	87
5.3 Conclusion .....	88
5.4 Sources for inaccuracies .....	90
6. List of references .....	93
7. Appendix.....	100

## List of figures

FIGURE 1: YEARLY AVERAGE VALUES OF MEASURED AIR TEMPERATURE (BLACK), YEARLY AVERAGE MINIMUM VALUES (BLUE) AND YEARLY MAXIMUM VALUES (RED) & SMOOTHED MEAN OVER 7 YEARS (BOLD). SOURCE: LÜERS ET AL. (2014). .....	4
FIGURE 2: PRECIPITATION VALUES (MM) FROM 1850 TO 2010. SOURCE: LÜERS ET AL. 2014. ....	5
FIGURE 3: LEFT: LOCATION OF THE RURAL SITE. SOURCE: URLAUBSZIELE.COM/BILDER/KARTEN/STAEDTE/472/KARTE-BAYREUTH-100.PNG, RIGHT: LOCATION OF THE WEATHER STATION IN THE BOTANICAL GARDEN (RED). ....	17
FIGURE 5: BIOCLIMATE ENVELOPE OF T. CORDATA WITH ACTUAL AND PREDICTED CLIMATE. SOURCE: KÖLLING & ZIMMERMANN (2007) .....	18
FIGURE 4: GEOGRAPHICAL EXTENSION OF THE OCCURENCE OF T. CORDATA. SOURCE: KÖLLING & ZIMMERMANN (2007) .....	18
FIGURE 6: ROBINIA PSEUDOACACIA. SOURCE: HOLZWURM-PAGE.DE .....	20
FIGURE 7: LEFT: LOCATION A, B, C, D & E OF MEASURING DEVICES IN SUBGROUP 1. RIGHT: STUDY SITE OF SUBGROUP 1. ....	22
FIGURE 8: FIRST: LOCATION A, B, C, D & E OF MEASURING DEVICES IN SUBGROUP 2. SECOND: STUDY SITE WITH SUBGROUP 2. ....	22
FIGURE 9: STUDY SITE WITH SELECTED TREES, SITES FOR STREET MEASUREMENTS AND LOCATION OF CLIMATE STATIONS. ....	24
FIGURE 10: CATEGORIES FOR OBSERVATION OF THE MICROCLIMATE OF THE STUDY SITE .....	25
FIGURE 11: HOBO MICROSTATION AS IT WAS USED IN THE STUDY AT HAND. SOURCE: FS.FED.US .....	26
FIGURE 12: CONTROLLING DEVICE IN A RURAL SURROUNDING. ....	26
FIGURE 13: SHT21-SENSOR WITH A FILTER FOR PROTECTION ALREADY PUT ON THE BASE OF THE RADIATION PROTECTION. ....	28
FIGURE 14: RADIATION PROTECTION FIXED ON A PVC-BASE. ....	28
FIGURE 15: ALUMINUM-TUBE ATTACHED TO THE RADIATION SHIELD TO GET MORE ACCURATE DATA. ....	29
FIGURE 16: PHOTODIODE ATTACHED TO THE RADIATION SHIELD. ....	29
FIGURE 17: INFRARED-SENSOR AS A SINGLE COMPOUND (L) AND INSTALLED (R). ....	30
FIGURE 18: WIND SENSOR ATTACHED TO THE DEVICE. ....	30
FIGURE 19: BOARD (L) AND ROUTERS (R). ....	31
FIGURE 20: DAILY TEMPERATURE AND PRECIPITATION-VALUES DURING THE STUDY PERIOD .....	33
FIGURE 21: MEAN TEMPERATURE AT JULY 20TH AND 21ST AVERAGED FOR EACH CATEGORY (N=2). ....	36
FIGURE 22: MEAN RELATIVE AIR HUMIDITY AT JULY 20TH AND 21ST AVERAGED FOR EACH CATEGORY (N=2)..	38
FIGURE 23: AVERAGED DIURNAL VARIATIONS OF AIR TEMPERATURE [°C] MEASURED IN BOTANICAL GARDEN (RURAL AREA), ABOVE THE STREET, AT A PARKING LOT AND AT A GREENSPACE (N=61). ....	40
FIGURE 24: DENSITY FUNCTION OF AIR TEMPERATURE [°C] MEASURED IN BOTANICAL GARDEN (RURAL AREA) AND ABOVE THE STREET. ....	42
FIGURE 25: AVERAGED DIURNAL VARIATIONS OF INCOMING SOLAR RADIATION MEASURED IN BOTANICAL GARDEN (RURAL AREA, N=1) AND ABOVE THE STREET (N=1) DURING THE STUDY PERIOD OF 61 DAYS. ....	43
FIGURE 27: AVERAGED DIURNAL VARIATIONS OF RELATIVE AIR HUMIDITY MEASURED IN THE BOTANICAL GARDEN (RURAL AREA, N=1), ABOVE THE STREET (N=2), AT THE PARKING LOT (N=1) AND AT THE GREENSPACE (N=1) DURING THE STUDY PERIOD OF 61 DAYS. ....	45
FIGURE 28: DENSITY FUNCTION OF RELATIVE AIR HUMIDITY MEASURED IN THE BOTANICAL GARDEN (RURAL AREA) AND ABOVE THE STREET DURING THE STUDY PERIOD OF 61 DAYS. ....	46
FIGURE 30: AVERAGED DIURNAL VARIATIONS OF OBJECT TEMPERATURE MEASURED ABOVE THE STREET VIA INFRARED (N=2) AND AIR TEMPERATURE ABOVE THE STREET (N=2) DURING THE STUDY PERIOD OF 61 DAYS. ....	47
FIGURE 31: AVERAGED DIURNAL VARIATIONS OF WINDSPEED [M/SEC] MEASURED IN THE BOTANICAL GARDEN (RURAL AREA, N=1) AND ABOVE THE STREET (N=2) DURING THE STUDY PERIOD OF 61 DAYS. ....	48

FIGURE 32: AVERAGED DIURNAL VARIATIONS OF THE COOLING EFFECT OF URBAN TREES (BLACK, N=12), STREET TEMPERATURE (=AIR TEMPERATURE ABOVE THE STREET, BLUE, N=1), OBJECT TEMPERATURE (=SURFACE TEMPERATURE OF THE URBAN ENVIRONMENT, GREEN, N=24) AND WINDSPEED (MEASURED ABOVE THE STREET, RED, N=1) ON A HOT AND SUNNY DAY. ....	49
FIGURE 33: TEMPERATURE MEASURED AT THREE DIFFERENT HEIGHTS (HIGH: N=12, MIDDLE: N=12, LOW: N=12) IN THE TREE CANOPIES WAS COMPARED TO TEMPERATURE MEASURED ABOVE THE STREET (N=1). ....	51
FIGURE 35: AVERAGED DIURNAL VARIATIONS OF RELATIVE AIR HUMIDITY MEASURED IN URBAN TREES (N=12) AND ABOVE THE STREET (N=1) IN COMPARISON TO INCOMING SOLAR RADIATION (N=1) ON A HOT AND SUNNY DAY (24.06.2016). ....	53
FIGURE 36: AVERAGED RELATIVE AIR HUMIDITY MEASURED AT POSITION A (N=12) AND D (N=12) COMPARED TO RELATIVE AIR HUMIDITY [%] MEASURED ABOVE THE STREET (N=1).....	54
FIGURE 37: AVERAGED SURFACE TEMPERATURE [°C] MEASURED IN THE SOUTH (N=12) AND THE NORTH (N=12) OF URBAN TREES AND AIR TEMPERATURE [°C] (N=1) AT A HOT AND SUNNY DAY. ....	55
FIGURE 38: AVERAGED SURFACE TEMPERATURE [°C] MEASURED IN THE SOUTH (N=12) AND THE NORTH (N=12) OF THE SELECTED URBAN TREES AS A FUNCTION OF AIR TEMPERATURE [°C] (N=1) AT A HOT AND SUNNY DAY. ....	56
FIGURE 39: AVERAGED DIURNAL VARIATIONS OF WINDSPEED [M/SEC] MEASURED AT TREES (N=4) AND ABOVE THE STREET (N=1) DURING THE STUDY PERIOD. ....	57
FIGURE 40: COOLING EFFECT OF R1, R2, T1 & T2 (ALL N=5) OVER THE STUDY PERIOD OF 61 DAYS. ....	58
FIGURE 41: AVERAGED COOLING EFFECT OF THE WHOLE PERIOD OF BOTH SPECIES (N=10 EACH) AND TEMPERATURE MEASURED ABOVE THE STREET (N=1). ....	59
FIGURE 43: AVERAGED COOLING EFFECT OF THE TREE SPECIES T. CORDATA (N=10) AND R. PSEUDOACACIA (N=10) AND STREET TEMPERATURE (N=1) ON AN EXEMPLARY HOT AND CLOUD FREE DAY.....	61
FIGURE 45: RELATIVE AIR HUMIDITY DIFFERENCES IN THE CANOPY OF EACH SPECIES (N=10 EACH) AND ABOVE THE STREET (N=1) AVERAGED OVER THE WHOLE PERIOD OF 61 DAYS. ....	62
FIGURE 46: COMPARISON OF INCOMING SOLAR RADIATION ABOVE THE STREET (N=1) AND SOLAR RADIATION IN THE TREE CANOPY OF EACH SPECIES (N=10 EACH). ....	63
FIGURE 47: AVERAGED COOLING EFFECT OF T. CORDATA (N=10) AS A FUNCTION OF AGE. ....	65
FIGURE 48: AVERAGED COOLING EFFECT OF ALL SELECTED T. CORDATA (N=10) AS A FUNCTION OF CROWN VOLUME. ....	66
FIGURE 49: TOP LEFT: AVERAGED HUMIDITY DIFFERENCES AS A FUNCTION OF AGE. TOP RIGHT: AVERAGED HUMIDITY DIFFERENCES AS A FUNCTION OF CROWN VOLUME. BOTTOM LEFT: AVERAGED SOLAR RADIATION DIFFERENCES AS A FUNCTION OF AGE. BOTTOM RIGHT: AVERAGED SOLAR RADIATION DIFFERENCES AS A FUNCTION OF CROWN VOLUME. ALL SELECTED T. CORDATA WERE CONSIDERED (N=10).....	67
FIGURE 50: IDEALIZED FORM OF THE SPATIAL AND TEMPORAL FEATURES OF URBAN AND RURAL SCREEN-LEVEL AIR TEMPERATURES GIVING RISE TO AN URBAN HEAT ISLAND EFFECT. SOURCE: T.R. OKE (1982). ....	74
FIGURE 51: STOMATA ARE AFFECTED BY ATMOSPHERIC VAPOR PRESSURE DEFICIT. AS A RESULT, STOMATA CAN PREVENT FASTER TRANSPIRATION AT LOW ATMOSPHERIC HUMIDITY BY CLOSURING. PATTERNS OF RESPONSE DIFFER BETWEEN SPECIES. THE GRAPH SHOWS TWO COMMON EXAMPLES. SOURCE: MOTT & PARKHURST (1991). ....	81
FIGURE 52: TEMPERATURE DIFFERENCE OF THE MEASUREMENTS OF THE USED DEVICES (N=1) IN COMPARISON TO TEMPERATURE MEASUREMENTS OF THE WEATHER STATION OF BAYREUTH (N=1) AS A FUNCTION OF INCOMING SOLAR RADIATION. ....	91
FIGURE 53: TESTING WITH DIFFERENT ADJUSTMENTS OF RADIATION PROTECTION (N=5). GREEN LINE SHOWS RESULT FOR THE RADIATION PROTECTION WITH AN ALUMINIUM-TUBE. LESS TEMPERATURE FLUCTUATIONS CAN BE SEEN. ....	101
FIGURE 26: DENSITY FUNCTION OF INCOMING SOLAR RADIATION IN MV MEASURED IN THE BOTANICAL GARDEN (RURAL AREA, N=1) AND ABOVE THE STREET (N=1) DURING THE STUDY PERIOD OF 61 DAYS. .	102
FIGURE 29: DENSITY FUNCTION OF OBJECT TEMPERATURE [°C] (N=25) OVER THE WHOLE STUDY PERIOD (29.05.2016 - 29.07.2016). ....	103

FIGURE 34: AVERAGED COOLING EFFECT OF T1 (N=5), T2 (N=5), R1(N=5) & R2 (N=5) AVERAGED OVER THE STUDY PERIOD OF 61 DAYS. .... 104

FIGURE 42: AVERAGED COOLING EFFECT OF BOTH SPECIES (N=10 EACH) FROM 10:00 TO 18:00 AND AIR TEMPERATURE MEASURED ABOVE THE STREET (N=1). .... 105

FIGURE 44: AVERAGED COOLING EFFECT OF BOTH SPECIES (N=10 EACH) AND AIR TEMPERATURE MEASURED ABOVE THE STREET (N=1) AT AN EXEMPLARY HOT AND CLOUD FREE DAY FROM 10:00 TO 18:00. .... 106

## List of tables

TABLE 1: TEMPERATURE [°C] MEASURED IN BAYREUTH OF THE LAST 105 YEARS FOR THE MONTHS MAY, JUNE, JULY AND THE AVERAGE TEMPERATURE IN THOSE MONTHS.....	3
TABLE 2: AVERAGED PRECIPITATION VALUES [MM] FOR THE MONTHS MAY - JULY FROM THE YEARS 2007, 2008 AND 2009. ....	4
TABLE 3: MONTHLY TEMPERATURE AVERAGES FOR THE STUDY PERIOD IN COMPARISON TO LONG-TERM VALUES FOR BAYREUTH. ....	34
TABLE 4: MONTHLY PRECIPITATION [MM] AVERAGES FOR THE STUDY PERIOD.....	34
TABLE 5: DBH [CM], AGE, HEIGHT [M], CROWN POSITION [M], VITALITY, CROWN VOLUME [M <sup>3</sup> ], CROWN PROJECTED AREA [M <sup>3</sup> ], TREE PIT [M <sup>3</sup> ] AND MIN. DISTANCE TO THE NEXT BUILDING [M] FOR ALL SELECTED TREE INDIVIDUALS OF T. CORDATA AND R. PSEUDOACACIA. ....	35
TABLE 6: TEMPERATURE MAXIMA, AVERAGE & MINIMA FOR ALL FOUR STUDY SITES. ....	40
TABLE 7: SOLAR RADIATION MAXIMA, AVERAGE & MINIMA FOR ALL FOUR STUDY SITES. ....	43
TABLE 8: RELATIVE AIR HUMIDITY MAXIMA, MEAN AND MINIMA FOR ALL FOUR STUDY SITES. ....	46
TABLE 9: AVERAGE COOLING EFFECT AT A HOT AND SUNNY DAY. ....	50
TABLE 10: AVERAGED SURFACE TEMPERATURE MAXIMA AND MINIMA FOR THE 24.06.2016 IN THE SOUTHERN (N=12) AND NORTHERN (N=12) DIRECTION WITH UNDERLYING AIR TEMPERATURE (N=1). ....	55
TABLE 11: COOLING EFFECT MINIMA, MEAN AND MAXIMA OF T. CORDATA AND R. PSEUDOACACIA AVERAGED OVER THE WHOLE PERIOD. ....	60
TABLE 12: TREE'S AGE (LEFT) AND CROWN VOLUME (RIGHT), MODELLED BY CAILLIAU (2016).....	64
TABLE 14: POSITIONS OF ALL DEVICES, MEASURED WITH LEICA DISTO. ....	100
TABLE 15: COOLING EFFECT BY MACK (2016) AND CAILLIAU (2016).....	107

## Summary

The IPCC report (IPCC 2013) projects many consequences of climate change, such as temperature increase. Due to altered energy balances those consequences will be felt particularly strong in cities and because of increasing urbanization, the majority of the world's population will be affected (Oke, 1982). Many factors, such as surface materials and architecture lead not only to increased temperature, but also to altered radiation schemes, moisture content and aerodynamics and are influencing every urban microclimate. The microclimate of the study site was analyzed for different categories and surface materials. Different climatic parameters taken within the urban environment were compared to data, which was collected in the rural environment. For data collection, devices which were self-constructed, measured temperature [°C], relative air humidity [%], solar radiation [mV], object temperature via infrared diode [°C] and windspeed [m/sec]. During the study period of 61 days (29.05.2016 – 29.07.2016), air temperature was ranging from 6.5 – 24.5 °C. Mean solar radiation was slightly lower at the urban site, but maximum value was registered above the street. In comparison to the rural site, lower relative air humidity was found above the street, most likely due to impervious surface materials. Due to material choice, surface temperatures in the urban environment were always higher than air temperature. Windspeed at the botanical garden was at any time greater than at the urban site because of its increased resistance. Temperature difference between the urban and the rural site was 1.3 °C on average. Highest temperatures were measured above the street due to heating materials. Temperature measurements at an urban greenspace were slightly lower. At the rural site, quick cooling in the evening and very low temperatures during the night stood opposed to rather high temperatures during the day. On average, warmer temperatures were measured in the urban environment and verified an existing urban heat island effect in Bayreuth.

Urban trees and all other vegetation types can help to buffer altered climatic conditions in the urban environment, such as the Urban Heat Island Effect. The study at hand focused on the cooling effect through shading and evapotranspiration. It was assumed, that urban trees significantly reduce heat stress on streets. The cooling effect of *Tilia cordata* and *Robinia pseudoacacia* was studied. On a hot and sunny day of 24 h, average cooling effect of 0.77 °C was documented. During the night a negative cooling effect was observed, which might be due to

reradiating surfaces. Because of photosynthetic activity, cooling effect was on average 1.76 °C in the tree canopy during the day. During the day, relative air humidity values were always higher in tree canopies than above the street due to evapotranspiration. The opposite was observed during the night. Because of shading, surfaces in the northern direction of the tree heat up less and slower than surfaces in the southern direction of the tree. Also windspeed was at any time greater above the street than in tree canopies because of increased resistance. Furthermore, it was assumed, that the species *T. cordata* and *R. pseudoacacia* have different cooling effects on streets. Both are commonly used, but demands differ, as *T. cordata* is tolerating shade, while *R. pseudoacacia* is light-dependent. Averaged cooling effect of *T. cordata* was slightly greater during the day with maximum differences between the species of 0.17 °C. Differences became more distinct, when temperature above the street exceeded 36 °C. Also relative air humidity was almost constantly 0.5% greater in *T. cordata*. Radiation differences were greatest in the morning with higher radiation values in canopies of *R. pseudoacacia*. Moreover, it was assumed, that cooling effect changes with size and the age. In fact, increased cooling effect with greater age and size was observed. Cooling effect of a 50-year-old tree was 0.28 °C greater than that of a 20-year-old tree and a tree with a crown volume of 500 m<sup>3</sup> had a greater cooling effect of on average 0.3 °C than a tree with a crown volume of 100 m<sup>3</sup>. The same tendencies were observed in cases of increased relative air humidity [%] and shading. As the experimental group was small with n=5-12, results have to be understood as a tendency rather than definite numbers.

## 1. Introduction and research objectives

The IPCC report (IPCC 2013) projects many consequences of climate change, such as temperature increase. Due to altered energy balances those consequences will be particularly strong in cities and will affect the majority of the world' population (Oke, 1982). Urban trees and all other vegetation types can help to mitigate the so called Urban Heat Island Effect by cooling through shading and evapotranspiration mainly (Lindberg & Grimmond 2011).

Growing patterns and provided ecosystem services of urban trees were modelled for Munich, Würzburg and Bayreuth (Pretzsch et al. 2015). In 2016 two studies were conducted, of which one will focus on modelling (Calliau 2016), while in the second study, the study at hand, field experiments on cooling effects of the two tree species *Tilia cordata* and *Robinia pseudoacacia* were conducted.

The following three hypotheses were set: First it was assumed, that urban trees significantly reduce the heat stress on streets. Modelled results of Moser (2015) showed a significant cooling effect through the functions of urban trees. To see whether or not this is true, the first hypothesis concentrates on the cooling function of urban trees. Furthermore, it was hypothesized that the species *Tilia cordata* and *Robinia pseudoacacia* have different cooling effects on streets. Even though all urban trees increase cooling, the extent differs with species. Moreover, it was assumed, that cooling effect of an urban tree increases with size. Not only species choice might influence cooling effect. Other factors such as the size of the tree is also decisive.

## **2. Current state of knowledge**

### **2.1 Climate Change**

In its 5<sup>th</sup> report the Intergovernmental Panel on Climate Change (IPCC 2013) stated an increased probability of extreme events. Rising temperature especially in the summer months and changed precipitation patterns are expected in coming years. Particularly heat waves, which lead to heat stress are expected to occur more frequently, more intensely and to last longer. In the recent years an increased frequency of heat waves has already been observed (Pretzsch et al. 2015, TEEB 2016, Meehl and Tebaldi 2004, Lindberg & Grimmond 2011). Coumou and Robinson (2013) expect at the end of the century the coldest summer months to be as warm as the hottest summer months now (TEEB 2016).

Predictions show that climate change may have many consequences for human health especially because of higher temperatures. Heat waves increase the probability of heat stroke, hyperthermia and increased mortality rates (Bowler et al. 2010, Stott et al. 2004). In 2003 about 15.000 deaths in France were attributed to that year's heat wave (Bowler et al. 2010, Fouillet et al. 2006). Indeed, many authors found a link between heat waves, other extreme events and an increased rate of mortality and morbidity in the urban area (Norton 2013, Corburn 2009, Gosling et al. 2009, Kovats & Hajat 2008, O'Neill & Ebi 2009). City dwellers are at special risk as temperatures in cities are already higher than in the rural surroundings (Urban Heat Island Effect) (Bowler et al. 2010).

It is urgently necessary to help cities to adapt to the changing climate using the available knowledge about ecosystem services and effects of urban green spaces (Pretzsch et al. 2015). Increased CO<sub>2</sub>-concentration and more frequent extreme events like heat, drought and storms increase the need for compensating. The EU-Commission (2013) considers strengthening of green infrastructure as necessary (Wojtkiewicz et al. 2012).

## 2.2 Climatic conditions in Bayreuth, Germany

In Bayreuth reliable climatic records are available since 1850. The cities' weather station is one of the 30 first weather stations and the oldest one in northern Bavaria. Since 1994 the university of Bayreuth collects its own data.

The city of Bayreuth is located in a wide-ranging drainage basin of the Red Main. The city center is situated on a small lift within the catchment at 330 m above sea-level. The city is surrounded by a range of hills with heights of 400 – 500 m above sea-level. The highest elevation with a height of about 600 m is already 6 kilometers away from the city center. The university of Bayreuth is located at the southern edge of the city at about 350 m above sea-level.

The table below shows the measured temperature in °C of the last 105 years:

*Table 1: Temperature [°C] measured in Bayreuth of the last 105 years for the months May, June, July and the average temperature in those months.*

Time span	May	June	July
1911-1940	12,7	15,6	17,3
1921-1950	12,5	15,5	17,4
1931-1960	12,2	15,5	17
1941-1970	11,7	15,2	16,7
1951-1980	11,3	15	16,5
1961-1990	11,4	14,7	16,6
1971-2000	11,9	14,8	16,9
1981-2010	12,5	15,4	17,6
Average	12	15,2	17

Lüers et al. (2014) compiled a time series from 1851 to 2013 (163 years), where yearly average values of measured air temperature (black), as well as yearly average minimum values (blue) and yearly maximum values (red) can be seen with the smoothed mean (over 7 years) (bold):

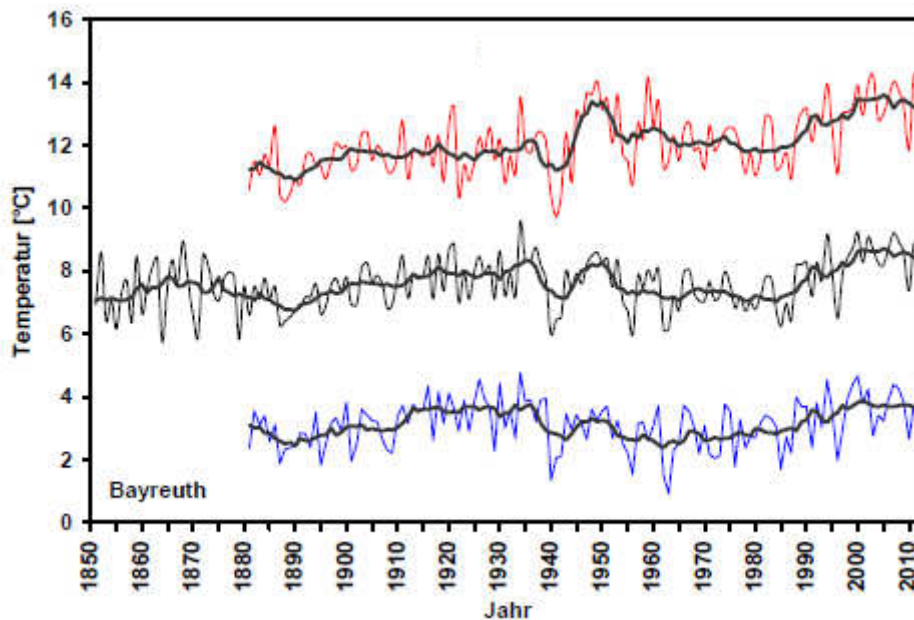


Figure 1: Yearly average values of measured air temperature (black), yearly average minimum values (blue) and yearly maximum values (red) & smoothed mean over 7 years (bold). Source: Lüers et al. (2014).

The impacts of global warming can already be seen in Bayreuth as temperatures tend to be warmer and yearly average temperature of the 30-year-period from 1981 to 2010 exceeded 8 °C for the first time.

Precipitation values show great fluctuations over the years. Comparisons are not easy as values vary even in small spatial scales. The occurrence of small-scale convective precipitation events is the greatest uncertainty factor during the summer. In the table below the average precipitation values for the months May, June and July for the years from 2007 – 2009 are shown:

Table 2: Averaged precipitation values [mm] for the months May - July from the years 2007, 2008 and 2009.

Year	May	June	July
2007	126	91	122
2008	10,7	44,9	72
2009	59,7	64,5	129

Lüers et al. (2014) described precipitation values (mm) from 1850 to 2010. Great fluctuations were present:

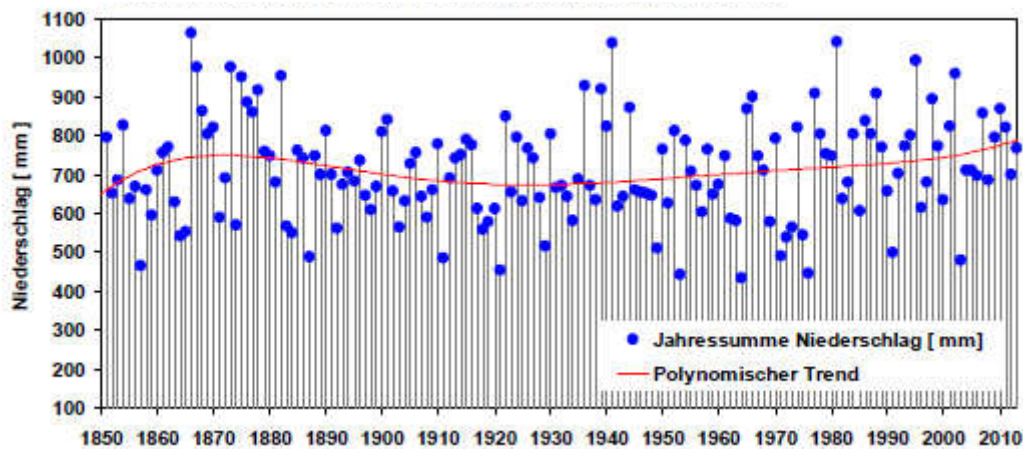


Figure 2: Precipitation values (mm) from 1850 to 2010. Source: Lüers et al. 2014.

Precipitation values fluctuated from a minimum of 432 mm in 1964 to 1062 mm in 1866. The yearly average from the last evaluated time period (1851-2013) is 712 mm. There was no significant increasing or declining trend.

### 2.3 Urbanization

Former UN-Secretary Kofi Annan had good reasons to state that we are living in an “urban millennium” as urban growth is a global trend, which leads to changes all over the world (TEEB 2016). Since 1950 the urban population has grown rapidly from 746 million to 3.9 billion in 2014. In 2007 the global urban population exceeded the global rural population for the first time in history. Seven years later the UN published findings, which state that 54% of the world’s population live in urban areas. This trend is expected to increase further as simulations project that 66% of the world's population will live in urban areas by 2050. Furthermore, it is very likely that by 2030 41 megacities inhabit more than 10 million people each (Bocquier 2005). Europe is a continent where urbanization increases, too. 2014 Europe placed third densest populated region (72% are living in urban regions) after Northern America and Latin America. In 2014 Europe is already home to 14% of the world's urban population. Even though rising urbanization is getting more stable and slower over the past two decades, the share of

people living in urban areas will further increase from 72% in 2014 to more than 80% in 2050 (Bocquier 2005). Germany is following the trend: 77% of the population lives in densely populated areas (TEEB 2016).

Urbanization is always coupled with sealing surfaces on a big scale. In 2004 still 131 ha per day were sealed in Germany. The most recent data from 2013 showed some improvement with 70,5 sealed hectares per day, which is still the area of almost 100 soccer fields and far off the target of the national strategic action plan, which states the aim to not seal more than 30 ha/day (TEEB 2016). In 2013 13,6% of the total area of Germany was covered by artificial materials (StBA 2015, TEEB 2016): Comprised of 51,3% buildings and associated space and 37,3% as traffic area (StBA 2015, TEEB 2016). As cities are so densely populated and need far more resources than the area can produce, sustainability is an important topic. The United Nations Conference on Sustainable Development in 2012 stresses the need for a holistic approach in urban planning and management to improve the living standards of dwellers and make urban societies economically, socially and environmentally more sustainable (Bocquier 2005). One reason for declined living conditions are the increased temperatures in the urban area. Vegetating urban areas is one proposed adaptation strategy (Gill et al. 2007, Bowler et al. 2010).

## **2.4 City Climate**

In general, the atmospheric situation is a result of exchange of energy, mass and momentum, which can be found in a wide range of spatial and temporal scales. Especially in urban areas those exchanges are very heterogeneous and include many factors (Oke 1982), leading to special meteorological properties in cities (Frezer 1995). Those special microclimates were observed in various studies as can be seen in the reviews of Oke (1974, 1979, 1990) and Matarakis (2001). The atmosphere above a city can be divided into two layers: First, the “urban canopy layer” (UCL), which is reaching from the ground to the mean roof level (Oke 1982). UCL encompasses two scales of climate: the micro-scale, which is the climate of individual elements in the city (as trees or buildings) and the local-scale, which are areas up to 10.000 m

and all the elements within (Grimmond & Oke 2002, Norton 2013). Second, the “urban boundary layer” (UBL), which is lying on top, forming a cap above the UCL (Oke 1976, Taesler 1981, Oke 1982) and is affected by regional climate processes (Norton 2013). Altered radiation schemes, moisture content and aerodynamics are the key influences of every urban microclimate.

#### **2.4.1 Radiation**

In the urban area the radiation scheme is altered. Typically, incoming sky radiation is decreased by about 10% (UV decreases up to 5%), while reflected shading can increase by 10% (TEEB 2016). Those alterations are mostly due to building structures and used materials. Building structures lead to varying shading patterns (Oke 1982) and decrease the average sunshine hours per day by up to 8 hours during summer (TEEB 2016). The results are smaller warming and cooling rates and no sharp temperature peak at sunrise or sunset. Furthermore, urban building structures lead to greater potential to absorb or emit radiation. Absorbed radiant energy is almost entirely converted into sensible heat (Oke 1982) while the small portion of latent heat is largely influenced by water availability (Coutts, 2007). Typical materials used for building increase the capacity to store and conduct heat and lead to multiple-reflection (Matzarakis 2001). Albedo describes the reflection rate of surfaces. Values are typically 0.05 to 0.1 lower in the city than in rural surroundings (Oke 1974, Oke 1982). Lowering the albedo by smart material choices can have a cooling effect (Shashua-Bar 2003).

#### **2.4.2 Moisture**

Moisture content is an important parameter for sensible heat. Energy exchange occurs either by the release of latent or sensible heat. While latent heat is related to changes in the phase of gas, liquid or solids, sensible heat is combined with changes in temperature. When moisture content is high, latent heat fluxes increase instead of sensible heat fluxes and therefore prevent urban heating. But as most surface types in cities such as paved roads, parking lots and

buildings are impervious, moisture has to be quickly discharged and evaporation is decreased by up to 50% (Matzarakis 2001, TEEB 2016). Regular irrigation may be a contemplable mitigation strategy to prevent heating (Oke 1982).

### **2.4.3 Aerodynamics**

Cities do have a greater aerodynamic roughness which leads to turbulences but can also function as an obstacle for wind currents (Matzarakis 2001). Goldbach & Kuttler (2013) presume that wind speed in cities is decreased by about 20% while squalls increase. This reduces cooling at night and sometimes even heating during the day, depending on many factors such as openness. Other influences are geographical compounds such as water bodies, topographic features, the nature of soils, present vegetation, land use of the region (Oke 1982) and combustion processes, which lead to release of heat and vapor (Matzarakis 2001). As cities are very complex and various materials are used, it is impossible to trust generalizations (Oke 1982, Shashua-Bar 2009).

### **2.4.4 Temperature - Urban Heat Island effect**

The Urban Heat Island effect is a phenomenon, which is defined as temperature differences between the warmest area in the city and the coolest temperatures in the rural surrounding. It can be measured through air temperature differences (Goldbach & Kuttler 2013). In 1833 Luke Howard was the first, who was able to show that temperatures in cities are higher than in the rural surrounding (Oke 1982). Today the urban heat island effect has become a serious environmental problem (Nakayama & Fujita 2010) particularly with regard to climate change. Variations of the urban microclimate, such as temperature increase can have impacts on human health and wellbeing (Lindberg & Grimmond 2011, Norton 2013). Fending for comfortable temperatures in our cities can simultaneously enhance indoor temperatures. Furthermore, it relieves the cardiovascular system. Respiratory problems can also be prevented because temperatures below 22°C decrease the probability of smog formation by 6% (Akbari et

al. 2001, Rosenfeld et al. 1995). As soon as night temperatures exceed 20°C sleeping quality is lowered and recovery hindered (Höppe 1999, Jendritzky & Grätz 1999, Scherer & Endlicher 2013, TEEB 2016). Studies show higher morbidity and mortality during and right after heat waves (Gabriel & Endlicher 2011, Heudorf & Meyer 2005, Michelozzi et al. 2009, TEEB 2016). During the European heat wave in 2003, 70.000 additional deaths were registered (Robine et al. 2008, Schär & Jendritzky 2004, TEEB 2016). It still seems to be unclear, which variables determine the intensity of the urban heat island effect to the biggest extent. There definitely seems to be a relationship between heat island intensity and city size (Oke 1973). Stone & Rodgers (2001) suggest that the urban heat island effect might be rather a result of urban design than of the density of building structures. Eliasson (1994) argues that energy absorbing surfaces and street geometry are primary causes. Others found winds, which facilitate mixing of heated and cool air masses and carry them downwind to be most important (Duckworth & Sandberg 1954, Oke 1982). Furthermore, anthropogenic heat sources which are mainly coming from transportation, building sectors and human metabolism influence the extent of heating (Coutts, 2007). Released air pollutants decrease permeability of the air for solar radiation and absorb longwave radiation (Matzarakis 2001). The absorbed energy is reflected to the surface and adds to the incoming sky radiation, adding to the total radiation. Those solar heated pollutants still radiate at night (Oke 1982). Further research is needed to clarify if either city size, population size, surface materials or architectural structures have the biggest influence (Oke 1982). Nevertheless, it can already be stated that the urban climate effect is one of the strongest anthropogenic-based climate effects on a small scale (Landsberg 1981, Beckroege 1984). On average about 2°C higher temperatures can be measured in urban areas, particularly at night (Oke 1987, Pretzsch et al. 2015, TEEB 2016). This effect is described as the Urban Heat Island Effect.

One of many factors is material choice. Urban areas are mostly covered by artificial surfaces, which cool slower and therefore increase warming. Thermal admittance of a surface indicates how quickly it can cool. Oke (1987) described thermal admittance for some materials and why gravel cools quicker than asphalt-stone covered areas (Eliasson 1994). Ca & Aseda (1996) described heat conductivity, specific heat, porosity and reflectivity for different surfaces, also asphalt and concrete. They found very high values for heat conductivity and specific heat of concrete and asphalt – two materials, which are often used in the urban environment. Poros-

ity and reflectivity is low in both cases. Therefore, it is not surprising that Eliasson (1996) noticed a temperature increase of 2.7°C in Sweden due to asphalt surfaces and that Leuzinger et al. (2010) detected the highest temperatures at a railway station (up to 60°C). Because of the reduced porosity of the used materials evapotranspiration rates are low in cities. Increasing the number of water bodies and plants helps to counter this effect (Spronken-Smith & Oke 1999, Chang et al. 2007, Nakayama 2011) due to increased transpiration rates, interception of solar radiation and shading (Oke 1989, Bowler et al. 2010). Increase of vegetation and low-albedo creation by only 7% already reduces urban temperatures (Akbari et al. 2001).

Street environments usually cover more than a quarter of the urban area (Shashua-Bar 2003). Therefore, urban climatologists use “street canyons” as a typical measure of street environments (Arnfield 1990). They consist of a roadway between two buildings and influence urban climate due to their distinct geometry (Oke 1982). Even though field studies showed, that background air temperatures are governed by regional factors, geometry and roughness of street canyons alter heating pattern as increased surface area leads to increased exposure to exchange processes (Oke 1982). Incoming solar radiation consists of shortwave and longwave radiation. Due to the geometry they get multiple-reflected. Particularly shortwave radiation is more likely absorbed and due to decreased openness longwave radiation cannot escape. Those geometric effects suffice to create an urban heat island effect (Matzarakis 2001, Oke 1982). Street orientation has an influence also because east-west canyons receive more solar radiation over the day than north-south oriented streets (Ali-Toudert & Mayer 2007, Norton 2013). But there are many additional influencing factors: heat emissions from buildings, surface materials with low-albedo, low moisture permeability and altered wind patterns. Furthermore, heat conductivity and storage capacity are increased in the urban environment (Matzarakis 2001). Oke (1982) studied energy flow of a canyon and found that 60 % of radiant surplus during the day was converted into sensible heat and further 30 % were conducted into heat storage. At calm nights 90% of longwave radiation was coming from storage, which led to higher average temperatures in the canyon than in the city center six hours after sunset.

Streets width and building heights (H:W ratio) are very important parameters to determine the heat risk of a street canyon (Norton 2013). The canyon’s H:W ratio determines the openness of the canyon and has an influence on shading. Studies showed that wide canyons with

low H:W ratios were on average hotter during the day and cooled quicker at night than narrow canyons with high H:W ratios. Here temperatures during the day were on average cooler because of the cooling effect of buildings shade but energy release during night was hindered (Johansson 2006, Swaid & Hoffman 1990, Norton 2013). Lindberg & Grimmond (2011) found highest temperatures in narrow street canyons and in sunlit areas under trees and justified results with hemispheric blocking of the cooler sky. Another measure to determine exposure to solar radiation is the sky view factor. While H:W ratio is only about building geometry, the sky view factor takes all shading factors into account, also trees and awnings (Coutts & Harris 2012, Norton 2013). During the night there is a linear negative relationship between sky view factor and measured temperature as many studies proved (Barring et al. 1985, Eliasson 1991, Oke et al. 1991, Oke 1981, Unger 2004). As a result, canyons, even if build relatively uniform are very complex and can still show great differences regarding radiative, thermal, moisture and aerodynamic properties. Taking into account the different orientations of the sun, different structures of buildings, different materials with different properties makes it impossible to draw general conclusions (Oke 1982), but rather show tendencies. It remains that temperatures in street canyons tend to be higher and therefore are key targets for mitigation and give possibilities to improve people's thermal comfort. East-west oriented streets have a higher priority due to their almost continuous exposure to solar radiation. Moreover, as the geometry of a canyon can only be altered with reconstruction processes, wide canyons are the better street type to work on mitigation on the short term (Norton 2013). One mitigation strategy is the plantation of trees. They have the same cooling effect in streets as on other sites (Shashua-Bar & Hoffman 1999). Oke (1989) showed in his article "The micrometeorology of the urban forest" that the energy absorption of urban trees is particularly large as they absorb direct solar radiation and reflect longwave and shortwave radiation from the urban environment. Depending on the water availability dissipation happens through evapotranspiration, latent and sensible heat and can lead to cooling (Shashua-Bar 2003).

## 2.5 Greens – One solution approach

### 2.5.1 Urban Green Spaces

Urban green infrastructure is a general term for remnant vegetation, parks, gardens, golf courses and street trees. New alternatives such as green roofs and green facades are on the rise (Norton 2013). Vegetation is an effective method to mitigate the urban heat island effect particularly during heat waves, which are expected to occur more often during climate change (Lindberg & Grimmond 2011, Bower et al. 2010, Gallo et al. 1993, Hamdi 2008, Norton 2013). It reduces temperature peaks and temperature variations (Jenerette et al. 2007, Luvall & Holbo 1989, Whitford et al. 2001) because energy is mainly emitted as latent heat and sensible heat flux is kept low (Grimmond et al. 1996, Coutts, 2007). Especially shading of urban trees at face level has a big influence on the wellbeing of dwellers (Rizwan et al. 2008). Nevertheless, it has to be kept in mind that vegetation has a very low albedo, so it absorbs a lot of incoming solar radiation and theoretically may lead to warming (Lawrence 2006). Evapotranspiration may counterbalance this effect. Moreover, vegetation modifies wind patterns (Norton 2013, McPherson et al. 1994, Oke et al. 1989, Taha 1997), which can support dispersal of heat. Vegetation also indirectly prevents warming as it absorbs carbon dioxide and buffers greenhouse gases in the atmosphere. Many studies all over the world studied the cooling effects of green spaces in cities. In London an average temperature reduction of 3.1 °C during summer was measured after urban green spaces were implemented (Lindberg & Grimmond 2011). Ca et al. (1998) found a park nearby in a hot-arid region can cool its surroundings by up to 2°C. Gill et al. (2007) points out that 1 ha is the minimum size of green space to have a cooling effect. Besides cooling, vegetation has many other functions. First, it benefits our environment (Norton 2013) as biodiversity habitats are created (Benedict & McMahon 2002), noise is reduced (Van Renterghem & Botteldooren 2009), storm water can be captured (Coutts et al. 2013) and air pollutants are reduced. Additionally, it enhances aesthetic values (McPherson et al. 2005), increases property values (Pandit et al. 2013), has a very important recreational value (Bolund & Hunhammar 1999) and increases human wellbeing (Lottrup et al. 2013). Surveys in German cities show that public green spaces are appreciated by urban dwellers and more than 75% of the participants would like to exclude them from saving measures (Forsa 2014). The effects mentioned above heavily depend on the vegetation type and moisture content (Norton 2013).

As an example: Bowler et al. (2010) suggest that tree cover may trap heat under the canopy whereas an open grass field provides low resistance to airflow and may cool by convection. Using urban green spaces for mitigation is very attractive because it does not increase energy use or greenhouse gas emissions as most technical cooling alternatives do. Furthermore, it's easier to implement than to modify urban geometry and material choices because it fits in already existing urban areas. To bring discussions on a concrete level, the Millennium Ecosystem Assessment (MA 2005) and TEEB-reports aim to systematically assess ecosystem services provided (TEEB 2016). Further work is necessary to predict how a changed climate leads to changing growing pattern of urban greenery and may restrict the ability to provide those services (Pretzsch et al. 2015, TEEB 2016). Pretzsch et al. (2015) simulated the changed climate for the years 2071 – 2131 in Munich and Würzburg and found averaged decreasing transpiration rates of *R. pseudoacacia* and *T. cordata* by 25% and 27% less cooling effect.

### **2.5.2 Urban trees**

Trees, as relatively big and high structures can create microclimates on the scale of tenth of meters with special interactions between wind, solar radiation, humidity and tree foliage (Miller 2015). In contrast to short, ground covering vegetation, trees are the optimal solution to provide shade not only on the streets (Norton 2013), but also for buildings, where it prevents heating and potentially decreases cooling-energy-costs (Akbari et al. 2001). Leuzinger et al. (2010) found shade of trees or buildings to be the coolest surfaces in cities after water bodies. Also Rosenzweig et al. (2006) rated tree planting as the best measure to reduce temperature at the local scale. Results from Melbourne show particular effectiveness at hot days (Coutts & Harris 2012). The downside is, that emitted heat from ground surfaces during night might be trapped under the canopies (Norton 2013, Spronken-Schmith & Oke 1999) and Grimmond et al. (1996) described how temperatures can be higher above the tree's canopy because of the overall increase of radiation fluxes (Coutts, 2007).

Urban trees are one vegetation type, which can be implemented in cities. They generally have the same functions as all vegetation types, but their shading and evapotranspiration has major effects on the urban climate (Shashua-Bar 2003).

Transpiration describes a vaporization process over the leaf surface through stomata (Pretzsch et al. 2015), which increases air humidity and cooling. A full-grown, healthy tree can evapotranspire 50-70 l water a day, but numbers change substantially depending on the plant. Transpiration leads to the cooling of the urban environment and is particularly important on hot summer days. Measurements show a temperature decrease of 6°C at the two-meter level in an alley (Wilde 2011). Increased humidity is not always pleasurable but can also lead to uncomfortable mugginess (Matzarakis 2001). Solar radiation provides the energy used for transpiring processes. When energy is detracted from the atmosphere, it leads to cooling by converting it to latent heat rather than sensible heat (Pretzsch et al. 2015, Bowler et al. 2010). The process is driven by many biotic and abiotic factors. Most important is the availability of light. Without solar radiation the stomata are closed, which makes the process negligible during night (Shashua-Bar & Hoffman 2002). In addition, the availability of water is crucial. But also vapor pressure deficit, intensity of wind and stomatal activity (Lambers et al. 2008, Oke 1987, Miller 2015) draw a distinction. It's a common belief, that the most important biotic factor is the leaf area index. Recent studies showed that leaf area index, tree canopy properties and leaf characteristics (Wilde 2011, Norton 2013, Hunter Block et al. 2012) are similarly important.

Besides transpiration, shading is the most important contribution to thermal comfort in cities during hot periods (Lindberg & Grimmond 2011). Although shadows from buildings might be the primary influence on the amount of shade in the urban environment (Lindberg & Grimmond 2011), shade from trees should not be underestimated. Only 30 % of incoming solar radiation can penetrate a leaf, which highlights the importance of shading of urban trees for microclimate alterations. Additionally, urban trees have a very low albedo and therefore reflect only 8% of the incoming energy (Wilde 2011). Other surfaces commonly used in cities reflect much more and enhance warming of the immediate surroundings (Wilde 2011). A study made in Basel shows the dimensions: While unshaded roofs heated up to more than 60°C at sunny days, temperature under trees remained relatively cool with 26°C on average (Leuzinger 2010). Again, the extent of this service is dependent on the characteristics of individual trees. The degree of permeability determines the amount of shade provided (Norton 2013), which means that general foliage density and leaf area density are influencing shading effect most (White et al. 2012). Therefore, broadleaf species are beneficial (Leuzinger et al. 2010, White et al. 2012). Moreover, canopy shape and depth varies within the species and

influences shade pattern. Shorter trees, for example, provide more shade for pedestrians (White et al. 2012), while taller trees are needed to shade buildings (Tooke et al. 2011). But also extrinsic factors are of influence. The background air temperature should be the basis for comparisons, while other factors such as geometric configuration of the site, tree characteristics and growth factors should be threatened as influencing factors (Shashua-Bar & Hoffman 1999).

### **2.5.3 Species differences**

Living conditions for trees are harsh in the urban environment. Temperatures in cities tend to be higher and root zones are generally smaller. Therefore, the risk of drought is present (Leuzinger et al. 2010). Kjelgren & Montague (1998) showed that trees growing above concrete are generally poorer in health than trees grown above grass. This effect is also caused by higher radiation levels in urban areas especially because of re-radiation from asphalt and concrete. If temperatures exceed a certain limit, trees tend to close their stomata, which leads to a positive feedback mechanism and the area heats up even quicker. Species' ability to cope with difficult circumstances varies, but nevertheless life spans of urban trees can be expected to be shorter (Hunter Block et al. 2012, Norton 2013). Species choice is still very important. Even though all vital trees provide important services in the urban environment, not all species accomplish the same level. They differ regarding their size, leaf size and canopy architecture, which affect penetration of solar radiation and water use and consequently also transpiration rates. Generally small-leaved trees remain cooler than bigger leaved ones, but might produce less shade (Norton 2013). Trees with lower foliage temperature have a greater cooling effect (Leuzinger et al. 2010). Furthermore, foliage temperature can influence stomata activity, since they get closed when temperature exceeds a certain level and evapotranspiration is stopped. Also water use varies among species, which results in different transpiration rates (McCarthy & Pataki 2010, Pataki et al. 2011). The situation gets more complex as species which have the greatest cooling effect at ambient temperatures are not necessarily coolest at extreme temperatures (Leuzinger et al. 2010).

#### 2.5.4 Previous studies in Munich and Würzburg

The study at hand is imbedded into a study of the TU Munich (Pretzsch et al. 2015). Aim of the study was to quantify and model growth dynamics of the four tree species: *Tilia cordata*, *Robinia pseudoacacia*, *Platanus x hispanica* and *Aesculus hippocastanum* in six cities (Munich, Würzburg and Bayreruth). The measurements included stem diameter, crown width and height, as well as sealed surface close to the trees and distance to the next buildings in all directions. Furthermore, vitality and competition with other trees was determined. Temperature and precipitation data were used to include living conditions and calculate tree age. Ecosystem services like shading, cooling through evapotranspiration, carbon sequestration were modeled. Results from trees of the same age showed that *R. pseudoacacia* was able to sequester almost double as much carbon than *T. cordata* (301/597 kg C). Furthermore, on average *R. pseudoacacia* shaded a slightly bigger area per tree (508/583 m<sup>2</sup>). *T. cordata* on the other hand removed more energy from the atmosphere which leads to increased cooling (4797/6350 kWh). Throughout the whole study results from trees growing on streets, on squares and in parks were grouped and compared. It was possible to show that trees on streets were performing worse than the ones on squares and parks. Another focus of the study was to model the mentioned services in different future scenarios. The impacts of two scenarios (wet and dry) on tree services were modeled for the years 2071 to 2131, where the expected temperature increase particularly during summer months was included. In general, a decrease of all addressed ecosystem services was observed, but results have to be treated carefully depending on tree species and site conditions. Comparisons of the two cities Würzburg and Munich showed less services provided in Würzburg than in Munich, which might be due to less precipitation.

### 3. Materials and Methods

#### 3.1 Underlying conditions

##### 3.1.1 Climatic conditions in Bayreuth during the study period

As Shashua-Bar & Hoffman (1999) already described, underlying climatic conditions are the most important factor, when temperature patterns are analyzed. Since 2001 the main weather station for Bayreuth is situated in the botanical garden, south of the university. Data from the station was used to describe climatic conditions during the study period. The location of the station can be seen in the figures below:

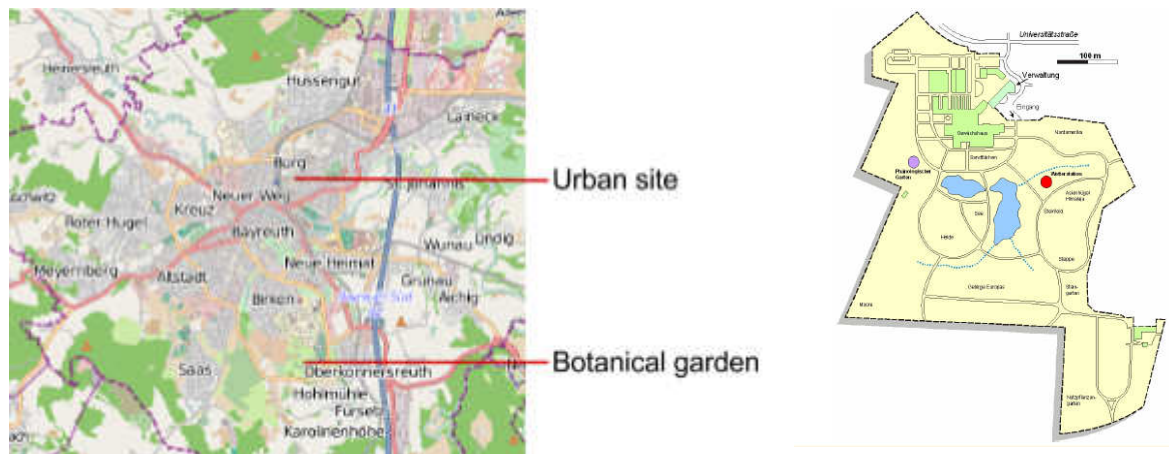


Figure 3: Left: Location of the rural site. Source: [urlaubsziele.com/bilder/karten/staedte/472/karte-bayreuth-100.png](http://urlaubsziele.com/bilder/karten/staedte/472/karte-bayreuth-100.png)  
Right: Location of the weather station in the botanical garden (red).

The pole with the main measuring devices is 17 m tall and is situated 365 m above sea-level. Temperature [°C], relative air humidity [%] and windspeed [m/sec] were collected 2 m above grassland. All data were read-out every 10 minutes and were transferred via radio to the Bay-CEER-computer system. Air temperature [°C] was measured by an actively ventilated and radiation protected psychrometer-thermometer. Daily averages were calculated as arithmetical mean from 10-minute-values. Precipitation [mm] heights were measured via the electrical weighing system “Pluvio” of the company Ott. Again daily averages were calculated from 10-minute values. For the study at hand, data from 01.05.2016 through 28.07.2016 was analyzed. Results can be seen in chapter 4.1.1.

### 3.1.2 Selected tree species

To ensure comparability, the study focuses on the same species *Tilia cordata* and *Robinia pseudoacacia* like the previous studies in Munich and Würzburg (Pretzsch et al. 2015). Originally, the species were chosen because of their different ecological niches. *T. cordata* is very shade tolerant while *R. pseudoacacia* is very light-dependent (Pretzsch et al. 2015). Moreover, both species are often planted within the urban environment (Pauleit et al. 2002).

#### *Tilia cordata* in detail

*Tilia cordata* Mill., is one of two *Tilia* species native to central Europe and is also called small-leaved lime. *T. cordata* is a genus of broad-leaved trees which belongs to the sub-family *Tilioideae* within the family of *Malvaceae*. The genus consists of about 45 species, but only three of them are native in Europe: *Tilia platyphyllos*, *Tilia cordata* and *Tilia tomentosa*. *T. cordata* is spread from southern Finland to southern Italy and from the Caucasus to north-west Spain (Aas 2016). More details about spatial expansion can be seen in figure 4. The small-leaved lime requires some warmth but not as much as *T. platyphyllos* (Eaton et al. 2016). Usually late or early frosts are not harming. Because *T. cordata* does not require much nutrients and humidity, but can



Figure 5: Geographical extension of the occurrence of *T. cordata*. Source: Kölling & Zimmermann (2007)

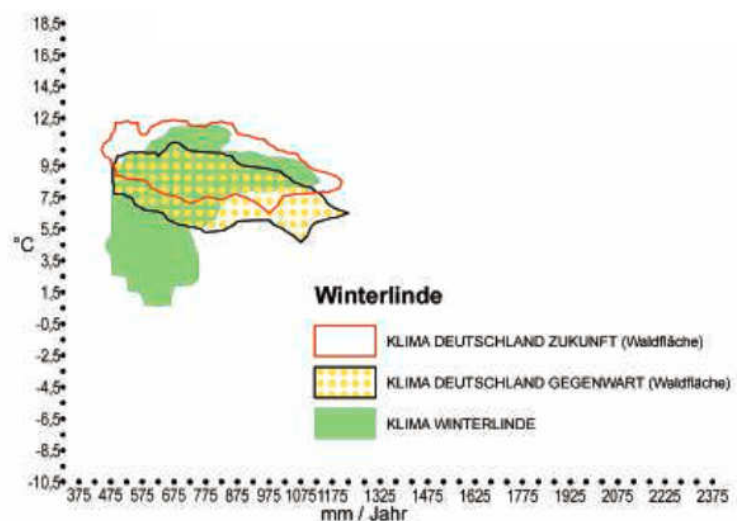


Figure 4: Bioclimate envelope of *T. cordata* with actual and predicted climate. Source: Kölling & Zimmermann (2007)

also tolerate stagnant moisture, it can grow in many different environments such as calcareous soils, podzols and brown earth, as well as on lime-rich soils, when there is enough precipitation (Aas 2016). Because of its modesty, small-leaved limes can be planted in almost every city in Europe. The species can reach a height of 30 – 40 m and trunk diameter of 1 m. Under good growing conditions it can survive for about a 1000 years (Eaton et al. 2016). Crowns grow very neat, also because of the regular, distichous phyllotaxy and ramification (Aas 2016). Leaves are about 9 cm long and heart-shaped. Both, crown and leaf shape embellish city scape. To distinguish between *Tilia platyphyllos* and *Tilia cordata*, vein axils on the lower surface of the leaves have to be checked for hairs, which can only be found at *T. cordata* (Aas 2016). Flowering starts in June. The small, pale flowers occur in clusters of 4 or 5 and attract many insects for pollination. Only individuals older than 30 or 40 years produce seeds (Eaton et al. 2016). Because of the very dense growing, light emitting efficiency is high and enables growing in relatively shaded areas such as street canyons in cities. Dense growing also increases shading, which is very important in urban areas to counterbalance increased heat (Eaton et al. 2016). Moreover, it is classified as relatively disease resistant. *Phytophthora plurivora*, a very aggressive soil born plant pathogen can harm *T. cordata*. Also the gypsy moth and aphids can be a problem. In cities, the honeydew can be a “disservice” if plastering cars or other objects of value (Eaton et al. 2016). Kölling & Zimmermann (2007) rate vulnerability of *T. cordata* to climate change as low. In figure 5 *T. cordata* and its bioclimate envelope can be observed in comparison to actual and predicted climate in Germany.

#### Robinia pseudoacacia in detail

*Robinia pseudoacacia* L., also called black locust is a deciduous tree native to North America and introduced to Europe in the early 17th. Century. Now the species is commonly planted in almost all European cities as a very undemanding but light dependent tree (Sitzia 2016).

The species belongs to the family of Fabaceae within the order of Fabales. The tribe Robinieae comprises of 4 to 10 species of which one is *Robinia pseudoacacia* L (Wojda et al. 2015).

Commonly, single trees reach about 20 m of height and have a typical life span of 60-100 years (Sitzia 2016). The trees can grow either as single- or as multi-stemmed trees. When they are older, the bark is vertically fissured. Leaves are composed, pinnate and up to 30 cm long. Commonly up to 12 pairs form one leaflet, they are mostly opposite with one at the end. The leaf blades are elliptic and about 2 to 5 times 2 cm. In winter the fruits, 5 to 10 cm long legumes are striking (Sitzia 2016). Nevertheless, the species reproduces mostly asexual through root elongation. Any damage favors clonal growth. As clonal re-



Figure 6: *Robinia pseudoacacia*.  
Source: holzwurm-page.de

production can occur even in great distances of up to 100 m, it is one of the 100 most invasive alien species in Europe (Sitzia 2016). *R. pseudoacacia* is appreciated for its durable and resistant wood, its quick growth, which makes it interesting for biomass production, the production of its fruity honey and its capacity as a fabaceae to fix free nitrogen gas from the air via Rhizobium bacteria, which enriches soil for other plants as well. Some more advantages were observed: within the stands of *R. pseudoacacia*, many rare and endangered fungi were found. Bats also appreciate the species for its rough bark, which can be used as shelter during the day (Wojda et al. 2015). Moreover, as it is no native species, there are only one gall midge and two moths which can potentially cause any threat. It can grow on almost any soils, also poor and degraded ones, only limited by low soil aeration and waterlogging, which also eases planting in cities (Sitzia et al. 2016). Furthermore, it is very drought resistant, which is one reason why the species is expected to expand even further with climate change (Pretzsch et al. 2015). *R. pseudoacacia* is also commonly planted in cities as a decorative, undemanding tree.

### 3.1.3 Selected tree individuals

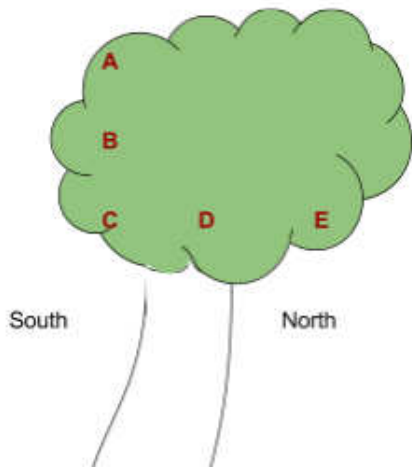
Within the city of Bayreuth individuals of the species *Tilia cordata* and *Robinia pseudoacacia* were selected. The experimental group was divided into two subgroups:

- 1) Two middle-aged *T. cordata* and two middle-aged *R. pseudoacacia*. This group was mainly used for species comparisons.
- 2) Eight younger trees of the species *T. cordata*. This group was mainly used for age differences.

All individuals' diameter was measured at 1.3 m height. Tree height and the height of the crown position were measured with a Leica disto device. Crown extent was plumbed at all subcardinal directions (N, NO, ...) by projecting it on the ground. Distances to the next tree and building in all subcardinal directions were also measured to evaluate competition and building intensity. Furthermore, vitality was rated after Roloff (2001). Devices were put in all selected individuals. Exact positions can be seen in the appendix A.

#### Subgroup 1

The tree individuals were located at a crowded street, where the soil is mostly covered with asphalt and concrete. Uncovered soil for surface roots was limited. The trees were planted as an alley in a distance of approximately six meters. *R. pseudoacacia*1 (R1), *T. cordata*1 (T1) and *R. pseudoacacia*2 (R2) were located next to each other, while *T. cordata*2 (T2) was on the other side of the street. Subgroup 1 offered a good chance to observe cooling effects of *R. pseudoacacia* and *T. cordata* side by side. Especially R1, T1 and R2 are exposed to similar conditions. They were very close to a building which was located less than three meters north and they had similar soil properties. Furthermore, all trees were of similar height (10 - 16,5 m). See figure 7 for further illustration. All four trees of subgroup 1 were equipped with five devices each (see positions in figure 7), which measured temperature, relative air humidity and radiation. Additionally, all trees measured infrared-radiation from the ground at position C and E. Furthermore, wind speed data was collected at T1 and R2.



Robinia1, Tilia1, Robinia2  
Tilia2

Figure 7: Left: Location A, B, C, D & E of measuring devices in subgroup 1. Right: Study site of subgroup 1.

### Subgroup 2

Subgroup 2 consisted of eight trees of the species *T. cordata*. It offered the possibility to gain a better insight into the cooling effects of this species. The tree individuals were located between a crowded street and a parking area as can be seen in figure 8. Close to the next building was a water body. The soil around the trees and at the parking site was almost totally covered. Soil for surface roots was limited to 1 meter in all directions. The trees were planted as an alley every eight meters. Even though all trees were of the same species, age differences were present (15 - 40 years). T11 was located next to a building which might bring interesting results due to the buildings' wall as a radiation emitting body. All trees of subgroup 2 were equipped with three measuring devices, which collected

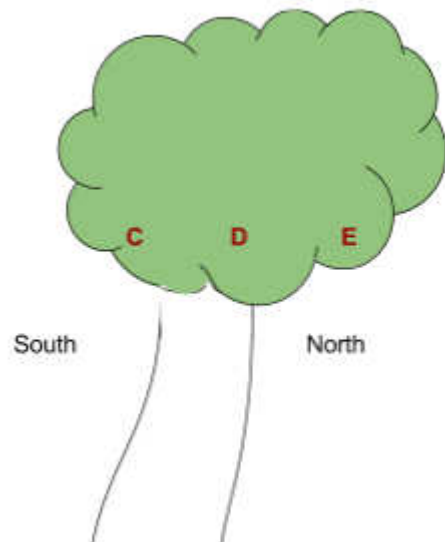


Figure 8: First: Location A, B, C, D & E of measuring devices in subgroup 2. Second: Study site with subgroup 2.

data on temperature, relative humidity and radiation. Positions can be seen in figure 8. Additionally, three trees have an infrared-sensor at position C and E, which was oriented towards the ground. Furthermore, wind speed was documented at T6 and T10.

#### **3.1.4 Study sites**

Urban site: It was necessary to make the study comparable to the previous studies in Munich and Würzburg. Those studies focused on trees on streets, on squares and in parks. Therefore, the focus needed to be on one of those sites. Furthermore, street environments are covering on average 25% of the urban area, which makes it the most important site of the discussed ones. The present study therefore focused on urban trees on streets.

The trees in focus were *Tilia cordata* and *Robinia pseudoacacia*, so a street was chosen where those trees stand side by side. The chosen site was located in the center of Bayreuth, Germany, close to the train station. Details can be seen in figure 9. The geometry of the chosen street was very complex and included buildings close to the street as well as an open area used as a parking lot. The street is oriented from south-west to north-east. As chosen trees were mostly on the northern side of the street, they received direct solar radiation almost all day. At the urban site many surfaces might lead to multi-reflections. The floor consisted of asphalt on the street, stones made out of concrete on the pavement as well as on the parking lot. Albedo and moisture permeability of asphalt was very low, heat conductivity and storage capacity was high. But concrete also stores a lot of heat and moisture could only penetrate through joints. The chosen street was straight for around 700 m which speeds up wind most likely. The parking lot and other unevenly build complexes might have also led to turbulences. Trees were planted at both sides of the street and also cover the parking lot. Furthermore, there was a water body close to the street which might have led to further cooling. All selected tree individuals and both street measuring sites were situated here.

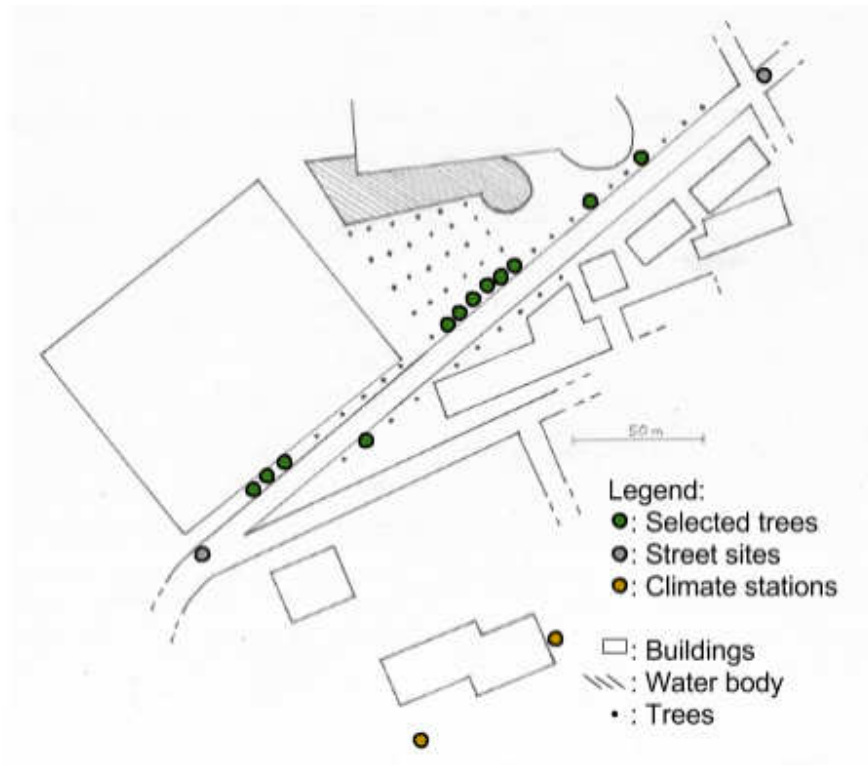


Figure 9: Study site with selected trees, sites for street measurements and location of climate stations.

The microclimate of the site was investigated with a Kestrel 4000. Accuracy is noted as  $\pm 3\%$  for windspeed,  $\pm 1\text{ }^{\circ}\text{C}$  for temperature and  $\pm 3\%$  for relative air humidity. The measurements were conducted at two days (20.07.2016 and 21.07.2016), when temperatures were high (max.  $34.2\text{ }^{\circ}\text{C}$ ), windspeed was low (max.  $3\text{ m/sec}$ ) and it was mainly cloud free. At both days, data was collected at 5:00, 10:00 and 15:00 in  $1.3\text{ m}$  height. To analyze the microclimate of the urban site in detail, it was classified into 11 categories, which can be seen in the figure below:

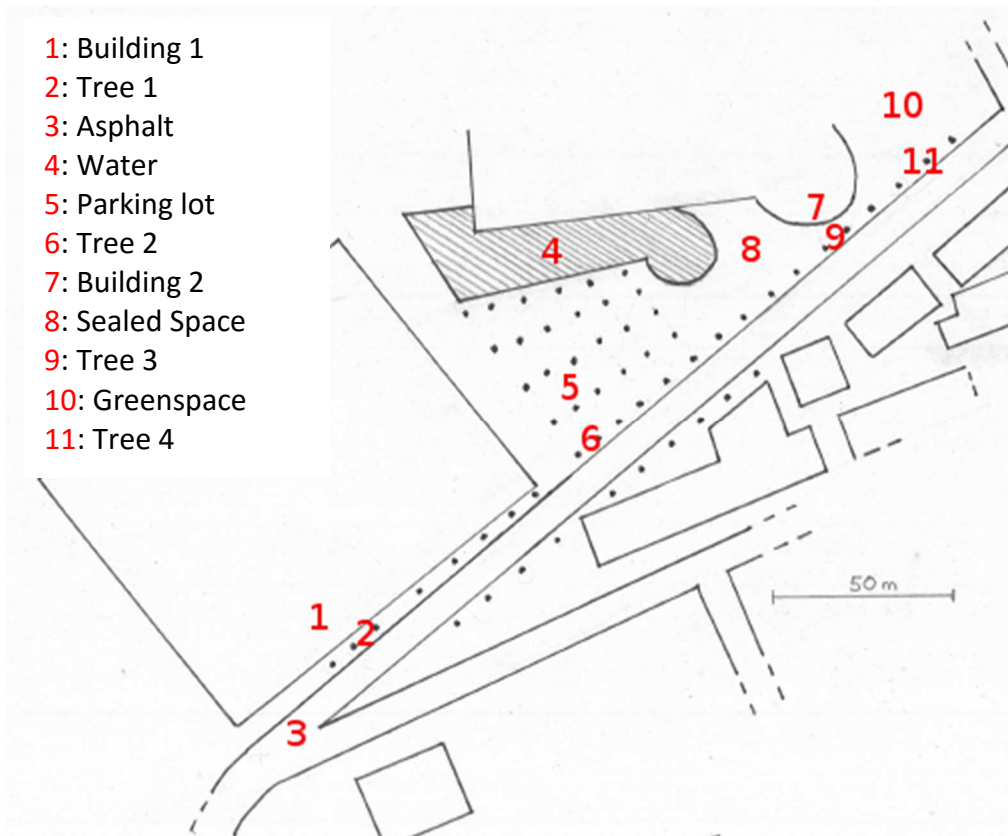


Figure 10: Categories for observation of the microclimate of the study site.

It was suspected, that two buildings had major effects on the microclimate at the study site, which are marked as Building 1 (1) and Building 2 (7). At both sites, data was collected close to the building walls to ensure the documentation of a possible heating effect. Four trees, which were exposed to different conditions were analyzed: Tree 1 (2) and Tree 3 (9) were located close to a wall (distances to buildings: 2.2 m, 9 m) and might have been influenced by reradiated heat. Tree 2 (6) was standing between a parking site, which was sealed but planted with trees and the asphalt covered street. Tree 4 (11) had a greenspace nearby, which might have had cooling effects but it might have also been influenced by the asphalt covered street on the other side. For all trees, data was collected close to the stem and both under the canopy in the sun (southern side) and under the canopy in the shade (northern side). Asphalt as the main street covering material was analyzed as well (3). Measurements were conducted once again in the sun as well as in the shade. As a potentially cooling factor, data was also collected at the waterside (4). The parking site (5) was sub-classified into three categories: conditions below a tree canopy on the parking site (shaded), above a car (potentially increased heating) and at an open, concrete covered place (sunny). Between the waterside and building 2, a relatively big open, concrete covered space was also included (8). In contrast to the categories,

which are typical for an urban environment, also a greenspace was included into the study (10). Measurements were conducted in the greenspace (shaded). The urban site was analyzed with the aid of 18 categories. Averaged mean temperature [°C] and relative air humidity [%] of both days can be seen in 4.1.3.

Study sites for comparison:

Weather stations: Two weather stations were set up close to the chosen study site described in 3.1.4.1. The position can be seen in figure 9 (marked as climate station). Both weather stations ran during the whole study period and documented temperature [°C] and relative air humidity [%]. Onsets' HOBO® Micro Stations with Temperature/RH smart sensor S-THB-M002 were used for measurements. Accuracy was  $\pm 0.2$  °C for temperature measurements and  $\pm 2.5$  % for relative humidity. Data was taken every minute and averaged over 10 minutes.

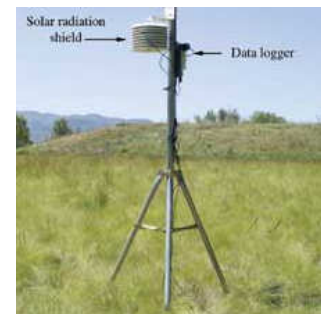


Figure 11: HOBO microstation as it was used in the study at hand. Source: fs.fed.us

Weather station 1 was put on a parking site. The site was covered with concrete stones and had only little vegetation. The parking lot was arranged around a tall building. Weather station 2 was put on a greenspace in the back of the building. The ground was covered with grass and some trees were standing nearby.

Rural site: To be able to compare data taken at the urban site with data from a rural site, a device was put in the botanical garden, which was already described and illustrated in 3.1.1. The device was set up close to the original weather station at 1.3 m of height. The site was located in a very natural environment with grass covered ground and trees in some distance. The device was documenting temperature [°C], relative air humidity [%] and incoming radiation.



Figure 12: Controlling device in a rural surrounding.

### 3.2 Main measurements

There are many different paths for gathering information about temperature patterns in urban areas:

Matzarakis (2001) developed a mobile vehicle which measured climatic parameters at face level. Leuzinger et al. (2010) overflew Basel, Switzerland with a thermal camera to describe different surface temperatures. Others installed a meteorological station in more than 40 meters of height to record foliar temperature (Miller 2015). To cover infrared radiation a pyrgeometer was successfully used by Ca & Aseda (1996). As wind speed recording with a cup anemometer is customary, it was used by many studies (e.g. Eliasson (1994)). In the study at hand, climatic conditions at the study sites were documented over a period of 61 days. Low cost devices had to be constructed, which produce high quality data and contain inexpensive off-the-shelf components. Devices had to accommodate various sensors which measure temperature [°C], relative air humidity [%], radiation [mV], object temperature [°C] and windspeed [m/sec]. Low power consumption was the aim, in order to reduce costs and to facilitate long-term measurements without further energy supply. With some further incidentals 74,31€ were spend for a fully equipped device. 53 devices were produced and installed, totaling 3938,58€. The compounds used were described in 3.2.1.

### 3.2.1 Components for measuring devices

Temperature & relative Humidity: For temperature and relative air humidity measurements a commercial SHT21 digital sensor from Sensirion was used. Every sensor was calibrated and had an accuracy of  $\pm 0,3$  °C and  $\pm 2$  % relative humidity. To protect the sensor against particles a filtering cover was put on top. Especially the quality of relative humidity measurements might have been improved due to the capping. The connected sensor was put in a naturally ventilated radiation protection.

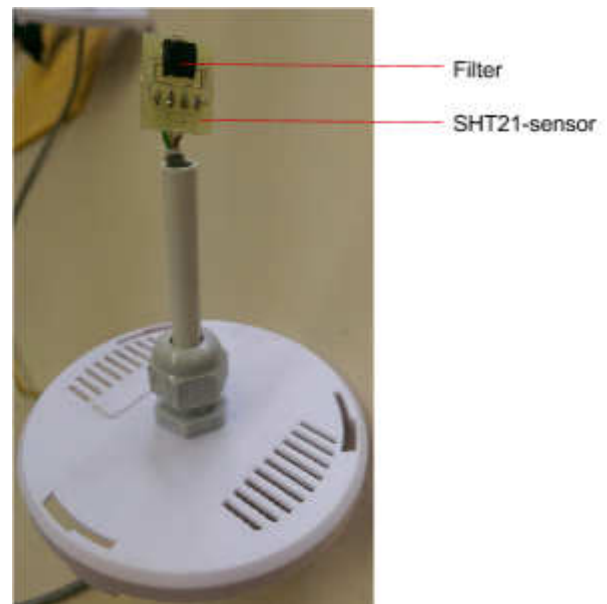


Figure 13: SHT21-Sensor with a filter for protection already put on the base of the radiation protection.

Radiation protection: As Thomas et al. (2013) described, it is necessary to put the temperature sensor in a radiation protection to shield the sensor from damage, keep the sensor dry, prevent the accumulation of particles on the sensor and minimize errors. Thomas et al. (2013) recommend naturally ventilated radiation shields because they require no electric power. Even though some progress was made to correct the radiation error there are still some serious uncertainties for temperature measurements in naturally ventilated protection shields (Lin et al. 2001). Uncertainties are dominated by wind speed differences inside and outside the shield, radiation penetration inside the shield (Richardson et al. 1999), simplifications and chosen variables.



Figure 14: Radiation protection fixed on a PVC-base.

Actively ventilated radiation protections, which actively circulate air close to the sensor and prevent heating are producing the most accurate results, but are very expensive and need an

energy supply. Therefore, a passive radiation protection was used. It shields the sensor from direct radiation and allows natural wind circulation. The small radiation protection was installed on a PVC-base, together with the housing for the board.

Tests of the radiation protection still showed some inaccuracy. To improve data quality. Different adjustments were tested as can be seen in the appendix B. The most precise results were achieved by covering the SHT-sensor with an aluminium-tube. The tube interior was sprayed black and was fitted with five ventilation holes on the sensor level. See figure 15 for illustration.



Figure 15: Aluminum-tube attached to the radiation shield to get more accurate data.

**Photodiode:** A photodiode was attached to the top of the radiation protection to measure incoming radiation from above. A simple silicon PIN SFH 203-diode was used, which was sensitive to a wavelength range from 400 to 1100  $\mu\text{m}$ . The analogue signals are converted to digital signals by MCP.

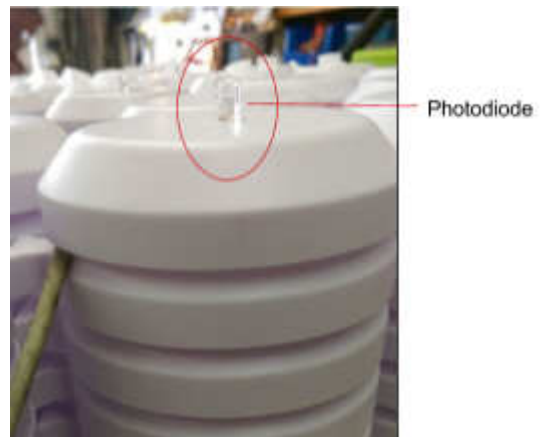


Figure 16: Photodiode attached to the radiation shield.

Infrared-sensor: A digital infrared sensor was used to measure infrared radiation originating from the ground. The digital sensor measures direct temperature values and is able to calculate the temperature of the object because of calibration.



Figure 17: Infrared-sensor as a single compound (l) and installed (r).

Wind-sensor: In order to measure wind speed a cup-anemometer was attached to the device. It records 1 impulse/sec at a wind speed of 1 m/sec. To save energy the device was in sleep-mode except for 100 sec/day activity and was connected via an interrupt entrance.



Figure 18: Wind sensor attached to the device.

Information processing: A board was brought into the housing, where all signals were readout by a microcontroller. Radio-modules (RF24) sent the data to a router. A G-Board-Pro was chosen, which had a microcontroller and a mobile phone chip incorporated. The router received the data, buffered it, averaged it over 10 minutes and sent it to a gateway. Until it reached the gateway it had a relative time stamp. Energy was provided by lithium button cell batteries or 1,5V AA-batteries respectively for the devices. Routers were equipped with rechargeable 12V lead acid batteries.

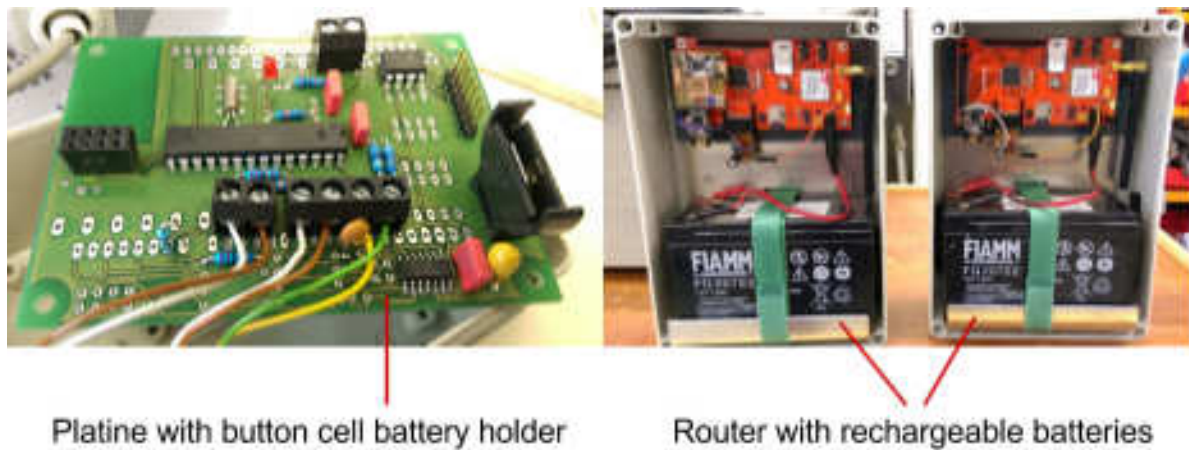


Figure 19: Board (l) and routers (r).

### 3.2.2 Data analysis

All data was collected on the BayEOS Server of Bayreuths' center of ecological and environmental research (BayCEER). To analyze the data, the software "R" and partly "Microsoft Excel" was used.

Statistics: Again the software R was used to do statistical testing.

Normal distribution: The Shapiro-Wilk test was applied to test for normal distribution. Null hypothesis  $H_0$  was set for normally distributed data. The level for significance was 95%. Null hypothesis  $H_0$  was rejected in all cases, data was never normally distributed.

Testing for homogeneity of variances: As collected data was not normally distributed, Wilcoxon signed-rank test was applied, when samples were not random and dependencies existed. In this study this was mostly the case as data was taken in the same environment with similar underlying forces. The test is a nonparametric hypothesis test, where two related samples are tested for rank differences. If the P-value was  $< 0.05$ , the null hypothesis  $H_0$  was rejected and the difference was considered as statistically significant. Independent datasets were tested with Mann-Whitney-U-test. Level for significance was 95%. Again the test is a nonparametric test, where the null hypothesis  $H_0$  is tested, which assumes, that two datasets do not differ significantly. If the P-value was  $< 0.05$ , null hypothesis  $H_0$  was rejected and the difference was deemed statistically significant.

## 4. Results

### 4.1 Underlying conditions

#### 4.1.1 Climatic conditions in Bayreuth during the study period

The results of this study were highly dependent on the climate conditions during the study period. Air temperature [°C] and precipitation [mm] were measured in the botanical garden of Bayreuth during the study period and can be seen below:

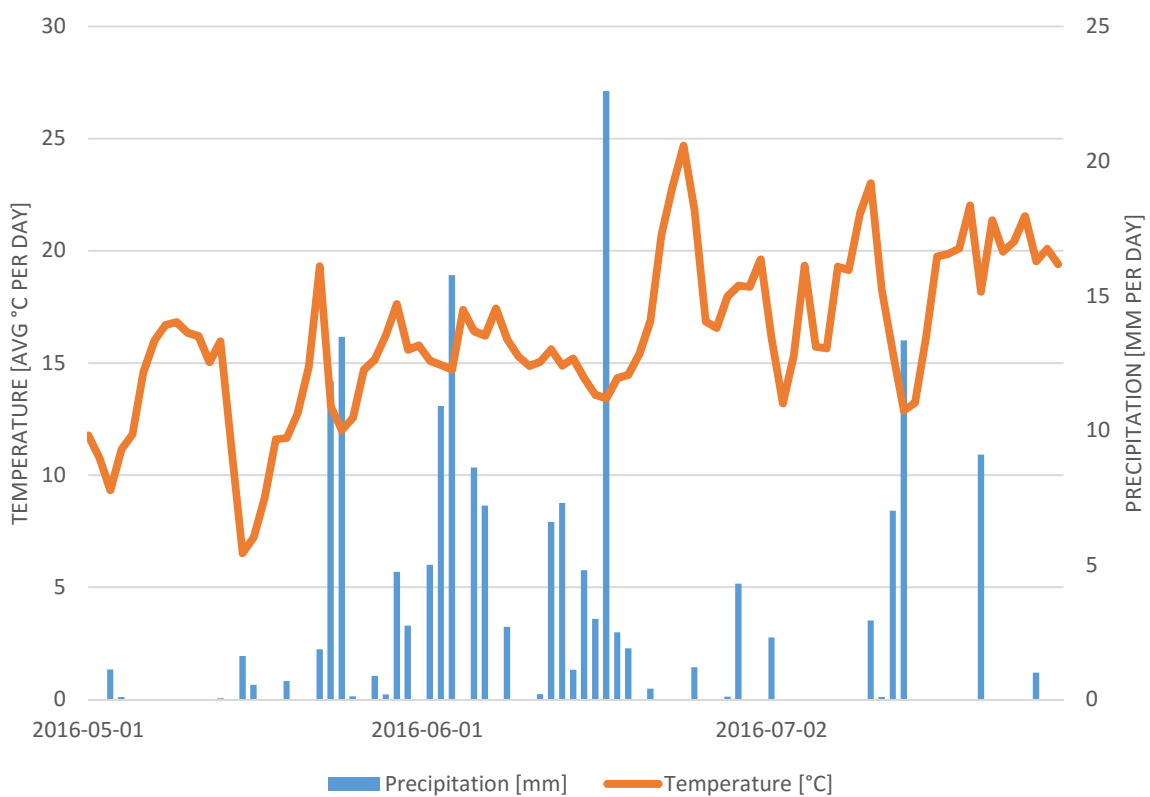


Figure 20: Daily temperature and precipitation-values during the study period.

Comparing values of 2016 with long-term values for Bayreuth, temperature development in the months May to July followed the normal trend. Temperature regularly fluctuated about 10°C. The figure visualizes how precipitation values of the months May, June and July differed: besides a wet period from the end of May until the end of June, precipitation values were on average lower than normal.

Figure 20 shows the weather conditions during the study period as daily values. The table below gives monthly averages.

Table 3: Monthly temperature averages for the study period in comparison to long-term values for Bayreuth.

	Temperature 2016 [°C]	Temperature average for Bayreuth [°C]
May	13.5	12
June	16.7	15.2
July (until 28th)	18.4	17

Temperature values during the study period were representative for the area as they fitted the long term averages pretty well. Values were constantly about 1.5°C higher than the long term averages calculated by Lüers et al (2014).

Table 4: Monthly precipitation [mm] averages for the study period.

	Precipitation [mm]
May	40
June	106
July (until 28th)	36

May and July were rather dry months (40, 36 mm), while there was a lot of precipitation in June (106 mm). Because of naturally fluctuating precipitation patterns, which are explained in 2.2, no direct comparison to previous years was done.

#### 4.1.2 Selected tree individuals

As already described in 3.1.3, all individuals' diameters, heights and the heights of the crown position were measured. Furthermore, crown extent and distances to the next tree and building in all subcardinal directions were documented. Vitality was rated after Roloff (2001). Cailliau (2016) calculated crown volume and modelled crown projected area. Results can be seen in the following table:

Table 5: Dbh [cm], Age, Height [m], Crown position [m], Vitality, Crown volume [m<sup>3</sup>], Crown projected area [m<sup>2</sup>], Tree pit [m<sup>3</sup>] and min. Distance to the next building [m] for all selected tree individuals of *T. cordata* and *R. pseudoacacia*.

Tree	Dbh [cm]	Age	Height [m]	Crown Pos. [m]	Vitality	Crown volume [m <sup>3</sup> ]	Crown projected area [m <sup>2</sup> ]	Tree pit [m <sup>3</sup> ]	Min. Distance to next building [m] (orientation)
<b>R1</b>	42,6	42,4	16,5	5,8	0	636,6	59,5	1,0	2,8 (N)
<b>T1</b>	42,4	53,3	13,8	5,3	0	486,4	57,2	1,0	2,2 (N)
<b>R2</b>	27,9	27,8	12,0	5,7	0	293,3	46,6	1,0	2,9 (N)
<b>T2</b>	35,0	43,8	10,5	4,3	1	294,0	47,4	5,2	12 (N)
<b>T3</b>	8,7	15,4	7,7	3,7	0	27,0	6,7	5,2	14,5 (S)
<b>T4</b>	8,2	16,1	9,3	3,3	0	47,0	7,8	5,0	15,6 (SO)
<b>T5</b>	8,5	17,2	10,4	3,0	0	58,5	7,9	5,3	13 (N)
<b>T6</b>	30,6	39,2	10,5	3,3	0	419,6	58,3	5,3	9 (N)
<b>T7</b>	25,7	34,4	10,8	3,0	0	385,3	49,4	5,6	14 (SO)
<b>T8</b>	25,5	33,3	9,6	3,3	0	179,9	28,6	5,3	9 (N)
<b>T9</b>	30,5	39,8	11,4	3,4	0	407,9	51,0	5,3	14 (SO)
<b>T10</b>	17,3	24,4	8,6	3,7	2	74,5	15,2	2,1	8 (S)

10 Trees were selected for the study at hand, of which 2 are of the species *R. pseudoacacia* and eight are of the species *T. cordata*. DBH was varying between 8.2 cm (T4) and 42.6 cm (R1) and age ranged between 15.4 (T4) and 53.3 (T1). Individuals were between 7.7 m (T3) and 16.5 m (R1) of height and had the lowest crown position at a height of 3 m (T7) to 5.8 m

(R1). Vitality was rated after Roloff (2001) and was mostly zero (best). Cailliau (2016) calculated crown volume, which varied between 27 m<sup>3</sup> (T3) and 636.6 m<sup>3</sup> (R1). Crown projected area was also computed and ranged between 6.7 m<sup>2</sup> (T3) and 59.5 m<sup>2</sup> (R1). The size of the tree pits varied from 1 m<sup>3</sup> to 5.6 m<sup>3</sup> (T7). In order to get an impression of the influencing surroundings, distance to the closest building was documented and varied between 2.2 m (T1) and 15.6 m (T4).

**4.1.3 Microclimate of the urban site**

Section 3.1.4 described the microclimate investigation of the selected urban site with a Kestrel 4000. The averages of the measurements on July 20<sup>th</sup> and 21<sup>st</sup> for each category can be seen as a bar plot below:

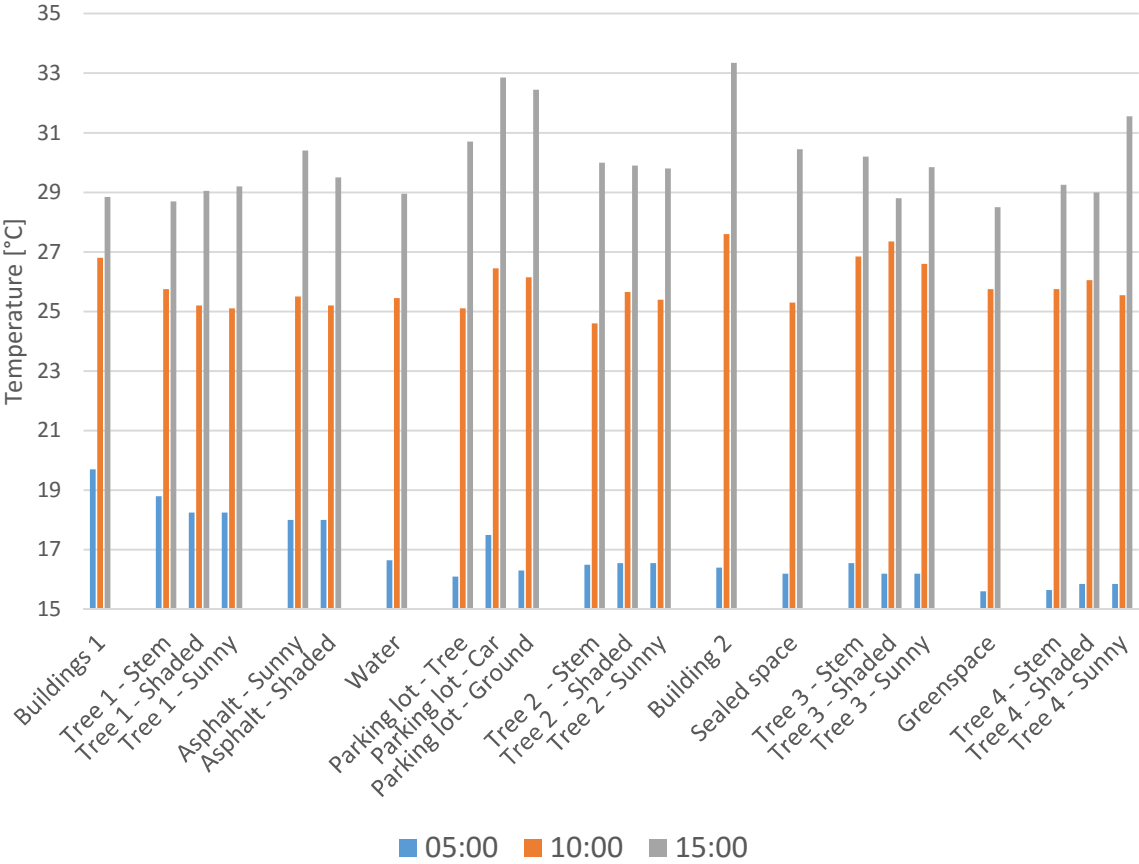


Figure 21: Mean temperature at July 20th and 21st averaged for each category (n=2).

Temperature measurements were conducted for all 18 categories. At 5:00 on average the highest values were found in the western part of the site, towards the train station. The highest temperature was measured at building 1 as 19.7 °C, while lowest the temperature was found at the greenspace with 15.6 °C. Tree canopies could not yet be differentiated between shaded and illuminated areas. At 10:00 the highest temperature was observed at building 2 with 27.6 °C, while the lowest temperature was found at the stem of Tree 2, which was located between the parking site and the street with 24.6 °C. Tree 3 and 4 already showed temperature differences between shaded and illuminated orientations of the canopy. Temperatures at both buildings differed, with lower temperatures observed at building 1. Neither temperatures at the greenspace nor at the waterside were lowest. At the parking site, the highest values were found above cars (26.5 °C), while it was coldest below the tree canopies (25.1 °C). Highest averaged temperatures were found at 15:00. The maximum value was measured at building 2 with 33.4 °C on average, while the lowest temperature was documented at the greenspace with 28.5 °C. Building 1 was again cooler (28.9 °C) than building 2 (33.4 °C). Temperatures below tree canopies were almost always lower in shaded areas than in illuminated areas with an average difference of 0.93 °C. Also averaged temperature difference between shaded and illuminated asphalt was 0.9 °C. In contrast to temperature at the greenspace (28.5 °C), temperature at the waterside was slightly higher at 29 °C. At the parking site, the averaged temperature difference was 2.2 °C between measurements below tree canopies (30.7 °C) and above cars (32.9 °C). Comparing all artificial surfaces, the concrete covered parking site was most heated at 32.5 °C, while asphalt (30.4 °C) and the sealed space (30.5 °C) showed similar results. All in all, maximum temperature differences were 4.1 °C at 5:00, 3 °C at 10:00 and 4.9 °C at 15:00.

Also relative air humidity [%] was measured for all 18 categories. The results can be seen below:

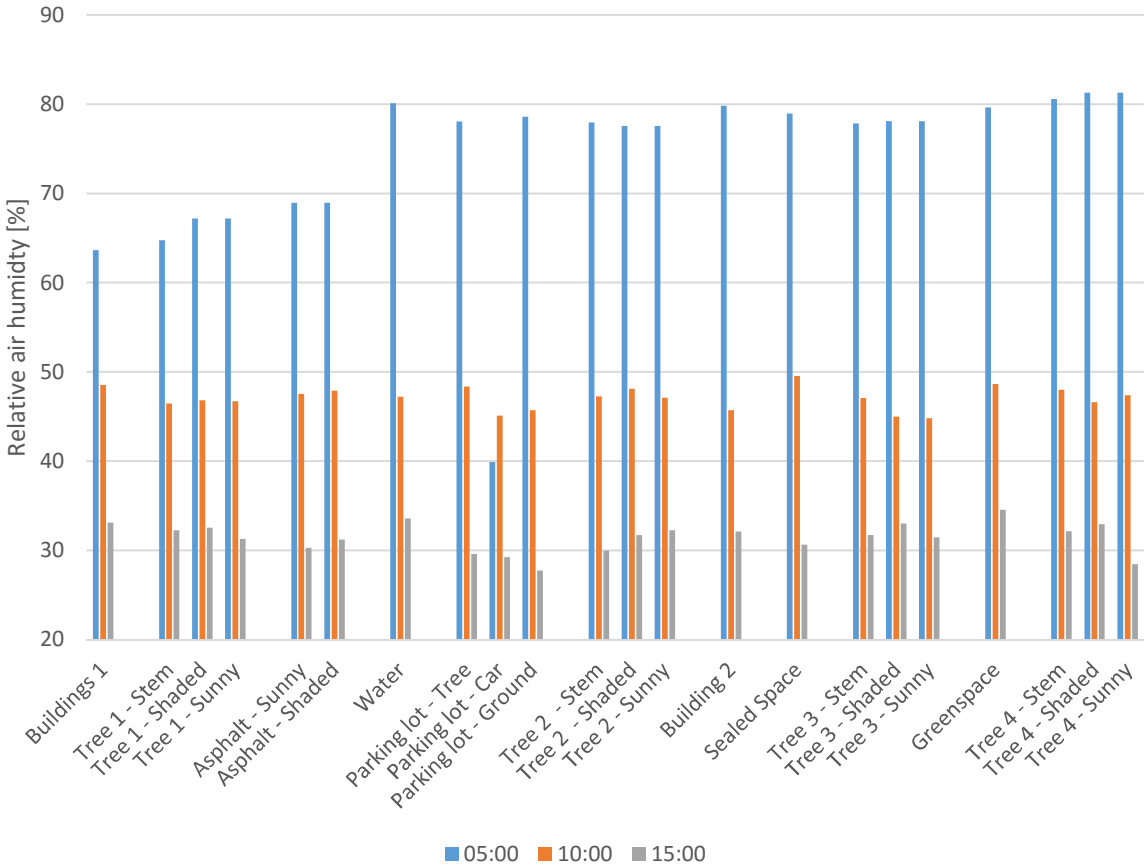


Figure 22: Mean relative air humidity at July 20th and 21st averaged for each category (n=2).

Relative air humidity varied between 81.3 % and 27.8 %. At 5:00 in the morning, the greatest air humidity was measured with particular great values at the east of the site, which is furthest from the train station. At 5:00, the maximum value was found at tree 4 (81.3 %), located close to a greenspace. The lowest value was measured above a car with 39.9 %. Humidity values were greater at building 2 (16.2 %), which was closer to the greenspace than at building 1. Humidity at the trees varied between 65 % and 81.3 %, while air humidity measured at the tree stems was generally lower than below the canopy. Comparing all sealing materials, the lowest values were found above asphalt with 69 %, while values measured above the parking site and at the sealed space were equally at 79 %. Air at the greenspace was slightly less humid (79.7 %) than at the waterside (80.1 %). Relative air humidity at 10:00 was already reduced by more than 20 % on average. Most relative humidity was found at the sealed space (49.6 %), while lowest values were found below tree 3, when there was no shade (45 %). Even though

air at building 2 was more humid at 5:00, the higher air humidity was now found at building 1 with 49 %. Apart from tree 4, all trees showed higher values in the shade than in the sun. Of all sealed surfaces, air at the sealed space was most humid (50 %), while the parking ground was driest at 46 %. Relative air humidity at the greenspace was 1.5 % higher than above the waterside (47.2 %). Conditions at the parking site differed by 3.3 % with greatest values below the tree canopy (48.4 %) and lowest above cars (45.1 %). Relative air humidity at 15:00 was again decreased by about 15 %. The greatest value was found at the greenspace at 34.5 %, while it was less humid above the parking ground at 27.8 %. Comparing the two buildings, humidity was 1 % greater at building 1 at 33.1 %. Air humidity was on average 1.7 % greater in the shade of trees than in illuminated areas below the canopy. Of all sealed categories, lowest values were found at the parking site, with 27.8 %, while conditions above asphalt and at the sealed space were similarly around 30.5 %. Moreover, conditions at the greenspace and above the water did only differ by 1 %, with higher values at the greenspace (34.6 %). Generally relative air humidity at the parking site was lowest, with minimum values above the ground (27.8 %). All in all, maximum relative air humidity differences were 17,6 % (leaving out the heated car) at 5:00, 4,6 % at 10:00 and 6,7 % at 15:00.

## 4.2 Main measurements

### 4.2.1 Urban climate

#### 4.2.1.1 Temperature

Temperature measurements were done at four sites: above the street and at a parking lot as typical urban environments as well as at a greenspace and in the botanical garden as vegetated comparisons. In the figure below the measurements were averaged over the whole period of 61 days:

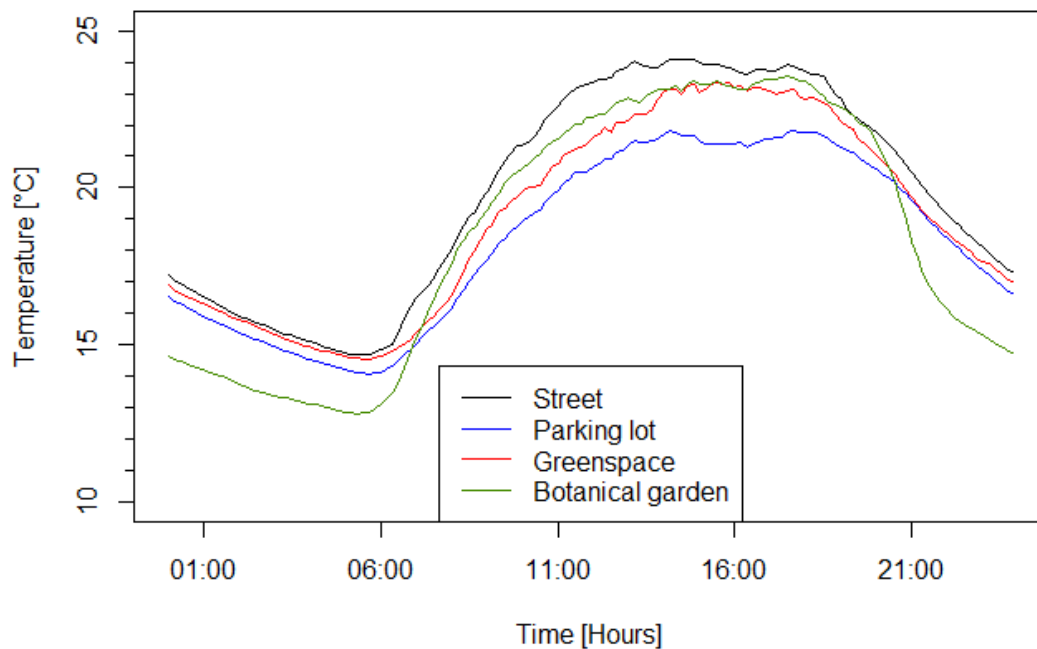


Figure 23: Averaged diurnal variations of air temperature [°C] measured in botanical garden (rural area), above the street, at a parking lot and at a greenspace (n=61).

Table 6: Temperature maxima, average & minima for all four study sites.

Temperature [°C]	Street	Parking lot	Greenspace	Botanical Garden
Maximum	24.1	21.8	23.3	23.6
Average	19.9	18.4	19.1	18.5
Minimum	14.6	14.1	14.6	12.8

The temperature above the street was the highest at any time. During the day, lowest temperatures were measured at the parking lot, while it was coolest at the botanical garden dur-

ing the night. The maximum average temperature was 24.1 °C documented at 14:40. The minimum average temperature was 14.6 °C measured at 5:30. Between 14:20 and 18:00 a slight temperature drop could be observed above the street, at the parking site and at the botanical garden.

Surprisingly, in comparison to measurements above the street and at the greenspace, the temperature was lowest at the parking site with an averaged maximum of 21.8 °C at 15:50. The temperature at the greenspace was even lower with a minimum of 14.1 °C at 5:40. During the night, temperatures at the greenspace were similar to the temperatures above the street. The minimum average value at the greenspace was documented at 5:30 at 14.6 °C. During the day, temperature at the greenspace was almost as high as in the botanical garden and reached the same maximum temperature at 15:30 with 23.3 °C. Temperature differences between night and daytime were greatest in the botanical garden: while at night it was by far the coolest in the botanical garden, it was second hottest there during the day. At 5:20 the minimum average was 12.8 °C, while the averaged maximum was 23.6 °C at 17:30. Particularly in the evening around 19:00, temperatures in the botanical garden were very similar to temperatures above the street. The greatest differences between those two were observed during the night, with a maximum of 3.1 °C at 22:10. While temperatures were changing quickly between 7:30 and 11:00 and between 8:00 and 21:30, in the evening, temperatures in the urban and the rural environment were very similar. In the afternoon, when averaged temperatures were highest, the temperature difference was less than 1 °C.

Whether the data measured above the street (urban site) and in the botanical garden (rural site) differ significantly was checked using the Wilcoxon signed-rank test. The P-value was  $2.2 \cdot 10^{-16}$  ( $V=10440$ ) and therefore  $< 0.05$ .  $H_0$  was rejected for  $\alpha = 0.05$  and the difference was deemed statistically significant.

Additionally, temperature taken in the botanical garden and above the street during the study period of 61 days were analyzed using a density function:

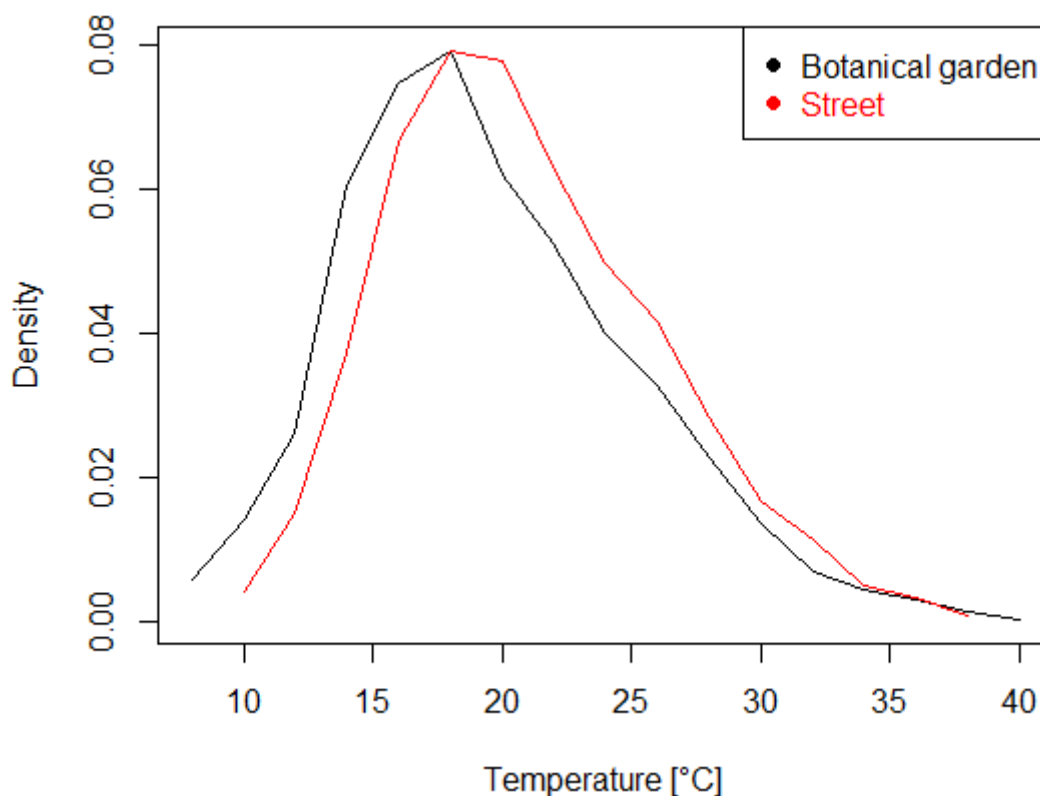


Figure 24: Density function of air temperature [°C] measured in botanical garden (rural area) and above the street.

Generally, warmer temperatures were more often measured in the urban than in the rural environment, even though both density functions found their maximum at an air temperature of 17.5 °C. The minimum temperature measured in the urban environment was 10°C, while the minimum temperature in the rural environment was about 1°C cooler. Nevertheless, also the highest temperature was found in the botanical garden at about 40°C. The temperature maximum in the city was about 1°C lower.

#### 4.2.1.2 Radiation

A photodiode was attached to all devices, which measured incoming solar radiation during the study period of 61 days.

Table 7: Solar radiation maxima, average & minima for all four study sites.

Incoming radiation [mV]	Street	Botanical Garden
Minimum	0	0
Mean	60.40	63.1
Maximum	185.90	180.3

The table gives an overview of the measured solar radiation at the urban and the rural site. Even though mean incoming solar radiation is greater at the botanical garden (63:60 mV), the greater maximum value was measured above the street (186:180 mV).

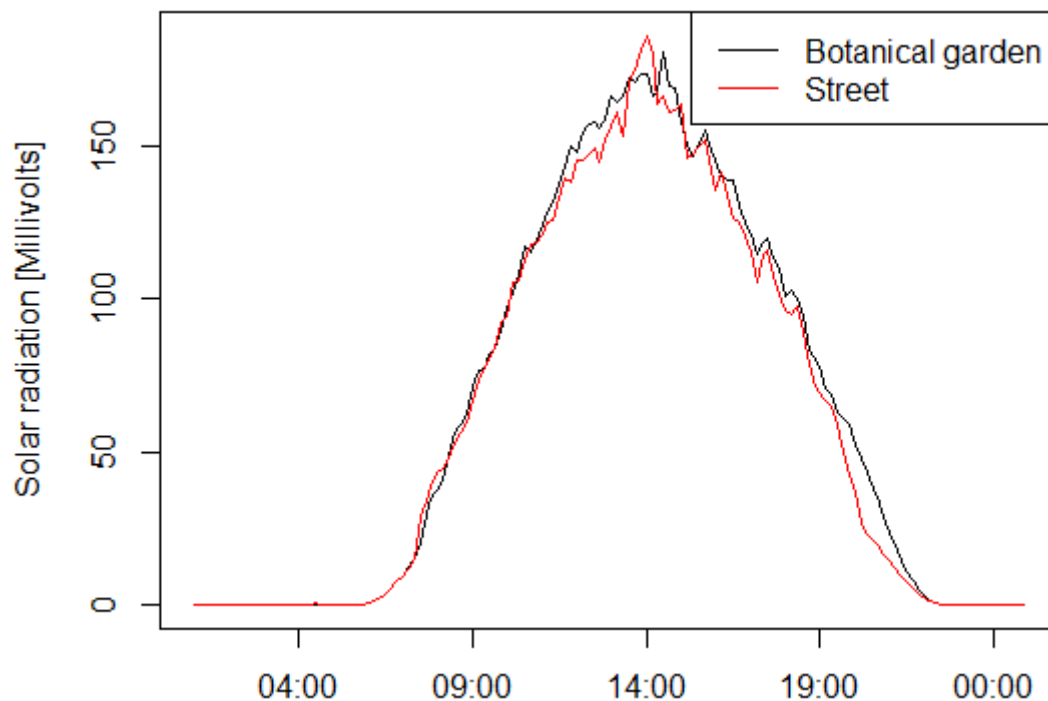


Figure 25: Averaged diurnal variations of incoming solar radiation measured in botanical garden (rural area, n=1) and above the street (n=1) during the study period of 61 days.

Figure 25 shows the average incoming solar radiation during the study period from 29.05.2016 to 29.07.2016. Generally, the same pattern can be observed at the rural site (botanical garden) as well as above the street. There was a slight tendency of less solar radiation at the urban site. Maximum values of 186 mV were found at around 14:00 above the street.

Whether the data measured above the street (urban site) and in the botanical garden (rural site) differ significantly was checked using the Wilcoxon signed-rank test. The P-value was  $2.2 \cdot 10^{-16}$  ( $V=10440$ ) and therefore  $< 0.05$ .  $H_0$  was rejected for  $\alpha = 0.05$  and the difference was statistically significant.

Data was furthermore analyzed using a density function. The result can be seen in the appendix C.

#### **4.2.1.3 Moisture**

Relative air humidity [%] was measured during the whole study period. In the figure below the averaged results measured above the street, at the parking lot, at the greenspace and in the botanical garden can be seen in comparison:

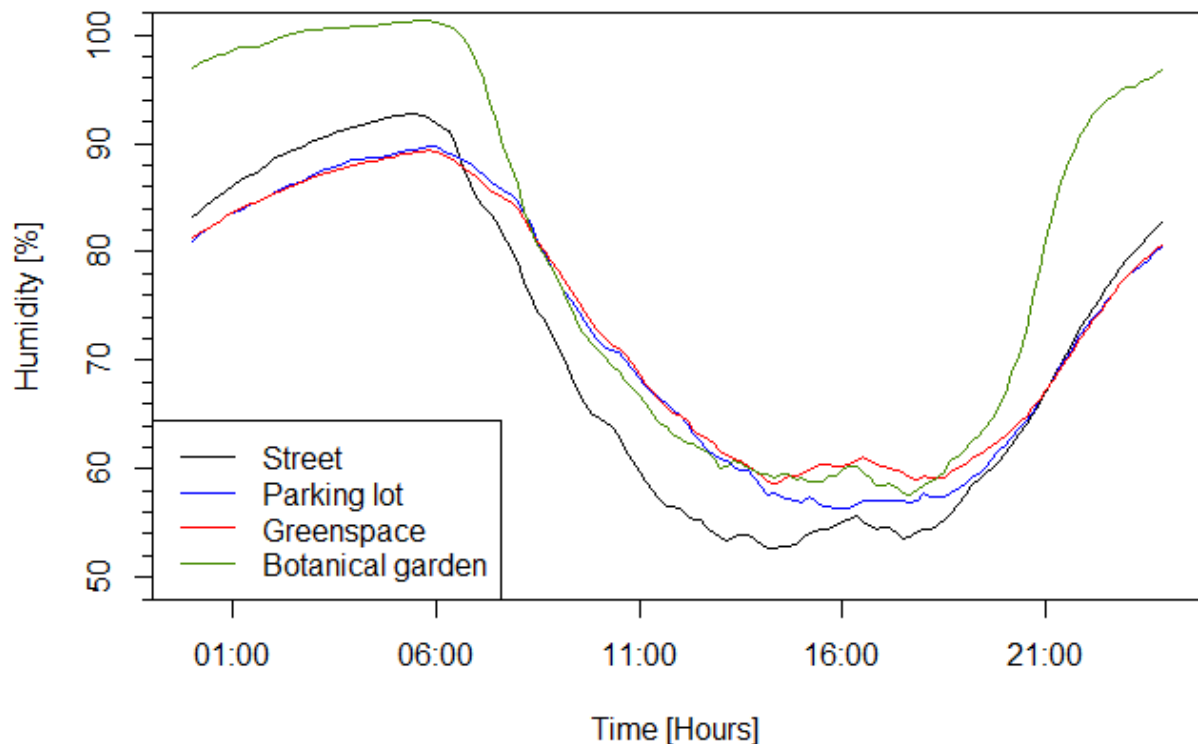


Figure 26: Averaged diurnal variations of relative air humidity measured in the botanical garden (rural area,  $n=1$ ), above the street ( $n=2$ ), at the parking lot ( $n=1$ ) and at the greenspace ( $n=1$ ) during the study period of 61 days.

Generally, all datasets showed the same daily pattern, as relative air humidity was high during the night, decreased at about 5:20 and stayed low until it rose again in the evening at 19:00. Comparing all datasets, during the day relative air humidity was at its lowest above the street. The minimum value of 52.7 % was measured at 14:10, just before it started rising by 2.5 percentage points. Humidity at the parking site and at the greenspace was very similar particularly from 19:00 to 14:00. The averaged maximum value measured was 89.3 % at the parking site at 5:50 and 89.8 % at the greenspace at 6:00. The averaged minimum was found in the afternoon at 58.7 % at the parking site (14:20) and at 56.3 % at the greenspace (16:00). Again a small increase of about 2.5 percentage points was measured in the afternoon at the greenspace. By far the highest relative air humidity was measured in the botanical garden with an average of 80 % (see table 8 for comparison). Particularly from 19:00 to 8:00 high values were documented. Highest documented value was 101.3 at 5:40. During the day, values were decreasing to a minimum of 57.6 % at 17:40. In the morning between 9:00 and 13:00 values were even lower than at both weather stations. Again, a slight rise in the afternoon at about 16:00 was observed.

Results of the Wilcoxon signed-rank test: Data taken above the street was tested against data taken at the botanical garden. The P-value was  $2.2 \times 10^{-16}$  (V=0). Data taken above the street was tested against data taken at the greenspace. The P-value was  $6.043 \times 10^{-8}$  (V=2503). Data taken above the street was tested against data taken at the parking lot. The P-value was  $5.881 \times 10^{-5}$  (V=3205). Data taken at the greenspace was tested against data taken at the botanical garden. The P-value was  $2.406 \times 10^{-10}$  (V=2044). Data taken at the greenspace was tested against data taken at parking site. The P-value was  $5.39 \times 10^{-6}$  (V=2938.5). P was < 0.05 in all cases, so  $H_0$  was rejected and the differences were statistically significant.

Table 8: Relative air humidity maxima, mean and minima for all four study sites.

Relative air humidity [%]	Street	Parking lot	Greenspace	Botanical Garden
Maximum	92.7	89.3	89.8	101.3
Mean	71	72.7	73.3	80
Minimum	52.7	58.7	56.3	57.6

The density function shows the density function of the relative air humidity during the study period from 29.05.2016 to 29.07.2016:

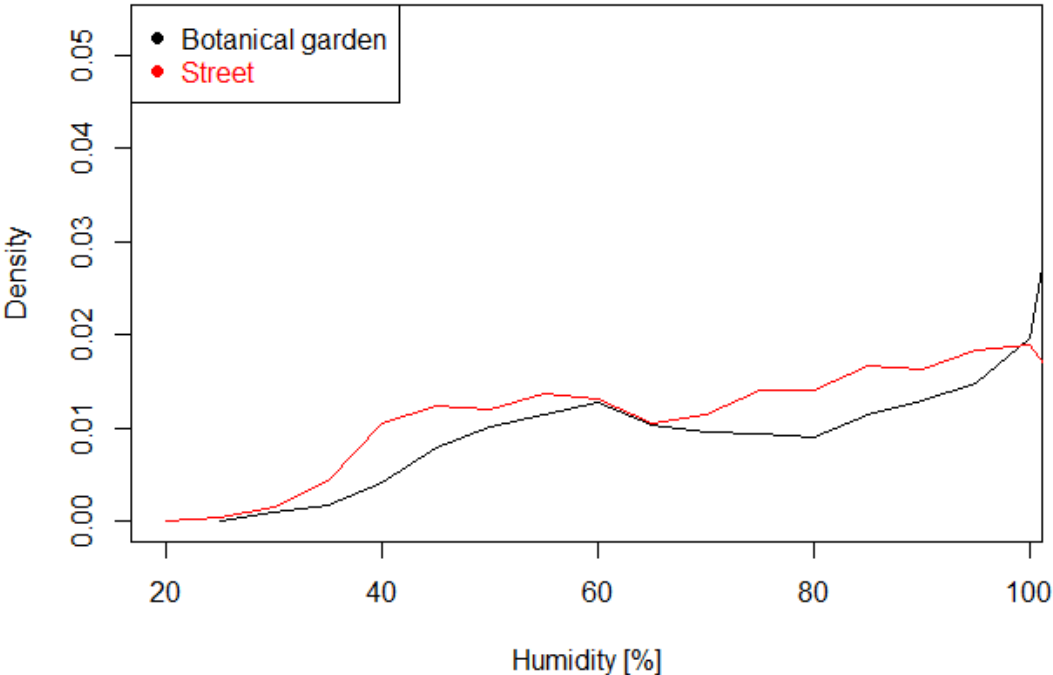


Figure 27: Density function of relative air humidity measured in the botanical garden (rural area) and above the street during the study period of 61 days.

Relative air humidity values ranging from 30 % to almost 100% show higher density values above the street. Very high air humidity values were mostly found at the rural site.

#### 4.2.1.4 Ground temperature

Object temperature was measured via an infrared diode over the whole study period at the urban site. Infrared-diodes were located above the street.

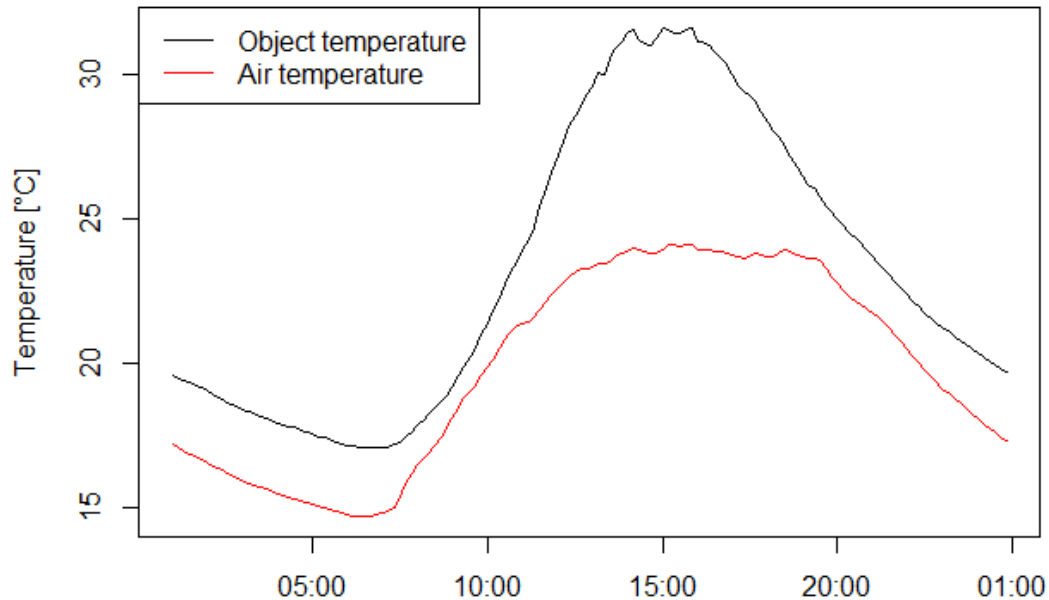


Figure 28: Averaged diurnal variations of object temperature measured above the street via infrared ( $n=2$ ) and air temperature above the street ( $n=2$ ) during the study period of 61 days.

The figure above shows the averaged diurnal variations of the object temperature above the street in comparison to the air temperature measured at the same locations during the study period from 29.05.2016 to 29.07.2016. Both, object temperatures of the surface materials at the study locations as well as air temperatures show the same pattern: minimum temperatures were measured in the morning at around 7:00 am, while the maximum temperature was measured in the afternoon at around 15:00. During the day the object temperature was always higher than the air temperature. Maximum differences were found between 11:00 and 20:00, when averaged air temperature stayed below 25°C and averaged object temperature exceeded 30°C. Moreover, a delayed cooling of the surfaces was observed in the evening after 20:00.

Whether the datasets differ significantly was checked through the Wilcoxon signed-rank test. The P-value was  $2.2 \cdot 10^{-16}$  ( $V=10440$ ) and therefore  $< 0.05$ .  $H_0$  was rejected for  $\alpha = 0.05$  and the difference was deemed statistically significant.

#### 4.2.1.5 Aerodynamics

The windspeed measured at the urban site was compared to the windspeed measured in the botanical garden. The average diurnal variation can be seen in the figure below:

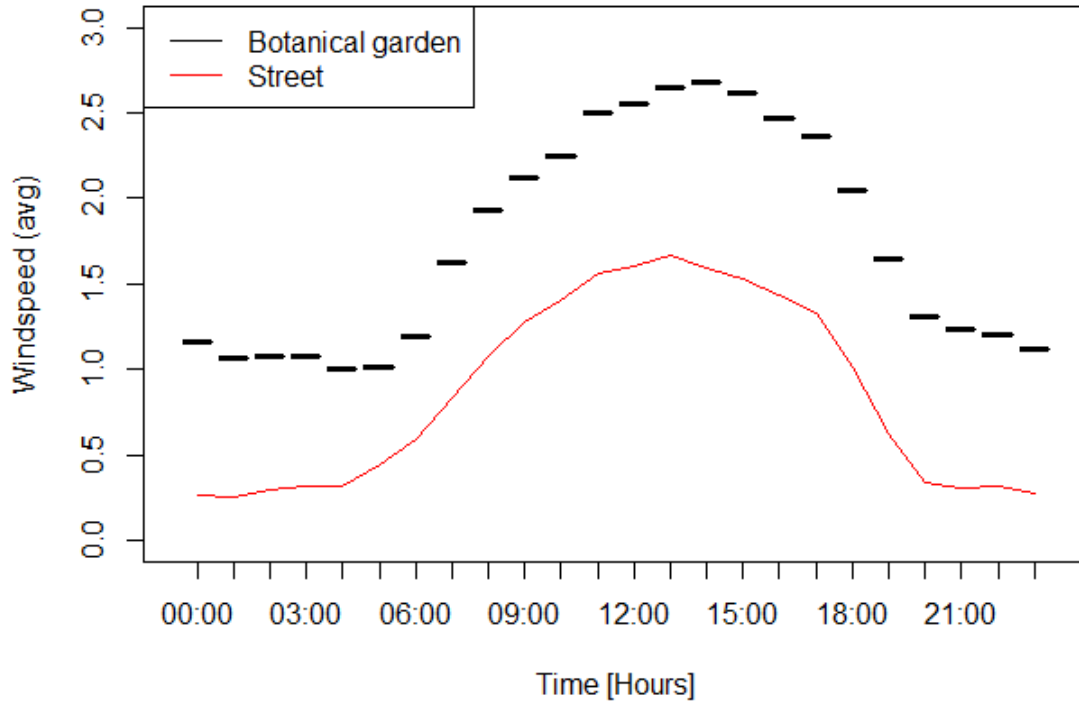


Figure 29: Averaged diurnal variations of windspeed [m/sec] measured in the botanical garden (rural area,  $n=1$ ) and above the street ( $n=2$ ) during the study period of 61 days.

The diurnal wind patterns in the botanical garden and above the street were following the same trend: at both sites windspeed was lowest during the night from 20:00 to 6:00. During the day the windspeed increased at both sites and was greatest in the afternoon at 13:00 above the street and at 14:00 in the botanical garden. Nevertheless, there were differences between the windspeed at the botanical garden and above the street as the windspeed in the botanical garden was at any time greater than at the urban site. Maximum differences were found in the afternoon at 14:00 and 15:00, when windspeed was on average 1.56 m/sec above the street and 2.65 m/sec at the rural site (difference of 1.09 m/sec). The minimum difference was documented at 5:00 with 0.56 m/sec difference (0.45 m/sec above the street, 1.01 m/sec at the rural site). The equity of central tendencies was checked by using the Wilcoxon signed-rank test. The P-value was  $1.937 \times 10^{-5}$  and therefore  $< 0.05$ . The null hypothesis was rejected. Windspeed values in the botanical garden and above the street were significantly different.

## 4.2.2 Effects of urban trees

### 4.2.2.1 Cooling effect of urban trees

The cooling effect of urban trees was calculated as difference between temperature measurements at all selected trees (position D, n=12) and the temperature measured above the street (n=1).

The cooling effect is particularly important on hot and sunny days. 24.06.2016 was chosen as an exemplary day, on which the cooling effect was analyzed. In the figure below, the cooling effect of urban trees (n=12) was drawn against air temperature measured above the street (n=1), surface temperature of the urban environment measured as object temperature via infrared (n=24) and windspeed measured above the street (n=1).

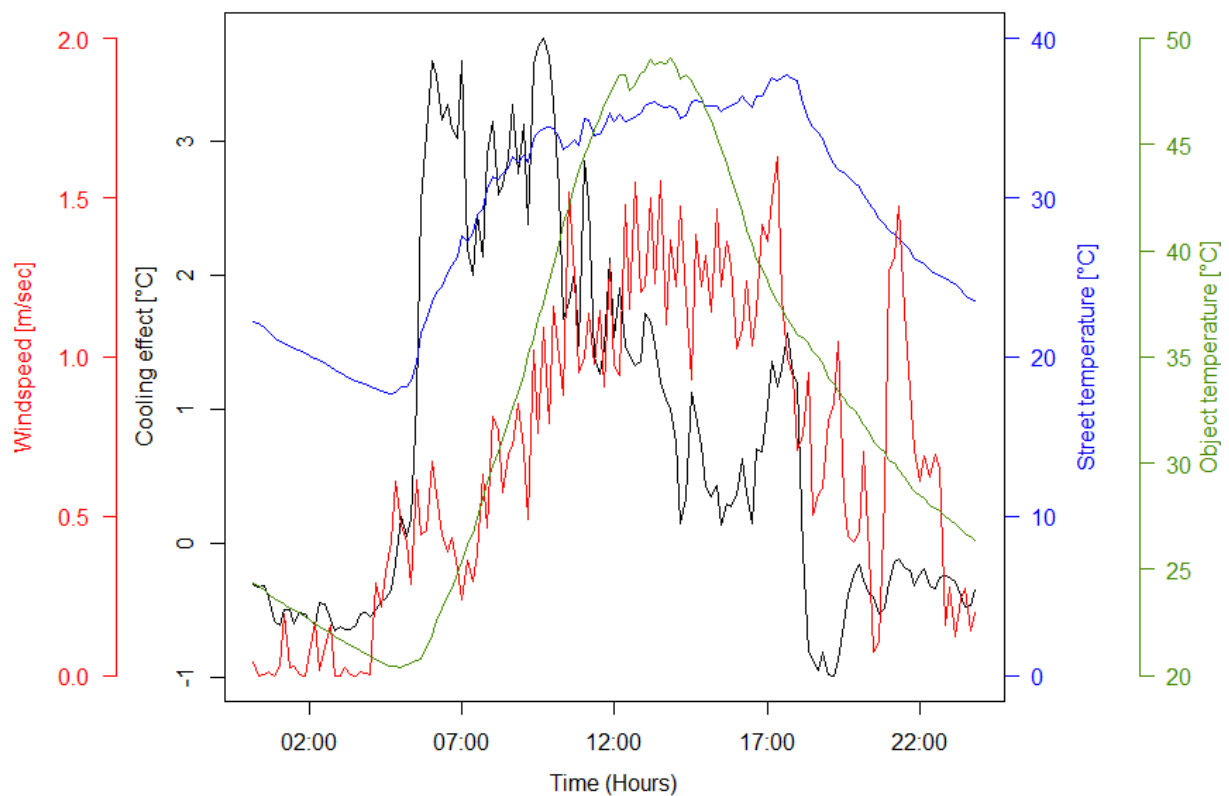


Figure 30: Averaged diurnal variations of the cooling effect of urban trees (black, n=12), street temperature (=air temperature above the street, blue, n=1), object temperature (=surface temperature of the urban environment, green, n=24) and windspeed (measured above the street, red, n=1) on a hot and sunny day.

Table 9: Average cooling effect on a hot and sunny day.

Average cooling effect [°C]	During the day (5:10 – 19:00) [°C]	During the night (19:10 - 5:00) [°C]
0.77	1.76	-0.45

Air temperature above the street (see figure 32, blue line) reached 37.7 °C in the late afternoon at 17:40 and was at its lowest at 4:40 with 17.7 °C. The cooling effect (black line) fluctuated a lot as well as windspeed (red line). The greatest cooling effect was found in the morning between 6:00 and 11:00 with the highest values around 3.8 °C. Around 14:00, when the surface temperature (green line) was at its maximum of 49.1 °C, the air temperature was 35.7 °C and windspeed was about 1.25 m/sec, while the cooling effect of the trees decreased and fluctuated between 0°C and 1,5 °C. At 17:20, when the windspeed was at its maximum of 1.6 m/sec, but also the object temperature had already decreased to 37.6 °C, street temperature as well as the cooling effect of the selected trees increased again until at 19:10 it dropped to its minimum of -0.98 °C. During the night from 19:00 to 5:00 the negative cooling effect of urban trees remained.

Results of the Wilcoxon-Mann-Whitney rank sum test: Street temperature was tested against cooling effect: The P-value was  $2.2 \cdot 10^{-16}$  (W=20449) and therefore  $< 0.05$ .  $H_0$  was rejected for  $\alpha = 0.05$  and difference was statistically significant. Street temperature was also tested against object temperature: The P-value was 0.001454 (W=7998) and therefore  $< 0.05$ .  $H_0$  was rejected for  $\alpha = 0.05$  and difference was statistically significant. Furthermore, Street temperature was tested against windspeed: The P-value was  $2.2 \cdot 10^{-16}$  (W=20449) and therefore  $< 0.05$ .  $H_0$  was rejected for  $\alpha = 0.05$  and difference was deemed statistically significant.

During the study period devices were put on the selected trees at three different heights. Details can be seen in 3.1.3. In the figure below, the averaged temperature at different heights was compared to the temperature measured above the street. The averaged maximum temperature above the street was 24.2°C.

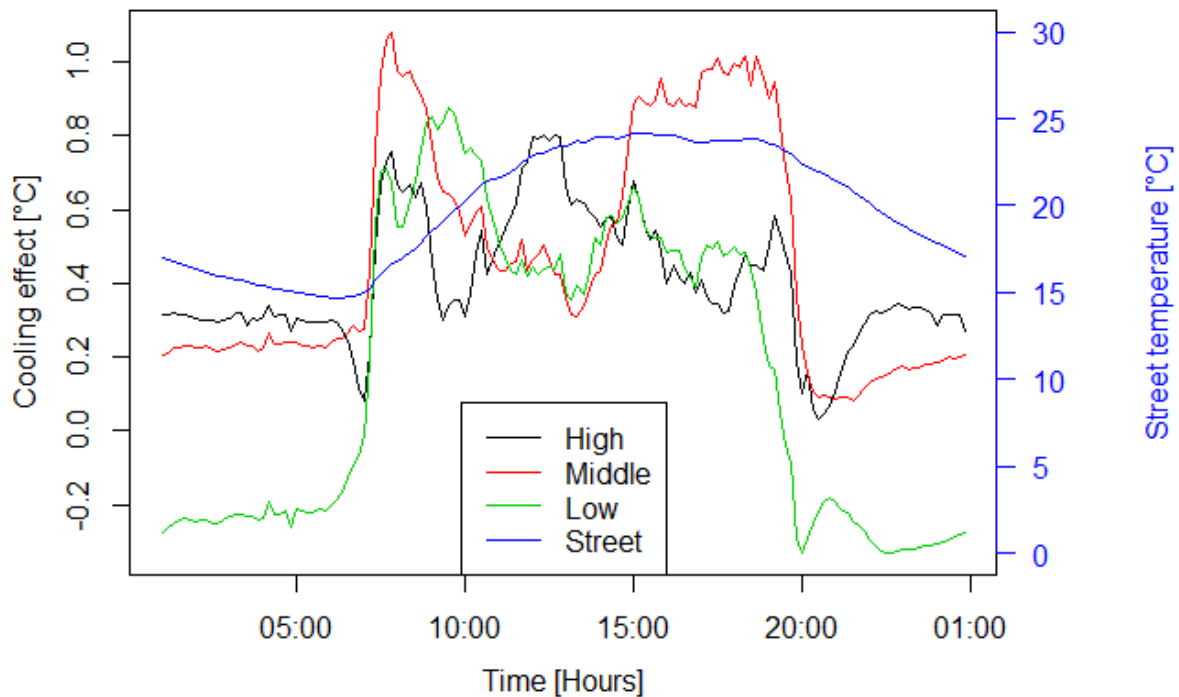


Figure 31: Temperature measured at three different heights (high: n=12, middle: n=12, low: n=12) in the tree canopies was compared to temperature measured above the street (n=1).

Temperature at the trees as well as above the street were lowest in the early morning at 5:20 with an average temperature of 14.7 °C above the street, 14.4 °C at the highest and at the middle position, and 14.9 °C at the lowest position. In the course of the morning, the cooling effect increased at all positions. The greatest averaged cooling effect of the day was documented at the middle position with 0.47 °C. Also, at 7:30 in the morning, the temperature difference already exceeded 1 °C. The maximum averaged temperature was already reached at 13:00 with 23.5 °C at the middle position and was decreasing afterwards. The cooling effect was lowest at 12:20 with 0.31 °C. Devices at the highest and at the lowest position documented very similar maximum temperatures at 14:30 (23.6 : 23.7 °C). The cooling effect diverged, as it was decreasing at the lowest position to 0.31 °C at 12:20, while it was 0.63 °C at the same time at the highest position. In the evening, the averaged temperature at all measuring groups was almost at 24 °C, with the highest temperatures above the street and at the lowest position. At the middle position another peak of the cooling effect was observed at

16:30 with 0.51 °C. At 20:00 the temperature above the street decreased slowly and the cooling effect in all heights was dropping quickly. Particularly the cooling effect at the lowest position dropped to negative values and was not rising until sunrise on the next morning.

The equity of central tendencies was tested with the Wilcoxon signed-rank test. Data taken at the highest position (A) was tested against data taken at the middle position (B): p-value was 0.04891 (V=6208). Data taken at the highest position (A) was also tested against data taken at the lowest position (C): The P-value was  $2.709 \cdot 10^{-13}$  (V=1555). Data taken at the middle position (B) was tested against data taken at the lowest position (C): The P-value was  $<2.2 \cdot 10^{-16}$  (V=577). Temperature values taken above the street were tested against middle position (B): The P-value was  $<2.2 \cdot 10^{-16}$  (V=10440). Therefore, all p-values were  $< 0.05$ . Null hypothesis was rejected in all cases and datasets were deemed significantly different.

The averaged cooling effect over the study period of subgroup 1 was analyzed for each individual. Results can be seen in the appendix E.

The cooling effect of urban trees is mainly due to shading and evapotranspiration. But also aerodynamics can be altered due to trees. Therefore, transpiration, shading and aerodynamics were analyzed in detail in the next sections. But the cooling effect differs depending on tree species and age of the tree. In 4.2.3 and 4.2.4 species and age differences were analyzed.

#### 4.2.2.2 Transpiration

Relative air humidity was observed at all positions (see 3.1.3) during the study period. The figure below illustrates data taken in tree crowns at position D in comparison to relative air humidity measured above the street and incoming solar radiation:

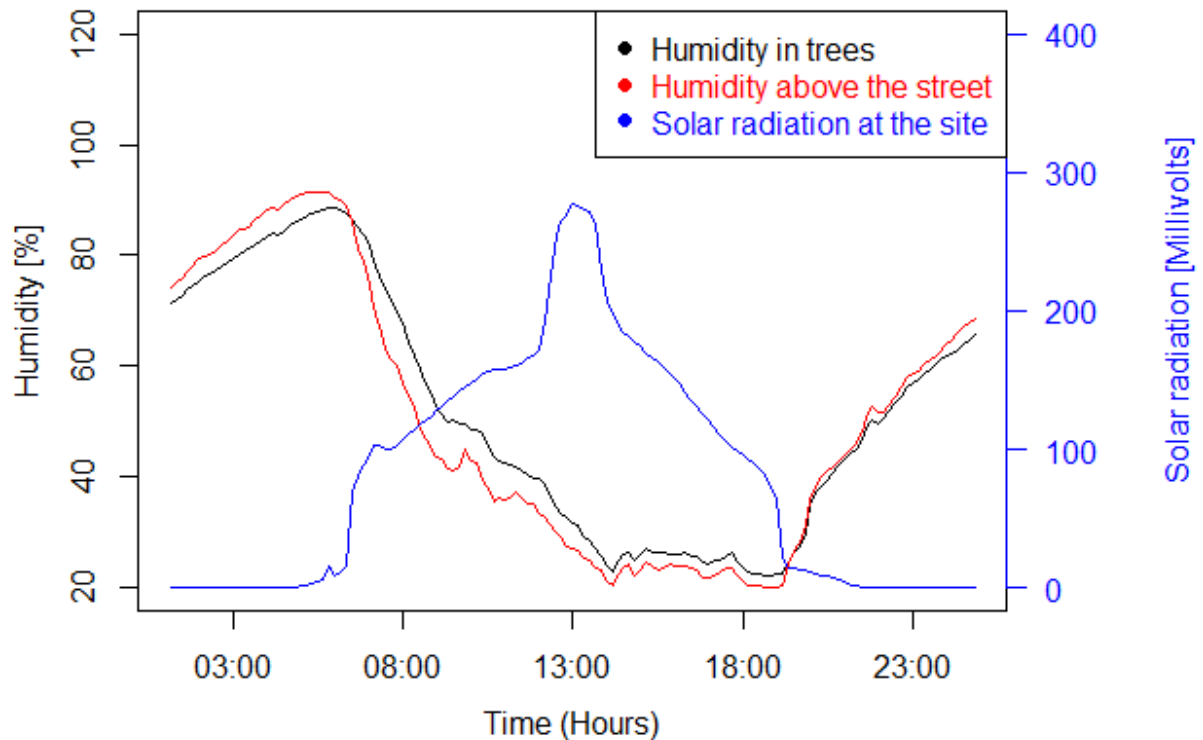


Figure 32: Averaged diurnal variations of the relative air humidity measured in urban trees (n=12) and above the street (n=1) in comparison to incoming solar radiation (n=1) on a hot and sunny day (24.06.2016).

Over the day humidity pattern developed inversely to incoming solar radiation: with rising solar radiation in the morning, humidity dropped. After some delay humidity levels always reacted to any changes in solar radiation levels. The lowest relative air humidity levels were measured after 14:00 (about 20 %) while the greatest solar radiation values (280 mV) were measured at 13:00. The greatest humidity was documented in the morning at 5:30, when solar radiation was low. During the day (7:00 – 20:00) the relative air humidity above the street was always lower than in the tree canopy, but higher during the night (20:00 – 7:00). Particularly above the street some fluctuations were observed in the morning around 10:00, when temperature increased very quickly. The relative air humidity increased after solar radiation decreased to almost zero after sunset (19:00). Any differences between results found above the street and in the tree canopies were rarely greater than 5%.

Results of the Wilcoxon signed-rank test: Humidity values measured in tree canopies were tested against values tested above the street. The P-value was 0.001148 ( $V=6762$ ) and therefore  $< 0.05$ . Null hypothesis was rejected datasets were deemed significantly different.

In the figure below, relative air humidity, which was measured at position A (top of the crown) and D (bottom of the crown) during the study period was compared to the humidity measured above the street. Details about the positions can be seen in section 3.1.3.

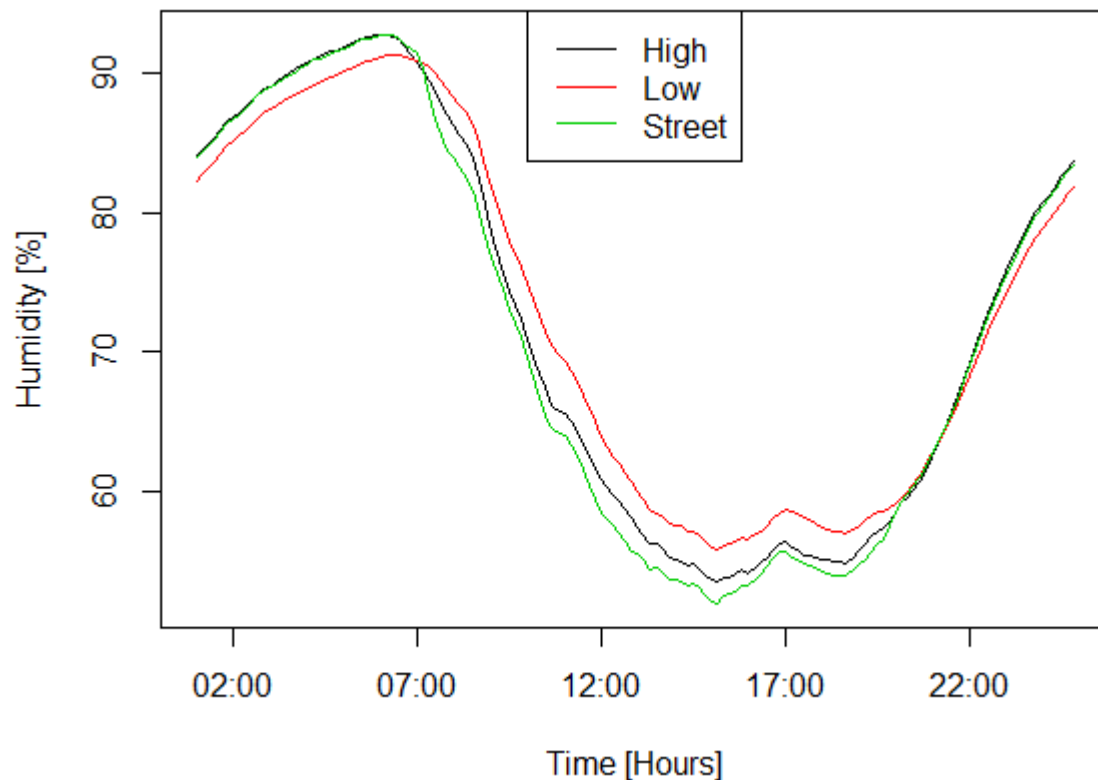


Figure 33: Averaged relative air humidity measured at position A ( $n=12$ ) and D ( $n=12$ ) compared to relative air humidity [%] measured above the street ( $n=1$ ).

Generally, all measurements showed the highest values in the early morning before sunrise and the lowest ones in the afternoon as already described in the previous figures. The values measured at the top of the trees and above the street were very similar particularly in the evening and during the night. The greatest differences were observed before the afternoon when the air humidity above the street was slightly lower. During the night the sensor at position D documented humidity values, which were less than 2 %. During the day, relative air humidity at position D was greater at any time with maximum differences of 4.3 %. A slight rise at 17:00 was observed.

The equity of central tendencies was tested with the Wilcoxon signed-rank test. Data taken at position A was tested against data taken at position D: The P-value was  $3.686 \times 10^{-7}$  ( $V=2670$ ). Data taken at position A was tested against data taken above the street: The P-value was  $< 2.2 \times 10^{-16}$  ( $V=9923$ ). Data taken at position D was tested against data taken above the street: The P-value was  $8.686 \times 10^{-9}$  ( $V=8106$ ). Therefore, P-values were  $< 0.05$  in all cases and datasets were deemed significantly different.

**4.2.2.3 Ground temperature**

To observe the cooling effect resulting from shading, infrared-diodes measured surface temperature in the southern and northern direction of the tree (position C & E, cf. section 3.1.3).

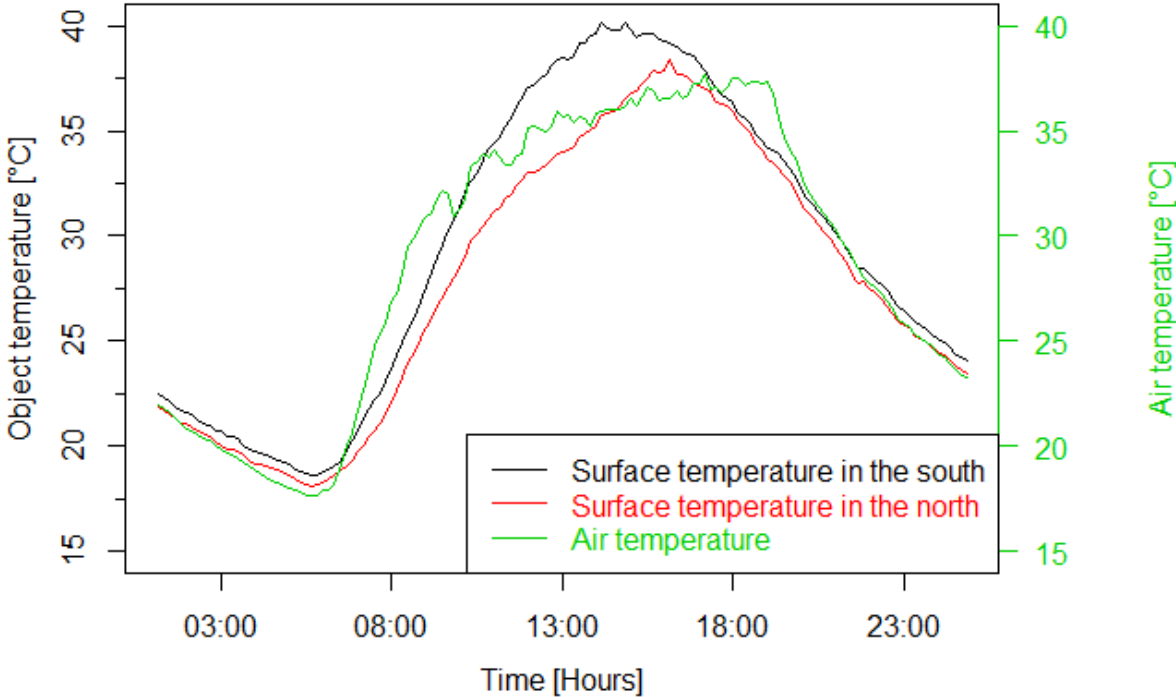


Figure 34: Averaged surface temperature [°C] measured in the south (n=12) and the north (n=12) of urban trees and air temperature [°C] (n=1) on a hot and sunny day.

Table 10: Averaged surface temperature maxima and minima for the 24.06.2016 in the southern (n=12) and northern (n=12) direction with underlying air temperature (n=1).

		Maximum	Minimum
Surface temperature [°C]	South	40.2	18.6
	North	38.3	18.1
Air temperature [°C]		37.5	17.6

In figure 37 surface temperatures in the south and in the north of all selected trees were averaged and plotted against air temperature on the hot and sunny day of the 24.06.2016. During the night, from 20:30 to 7:30, temperatures were very similar in all three datasets. The lowest surface temperature was found at 05:40 with 18.6 °C in the south and 18.1 °C in the north, when air temperature was also at its minimum of 17.6 °C. The surface temperature in the south of the tree exceeded the air temperature already at 10:30, while the shaded ground in the north of the tree stayed cooler until 14:30. The air temperature was highest at 17:00 with 37.5 °C before it dropped quickly. The surface temperature in the south of the tree was at its maximum at 14:50 with 40.2 °C, while the highest temperature in the north of the tree was measured more than two hours later at 17:00 with 38.3 °C. After 20:30 in the evening decreasing temperatures were very similar in all three datasets.

Results of the Wilcoxon signed-rank test: The P-value was  $2.2 \cdot 10^{-16}$  ( $V=10296$ ) and therefore  $< 0.05$ .  $H_0$  was rejected for  $\alpha = 0.05$  and the difference was statistically significant.

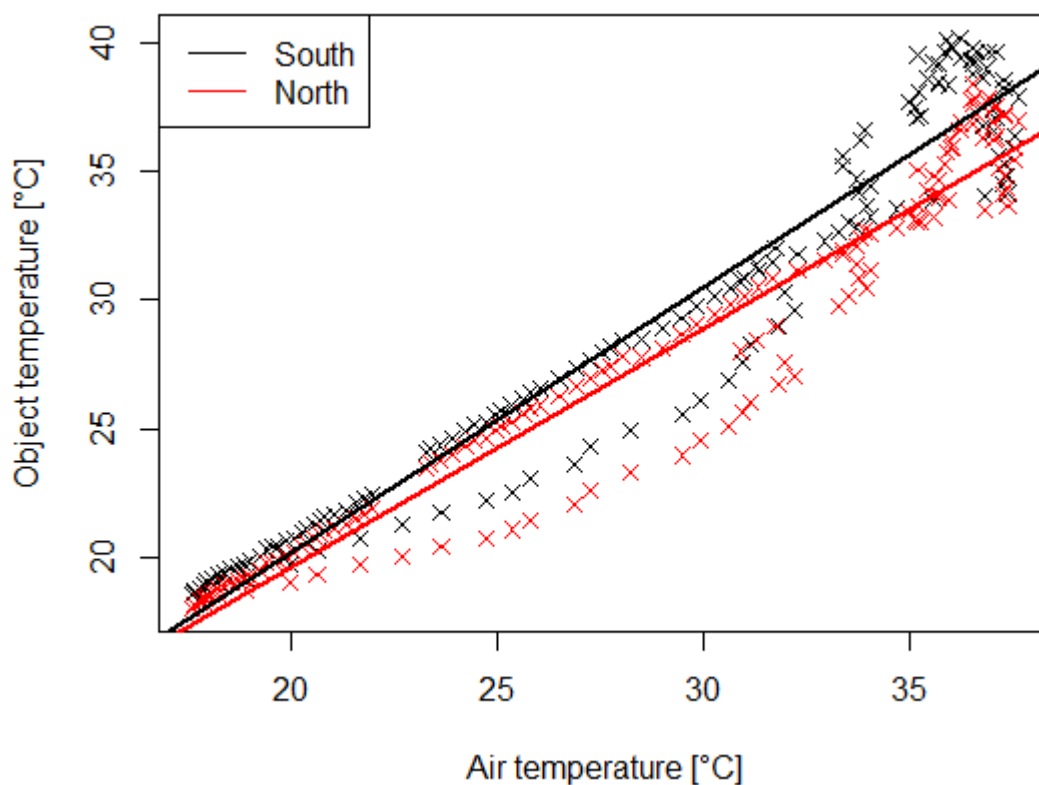


Figure 35: Averaged surface temperature [°C] measured in the south ( $n=12$ ) and the north ( $n=12$ ) of the selected urban trees as a function of air temperature [°C] ( $n=1$ ) on a hot and sunny day.

Figure 38 shows averaged surface temperatures in the south and the north of all selected trees as a function of air temperature on the hot and sunny day of the 24.06.2016. It was observed, that surfaces in the northern direction of the tree heated up less with rising air temperatures than surfaces in the southern direction of the tree.

**4.2.2.4 Aerodynamics**

Two trees of subgroup 1 and two trees of subgroup 2 were equipped with cup anemometers at position C (see 3.1.3), which measured windspeed in meter per second during the study period of 61 days. In the figure below, averaged diurnal variation of windspeed measured in trees was drawn against windspeed measured above the street.

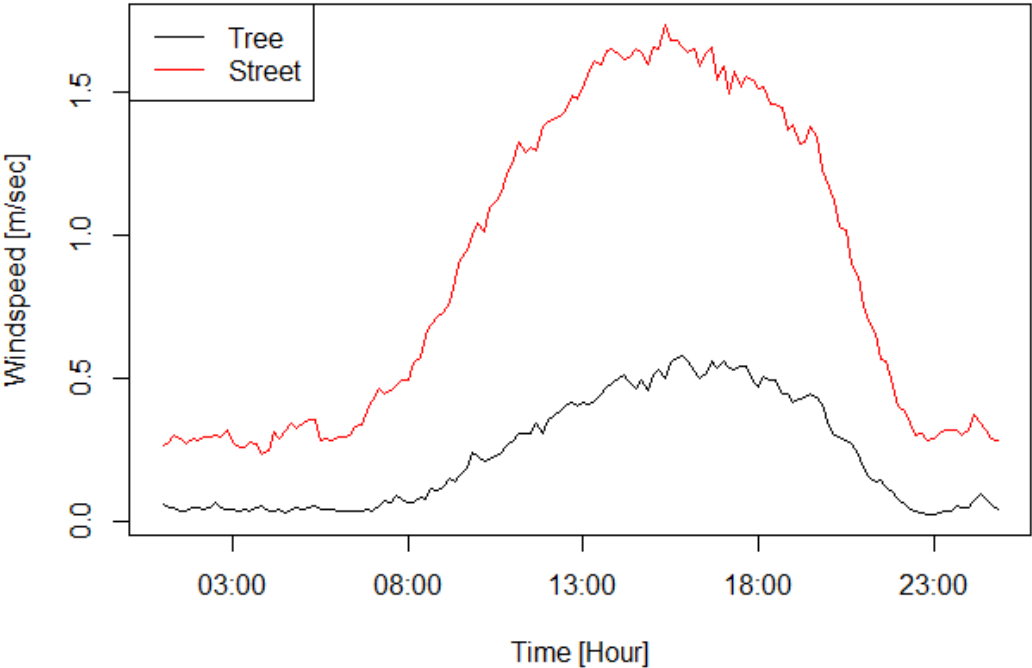


Figure 36: Averaged diurnal variations of windspeed [m/sec] measured at trees (n=4) and above the street (n=1) during the study period.

The windspeed pattern were following the general trend which was already observed in section 4.2.1.5: windspeed was lowest during the night and greatest during the day. Windspeed was at any time greater above the street than at the trees. Differences were greatest at 16:10 when averaged windspeed over the study period was 0.52 m/sec in the trees and 1.65 m/sec

above the street. The smallest differences were measured at 03:10 when windspeed above the street was only 0.23 m/sec greater than in the trees, where it was almost zero.

Results of the Wilcoxon signed-rank test: Windspeed measured in trees was tested against windspeed measured above the street. The P-value was  $2.2 \times 10^{-16}$  ( $V=0$ ) and therefore  $< 0.05$ . Null hypothesis was rejected and datasets were deemed significantly different.

#### 4.2.3 Species differences

Devices were put in *T. cordata* as well as in *R. pseudoacacia* of subgroup 1 to observe the cooling effect differences of the species. As can be seen in the following boxplot, cooling effect was different for each individual, even though differences were not significant:

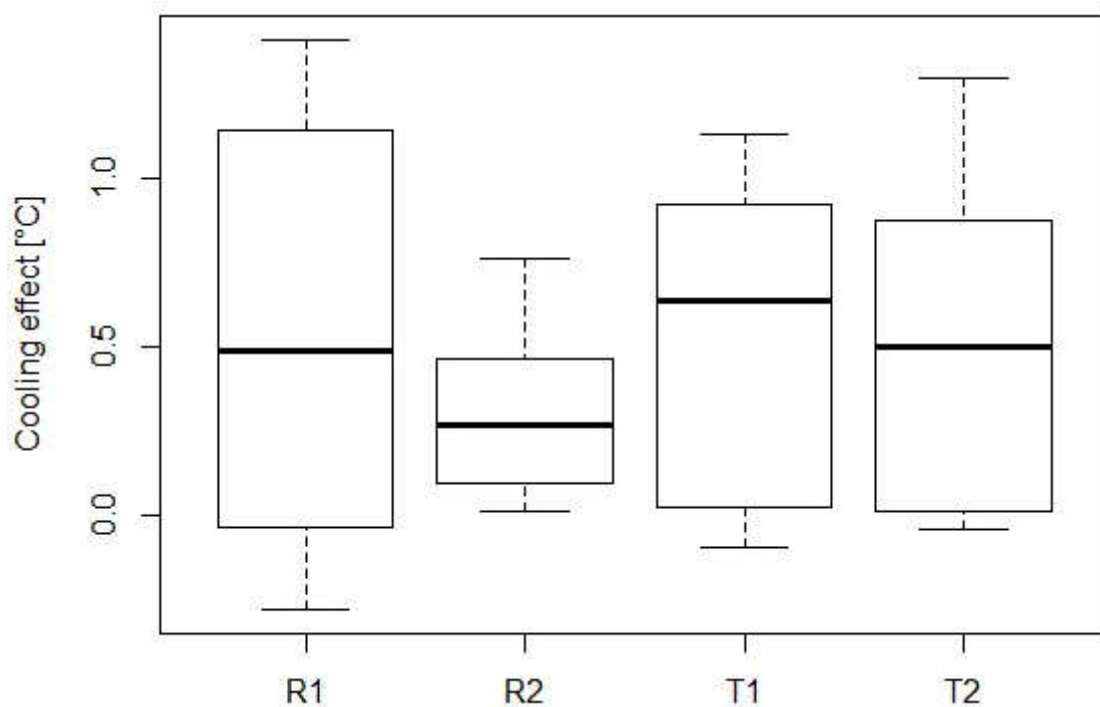


Figure 37: Cooling effect of R1, R2, T1 & T2 (all  $n=5$ ) over the study period of 61 days.

The cooling effect differed between the individuals. Greatest variations were observed at R1 with the mean 50% laying between 0 °C and 1.13 °C. Median was 0.5 °C. R2 on the other side cooled less, but fluctuations were also smaller. The mean 50% of the data laid between 0.1 °C and 0.48 °C. Median was 0.25°C. Cooling effect of both individuals of *T. cordata* was greater

than cooling effect of *R. pseudoacacia*. T1 and T2 showed similar results: Both dataset's mean 50% laid between 0 °C and almost 1°C. Median was 0.6 °C for T1 and 0.5 °C for T2.

If the cooling effect of T1, T2, R1 and R2 differed significantly was checked by Wilcoxon-Mann-Whitney rank sum test. Data of R1 was tested against R2: The P-value was 0.581 (W=10758). Data of R1 was tested against data of T1: The P-value was 0.666 (W=10063). Data of R2 was tested against T2: The P-value was 0.6527 (W=10050). Data of T1 was tested against T2: The P-value was 0.9121 (W=10446). Therefore, P was > 0.05 in all cases and differences were statistically not significant.

Nevertheless, averaged cooling effect of the whole period was plotted against temperature measured above the street:

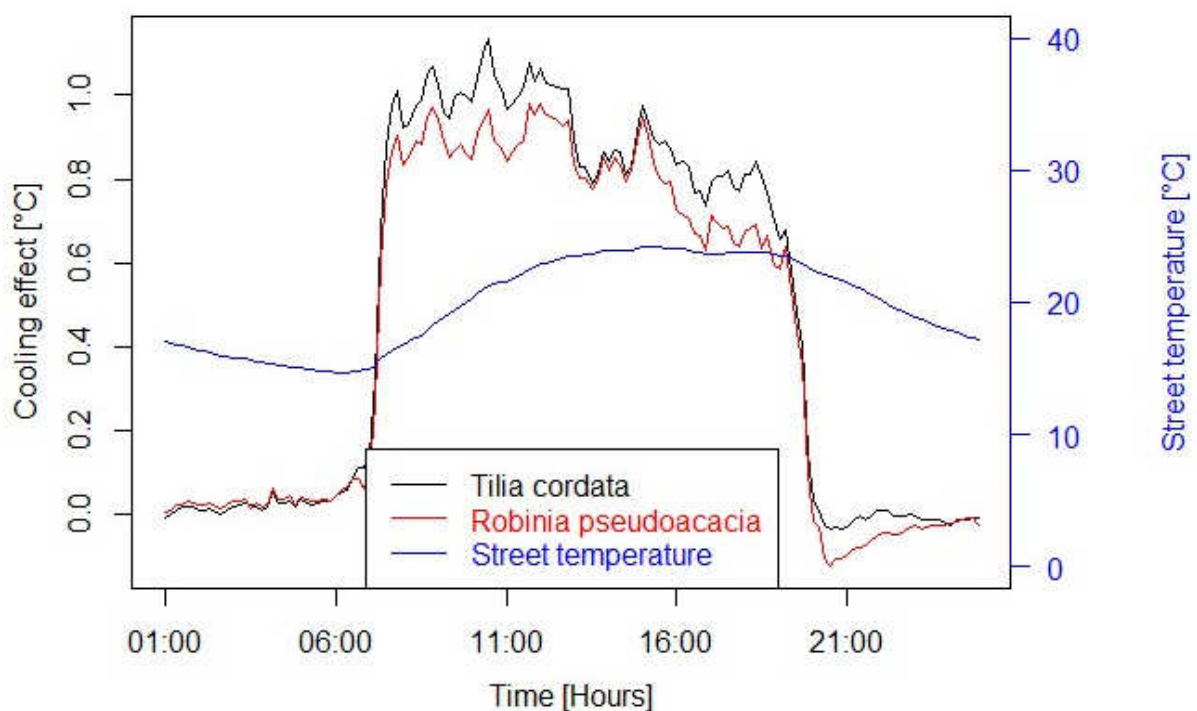


Figure 38: Averaged cooling effect of the whole period of both species (n=10 each) and temperature measured above the street (n=1).

Both species did not provide any substantial cooling effect during the night (20:30 – 6:30). Particularly *R. pseudoacacia* showed a negative cooling effect in the evening after sunset. Temperature in the canopies was 0.6 – 1.1 °C cooler during the day. Cooling effect of *Tilia cordata* was slightly greater at any time with mean cooling effect of 0.47 °C (*R. pseudoacacia*: 0.42 °C) and maximum cooling effect of 1.14 °C (*R. pseudoacacia*: 0.98 °C). Furthermore, both

species showed greatest effect before afternoon, when averaged temperature above the street did not yet exceed its maximum of 24.1 °C. Fluctuations were greatest during the day.

Table 11: Cooling effect minima, mean and maxima of *T. cordata* and *R. pseudoacacia* averaged over the whole period.

Cooling effect [°C]	<i>Tilia cordata</i>	<i>Robinia pseudoacacia</i>
Minimum	-0.04	-0.12
Mean	0.47	0.42
Maximum	1.14	0.98

If the cooling effect values of *T. cordata* and *R. pseudoacacia* differed significantly was checked by Wilcoxon-Mann-Whitney rank sum test. The P-value was 0.24 (W=9546), therefore  $> 0.05$ .  $H_0$  was not rejected for  $\alpha = 0.05$  and difference was statistically not significant.

In the previous figure greatest cooling effect was observed during the day. To analyze this part more in detail, averaged cooling effect of both species from 10:00 to 18:00 over the whole period was plotted against air temperature measured above the street and can be seen in appendix F.

As the cooling effect is most important at very hot summer days, June 24<sup>th</sup> was chosen as an exemplary hot and cloud free day. Average temperature measured at the botanical garden was 24.7°C, street control at the site recorded maximum temperature at 18:40 at 37,7°C:

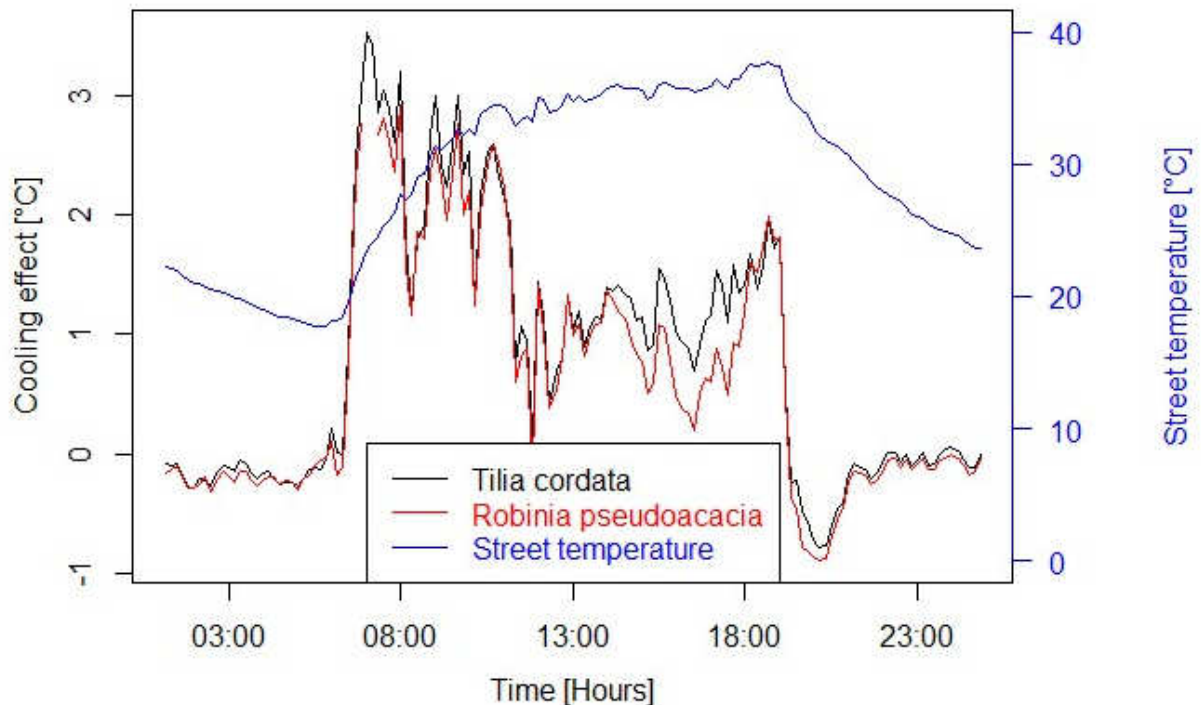


Figure 39: Averaged cooling effect of the tree species *T. cordata* (n=10) and *R. pseudoacacia* (n=10) and street temperature (n=1) at an exemplary hot and cloud free day.

In figure 43 the cooling effect of the tree species *T. cordata* and *R. pseudoacacia* can be seen in comparison to temperature measurements above the street. Both species showed more or less the same cooling pattern, but *T. cordata* had again a slightly greater cooling effect during the day than *R. pseudoacacia*. During the night, the air in the trees canopy stayed slightly warmer than the air above the street. Greatest cooling effect was observed in the morning at around 7:00, when temperature above the street was below 30°C. At around 14:30, when street temperature exceeded temperatures of 36°C, cooling effect decreased and differences between the two species became more distinct. When temperature fell between 19:00 and 20:00, cooling effect became negative until the next morning. Particularly at 20:30 the trees were almost 1°C warmer than the air around the street control. Results of the Wilcoxon-Mann-Whitney rank sum test: The P-value was 0.6375 (W=10554) and therefore > 0.05.  $H_0$  was not rejected for  $\alpha = 0.05$  and difference was deemed statistically not significant.

Again averaged cooling effect of both species from 10:00 to 18:00 was analyzed in detail in the appendix G.

Furthermore, relative air humidity was documented in both tree species as well as above the street over whole period. The humidity differences of each species in contrast to circumstances above the street were plotted with air humidity itself:

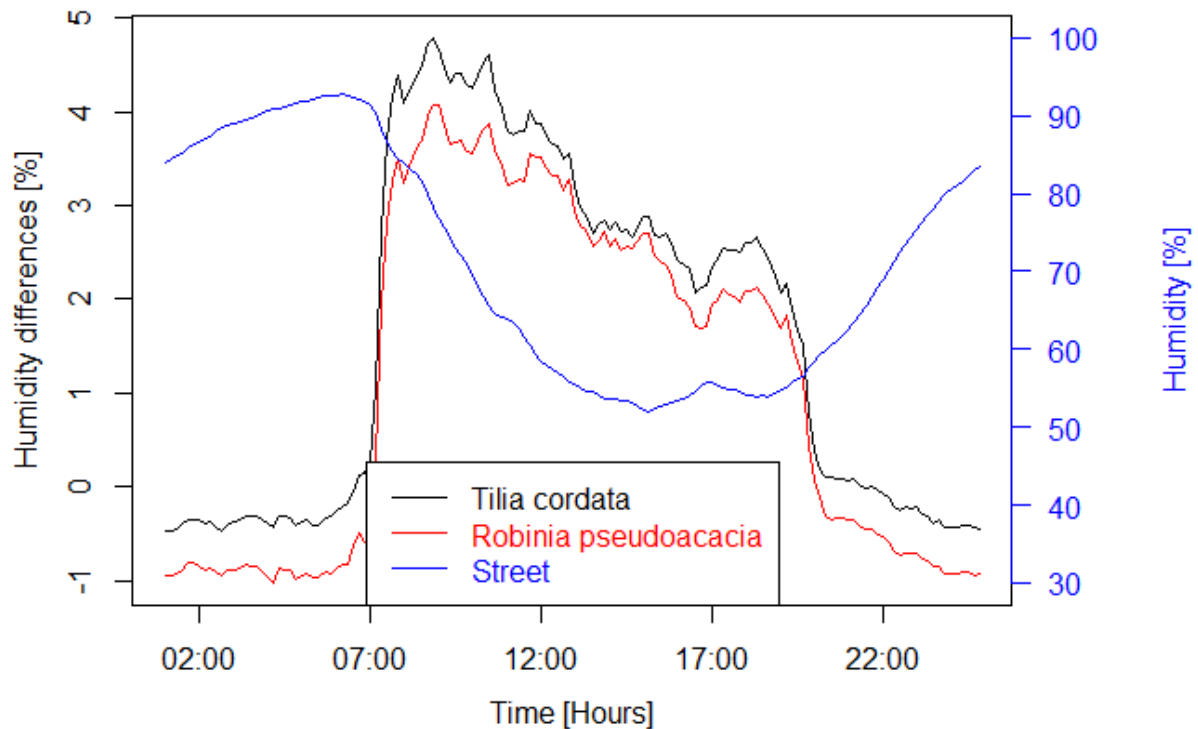


Figure 40: Relative air humidity differences in the canopy of each species (n=10 each) and above the street (n=1) averaged over the whole period of 61 days.

Averaged relative air humidity was increasing until 5:10 in the morning with a maximum value of 92.2 % and was decreasing afterwards until it reached lowest values at 14:00 with 52.1 %. Data measured in *T. cordata* were almost constantly 0.5% greater than data from *R. pseudoacacia*. Humidity values in the canopies were lower during the night after 20:00 until 7:00 than above the street. When relative air humidity was decreasing above the street at 7:00, air in canopies of both species stayed 3-5% more humid. Both species showed maximum increased humidity during the morning at 9:30 until it steadily decreased. Also during the day, humidity measured in the canopies of *T. cordata* was greater than in *R. pseudoacacia*: on average mean humidity difference was +1.6 % in *T. cordata* and +1.1 % in *R. pseudoacacia*. Maximum differences measured were 4.8 % for *T. cordata* and 4.1 % for *R. pseudoacacia*. Fluctuations were particularly strong during the day but were never greater than 1 %.

Results of the Wilcoxon-Mann-Whitney rank sum test: The P-value was  $7.47 \times 10^{-5}$  ( $W=13167$ ) and therefore  $< 0.05$ .  $H_0$  was rejected for  $\alpha = 0.05$  and difference was deemed statistically significant.

Measurements via photodiode enabled comparisons of incoming solar radiation above the street with solar radiation in the canopy of each species. To see species differences in detail, solar radiation measured in canopies of each species was subtracted from solar radiation measured above the street.

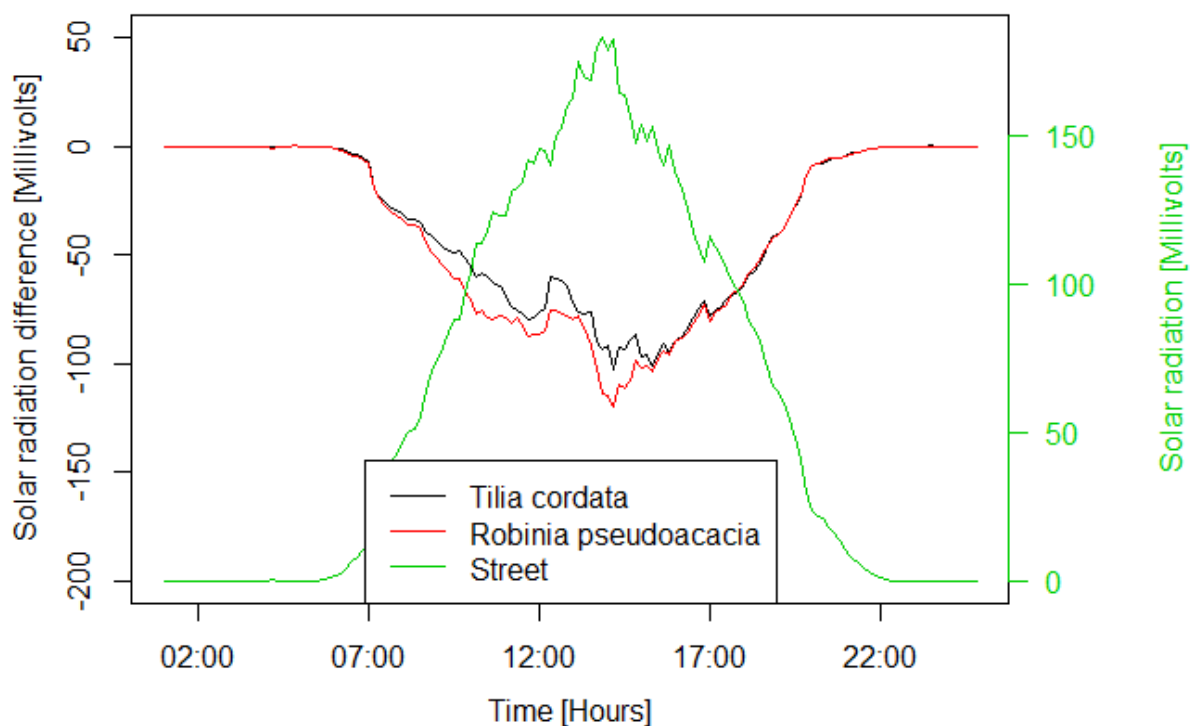


Figure 41: Comparison of incoming solar radiation above the street ( $n=1$ ) and solar radiation in the tree canopy of each species ( $n=10$  each).

Solar radiation was not present during the night, neither above the street nor in tree crowns. During the day solar radiation was rising above the street to a maximum value of 183 mV. With rising radiation above the street, in canopies differences were increasing. Maximum difference was -120 mV at 14:00. In the morning until 14:00, solar radiation measured in tree crowns of *R. pseudoacacia* was slightly lower. After solar radiation peak has been overcome, the radiation differences measured in canopies decreased. In that period, values of both species were very similar.

Results of the Wilcoxon-Mann-Whitney rank sum test: P-value was 0.1442 (W=9336) and therefore  $< 0.05$ .  $H_0$  was rejected for  $\alpha = 0.05$  and difference was statistically significant.

#### 4.2.4 Age differences

Cooling effect might change with the size and the age of the trees. With the aid of a process-based model, Cailliau (2016) determined the age and the crown volume of all selected trees. Contradictory to assumptions, age and crown volume was not always correlating, order was therefore changing. Results can be seen below, sorted by age or crown volume:

Table 12: Tree's age (left) and crown volume (right), modelled by Cailliau (2016).

Tree	Age	Tree	Crown volume [m <sup>3</sup> ]
T1	53.30	T1	486.4
T2	43.80	T6	419.6
T9	39.80	T9	407.9
T6	39.20	T7	385.3
T7	34.40	T2	294
T8	33.30	T8	179.9
T10	24.40	T10	74.5
T5	17.20	T5	58.5
T4	16.10	T4	47
T3	15.40	T3	27
Mean:	31.69		

To get a better insight into the correlation, averaged cooling effect of *T. cordata* of the whole period of 61 days was analyzed as a function of age using linear regression. Data of all five devices of all selected *T. cordata* (n=10) were considered:

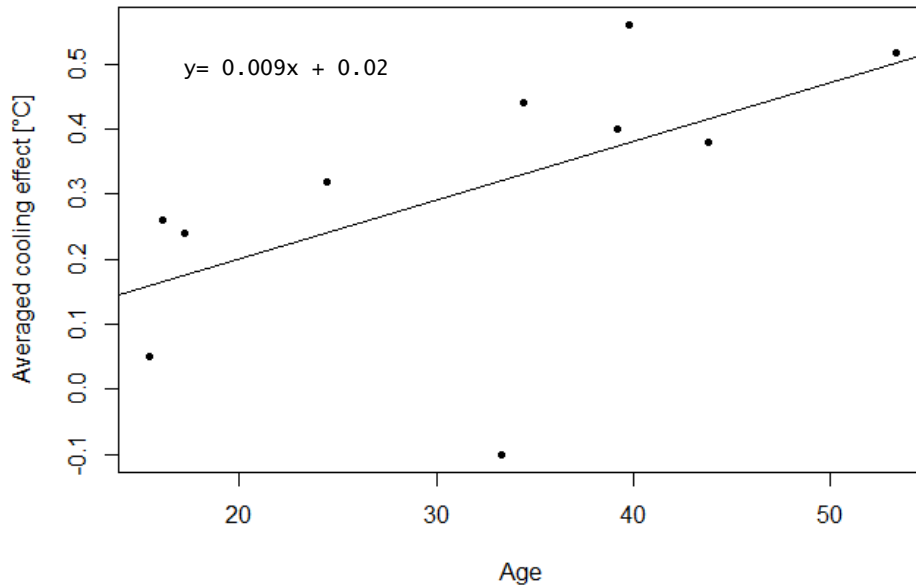


Figure 42: Averaged cooling effect of *T. cordata* (n=10) as a function of age.

A tendency of increased cooling effect with greater age was observed. While cooling effect of a 20-year-old tree was 0.2 °C, a 50-year-old tree was cooling on average 0.48 °C. Because experimental group was small, results have to be understood as a tendency rather than definite numbers.

In the figure below, averaged cooling effect [°C] was analyzed as a function of crown volume [m<sup>3</sup>] using linear regression:

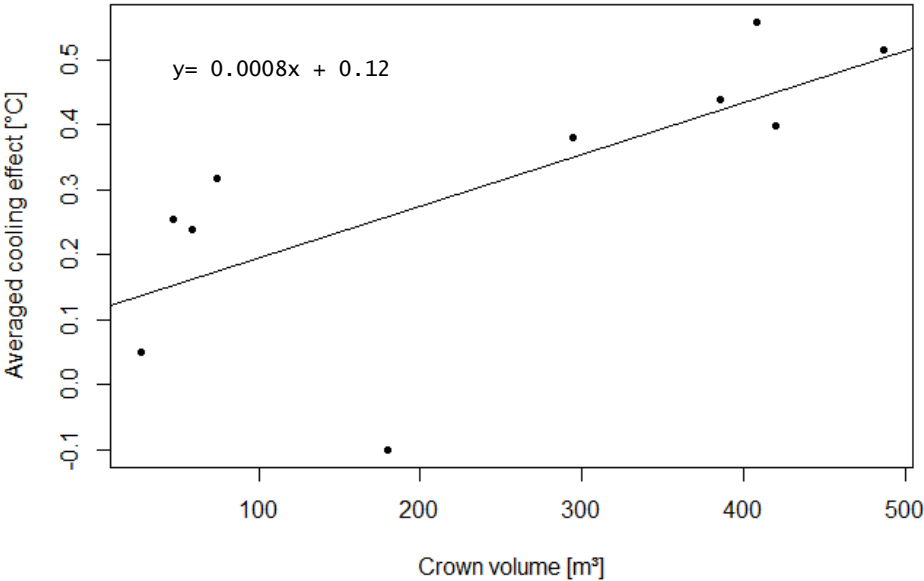


Figure 43: Averaged cooling effect of all selected *T. cordata* (n=10) as a function of crown volume.

Averaged cooling effect of *T. cordata* over the study period was rising with greater crown volume. While a tree with a crown volume of 100 m<sup>3</sup> was cooling on average by 0.2 °C, a tree with a crown volume of 500 m<sup>3</sup>, was cooling on average by 0.5 °C.

Transpiration and shading were supposed to be the main factors leading to the cooling effect of trees. Therefore, humidity differences [%] and radiation differences [mV] of tree canopies of *T. cordata* to conditions above the street were drawn against age and crown volume [m<sup>3</sup>] using linear regression:

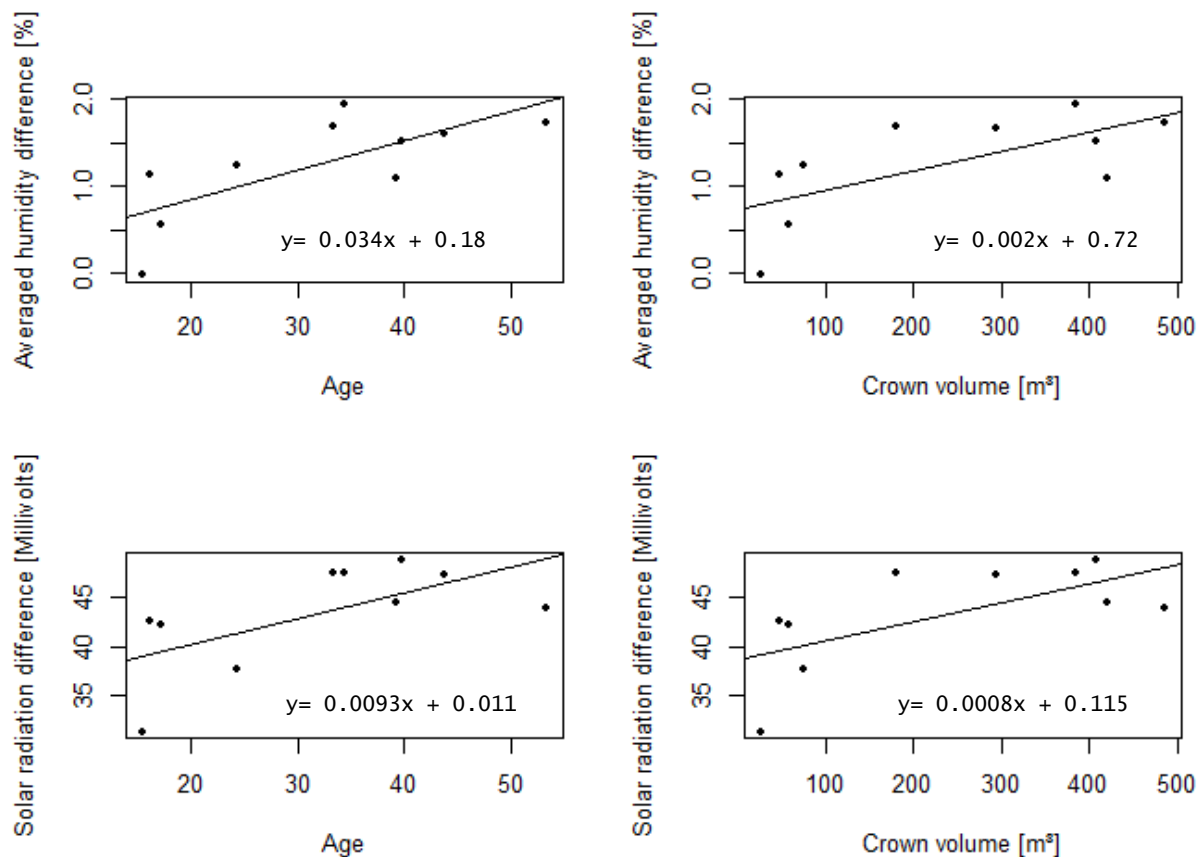


Figure 44: Top left: Averaged humidity differences as a function of age. Top right: Averaged humidity differences as a function of crown volume. Bottom left: Averaged solar radiation differences as a function of age. Bottom right: Averaged solar radiation differences as a function of crown volume. All selected *T. cordata* were considered (n=10).

In all cases, increased differences were observed with greater age and increased crown volume. In the canopy of a 20-year-old *T. cordata*, relative air humidity was 0.9 % greater than above the street, while it was 1.8 % greater in a 50-year-old tree. Air in a tree with a crown volume of 100 m<sup>3</sup> was 0.9 % more humid, while values were increased by on average 1.9 % in a tree crown of 500 m<sup>3</sup>. In case of solar radiation, the same pattern was observed: solar radiation in the canopy of a 20-year-old-tree was decreased by 40 mV, while it was decreased by 48 mV in case of a 50-year-old tree. A smaller crown with a volume of 100 m<sup>3</sup> was able to decrease solar radiation by 41 mV, while it was again decreased by 48 mV in case of a tree with a canopy of 500 m<sup>3</sup>.

## **5. Discussion**

### **5.1 Underlying conditions**

The study period was 61 days in June and July. Environmental conditions varied considerably over the course of the study. Daily averages were ranging from 0 – 22.5 mm precipitation and 6.5 – 24.5 °C air temperature at the rural site.

#### **5.1.1 Climatic conditions in Bayreuth**

The results of this study were highly dependent on the climate conditions during the study period. Air temperature and precipitation values during the study period were measured in the botanical garden of Bayreuth. Generally, neither temperature nor precipitation patterns deviated greatly from long term average values summarized by Lüers et al. (2014). Lüers et al. found a trend towards warmer temperature during the last 160 years. This trend is underlined by the temperature pattern of 2016, as temperature values were constantly about 1.5 °C higher than the average over the last 100 years. As already discussed, May and July were rather dry months (40 mm and 36 mm precipitation, respectively), while there was a lot of precipitation in July (106 mm). Lüers et al. (2014) did not find any trend in precipitation during the last 160 years. Precipitation patterns fluctuate a lot and vary greatly within small spatial scales. Small-scale convective precipitation events are the greatest source of uncertainty during the summer months. Therefore, comparisons to previous years are not yielding evidence and in the study at hand it was foregone to analyze those.

#### **5.1.2 Selected Tree individuals**

Ecosystem services, such as the cooling effect are influenced by many factors. Environmental conditions are as important a factor as trees species, age and health. All selected trees were described in 3.1.3 and in the appendix A.

10 trees were selected for the study at hand, of which 8 were *T. cordata* and two were *R. pseudoacacia*. Size and age varied considerably (DBH: 8.2 - 42.6 cm, Age: 15.4 - 53.3 years, Height: 7.7 - 16.5 m, crown position: 3 - 5.8 m). Vitality was best in most cases. Cailliau (2016) modelled crown volume: 27 - 636.6 m<sup>3</sup>, crown projected area: 6.7 m<sup>2</sup> - 59.5 m<sup>2</sup> and tree pits: 1 - 5.6 m<sup>3</sup>. Distance to the closest building was between 2.2 and 15.6 m. To test for hypothesis 1, which claimed urban trees would significantly reduce heat stress on streets, measurements were conducted in all selected trees independently of species, size and age. For Hypothesis 2, which focused on species differences, cooling effect of *T. cordata* and *R. pseudoacacia* was compared. To eliminate size and age as influencing factors as far as possible, only data taken from R1, R2 and T1, T2 were used as those individuals were of similar age. Hypothesis 3 referred to different cooling effects depending on the trees size, which correlates with age. Therefore, hypothesis 3 was checked for *T. cordata*, focusing on the individuals' size and age. The selected individuals represent an important range of urban trees. Nevertheless, it has to be pointed out that results are only valid for the selected trees. To transfer conclusions to other tree populations entails uncertainties. Further research with a greater experimental group is necessary but would have exceeded the scope of a master's thesis.

### **5.1.3 Microclimate of the urban site**

The microclimate of the selected urban site was investigated with a Kestrel 4000 three times a day on July 20<sup>th</sup> and 21<sup>st</sup>. Averaged values were shown in 4.1.3.

First, the site was divided into 18 categories. Temperature and relative air humidity was measured at the two buildings with the most influence. Buildings store and reradiate heat, so it was expected to measure relatively high temperatures and low humidity values here. Indeed, at any time of the day the highest averaged temperatures were measured at the buildings. At 5:00 the highest temperature and the lowest air humidity was found at building 1, which was closer to the main train station. Leuzinger et al. (2010) measured the highest temperatures at the railway station (up to 60°C), so the results found in the study at hand might also be due to the small distance to the station. Also at 10:00 and 15:00 the highest temperature was found at a building. As building 1 was shaded by trees, while building 2 was illuminated, building 1

was now slightly cooler. Relative humidity measurements showed higher values at building 2 only in the morning and higher values at building 1 for the rest of the day because of the shading patterns already explained.

Furthermore, surface materials are an important factor in the urban environment, as already discussed in 2.3.4.1. At the chosen site the street was covered by asphalt and the parking site as well as the open space were covered by concrete. Temperature differences between shaded and illuminated areas were not seen until 15:00. In the afternoon, when temperatures were at their highest, the parking site was most heated of all surface materials. The same results were found by Coutts & Harris (2012). Relative air humidity at 5:00 was lowest above asphalt. Surprisingly, the highest humidity values at 10:00 were measured above the sealed space, which might be explained by the waterside nearby. The concrete covered parking site was driest at 10:00 and at 15:00. Concrete is not able to store sufficient moisture, so no evaporation was able to occur in the afternoon, which led to the increased temperatures because of the transformation to sensible heat.

Four trees were analyzed in detail, which were located evenly across the street: Tree 1 and 3 were very close to a building and were most likely affected by its radiation emittance, Tree 2 was located between the parking site and the street and Tree 4 was located next to a green-space, which might have cooled the surrounding. At all trees measurements were taken at the stem and below the canopy in the sun as well as in the shade. Temperature measurements at trees were neither particularly low nor high. Because solar radiation was too low in the morning, differences between shaded and illuminated areas under the canopy were initially found at 10:00 and increased in the afternoon. Exceptional low temperatures were found at the stem of one individual at 10:00 which might have been due to measuring inaccuracies. At 5:00 maximum relative air humidity was measured at tree 4, but was greater below the canopy than close to the stem, even though transpiration due to photosynthesis and shading should not yet play a role. At 10:00 the opposite was measured, as lowest humidity values were measured at a tree (3). Relative air humidity was always higher in shaded areas than in the sun because of lower evaporation rates. Results showed no great effects issuing from the selected urban trees.

A waterside and a greenspace were supposed to be the “cooling categories” of the site. Measurements proved the fact, as particularly low temperatures were found at the greenspace. At

5:00 and at 15:00, the lowest temperatures were found at the greenspace, while temperatures at the waterside were always slightly greater. The reason might be effective air mixing, which was facilitated at the waterside because of increased openness. Regarding relative air humidity, values at the waterside were only greater at 5:00, but the greenspace had higher values at 10:00 and at 15:00. Particularly at 15:00 maximum humidity values were found here. Effective air mixing was rather happening above the waterside during the day because of less obstacles and increased windspeed. It led to quick removal of moisture.

As the parking site was supposed to heat up most (Coutts & Harris 2012), it was independently investigated. As the parking site was planted, values were taken below a tree, but also above a car and above the concrete covered ground. Measurements of the present study showed particularly high temperatures above cars throughout the day. Metal, which naturally emits energy easily was additionally heated due to driving activity. Dark colors intensified the effect. Lowest temperatures were found below trees because of shading. Also the highest relative air humidity was found below tree canopies at 10:00, while it was lowest above the car. The reason was high photosynthesis activity, which results in higher humidity values below the canopy and lower temperature because of latent heating. At 15:00 driest conditions were found above the ground, which was already discussed above.

All in all, maximum temperature differences were 4.1 °C at 5:00, 3 °C at 10:00 and 4.9 °C at 15:00, so the influence of cooling was greatest at 15:00. Relative air humidity was varying between 81.3 % and 27.8 %. Relative air humidity differences were greatest at 5:00, the time when values were generally greater.

## 5.2 Main measurements

### 5.2.1 Urban climate

#### 5.2.1.1 Temperature

In different temperature zones the intensity of the urban heat island effect varies throughout the year and the day. The greatest variation was found during summer and autumn (Chandler 1965, Lee 1979, Unwin 1980). Temperature measurements, the focus of the study at hand, were therefore done during the summer months June and July at four sites: above the street and at a parking lot as typical urban environments and at a greenspace and in the botanical garden as vegetated comparisons. The temperature difference between the urban and the rural site was on average 1.3 °C. Many studies describe the extent of the urban heat island effect. Akbari et al. (2001) found 2.5°C higher temperatures in a typical American city. Also Rosefeld et al. (1995) described 2-3 °C higher temperatures in Los Angeles due to the urban heat island effect. In Berlin city increased temperatures of 2-4 °C and in Aachen of 1-3 °C were found (TEEB 2016). In Bayreuth, a relatively small city, an urban heat island effect comparable to Aachen was found. Day-to-day variations of fluxes and timing of temperature peaks, which are due to differing water availability and other factors have to be acknowledged. Furthermore, effective air mixing among the sites reduced air temperature differences.

Highest temperatures were always measured above the street, which was due to material choice and other factors leading to urban heating (see 2.4.4 and 4.2.1). The average temperature above the street over the study period was 19.9 °C and was therefore greater than the temperature measured for Bayreuth during the study period, which was 17.6 °C (see 4.1.1). Surprisingly, at daytime the temperature was always lowest at the parking site. This result shows, that the chosen parking site had not the same typical characteristics as described in literature (Davis et al. 2010). A reason might be the size and the heterogeneity of the place: while parking lots are typically of greater size and uniformly build, the weather station had to be placed on a heterogeneous place in a passage, close to some greenery. Wind circulation might have led to cooling. The slight temperature drop, which was observed in the late afternoon, was also due to the locality: shade of the tall building reached the station and lowered

the air temperature. Night measurements at both weather stations and above the street were always very similar because of their small distance (see map in 3.1.4) and negligible differentiating factors like evapotranspiration, windspeed and solar radiation/shading during night. Both sites, the greenspace and the botanical garden were exposed to similar factors in regard to solar interception and cooling due to evapotranspiration of the underlying grass field. It led to similar temperature patterns during the day, while temperature at the greenspace was slightly lower because of less openness and more shading. At the botanical garden the very low temperatures during the night stood opposed to rather high temperatures during the day. In the evening temperature was decreasing quicker above the street than in the botanical garden, which might be due to earlier shading at the urban site because of decreased openness. Cooling during the night was much more effective at the rural site than in the city because of increased openness and less reradiating surfaces, which emitted energy during the night. Those findings are in line with documentations of Oke (1982). He described spatial and temporal features of urban and rural temperature developments. In his findings as well as in the findings of the study at hand, rapid cooling after sunset was observed at the rural site. Also, in the present study, the minimum average temperature was measured just before sunrise and explained by the absence of solar heating. Oke explained this process by the energy drain of the surface and the withdrawal of heat from the shallow layer of air above it. When the surface temperature decreased, the cooling rate also declined. The result can be seen in figure 50 of Oke (1982), which shows a simple exponential decay curve until sunrise and was found similarly in the present study. In the morning, the pattern was interrupted by warming and heating causing plausible heat fluxes. Uprising heat caused the mixing of air, which in turn decreased warming rates in the afternoon. Oke described maximal temperatures in the midafternoon, which is in line with the present results, that show maximum average temperature in the early afternoon. It was quite striking that the sharp peaks of the heating and cooling rates around sunrise and sunset were missing in the urban environment. In consequence, the heat island intensity was greatest just after sunset and decreased until sunrise when urban cooling counterbalances this effect. Also Oke (1982) showed that the biggest differences of

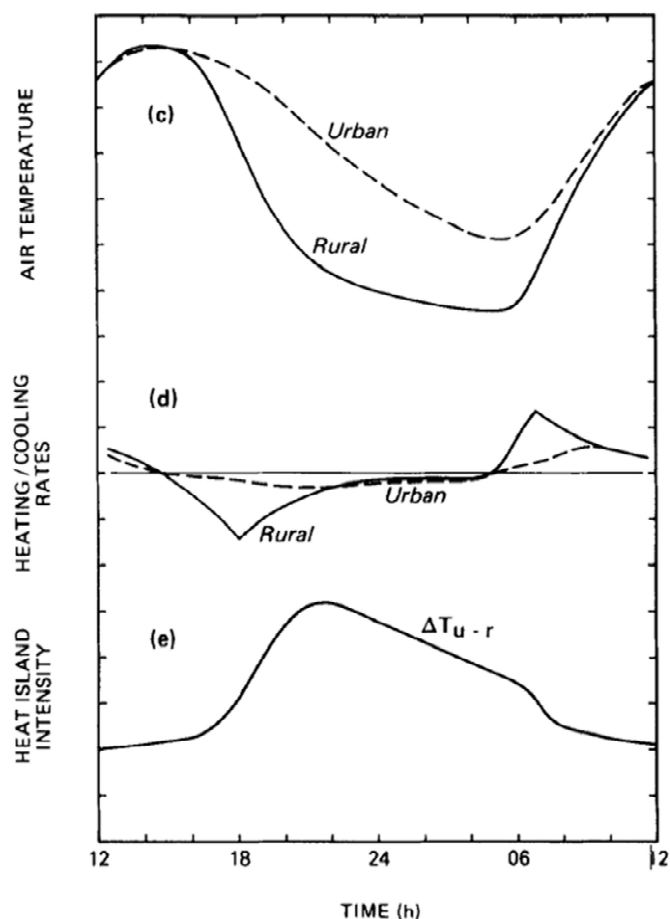


Figure 45: Idealized form of the spatial and temporal features of urban and rural screen-level air temperatures giving rise to an urban heat island effect. Source: T.R. Oke (1982).

cooling between urban and rural areas can be found three to five hours after sunset. Later at night he found a slight approximation because of greater urban cooling. The results of Oke (1982) and the study at hand bring further evidence that urban heat island is mainly a nocturnal phenomenon.

The results discussed above and the density function of air temperature [ $^{\circ}\text{C}$ ] showed that generally warmer temperatures were more often measured in the urban than in the rural environment and verified an existing urban heat island effect in Bayreuth.

Statistical testing showed statistically significant differences between the dataset of the botanical garden and data taken above the street.

### 5.2.1.2 Radiation

All devices had a photodiode attached which measured incoming solar radiation over the study period. Daily incoming solar radiation was averaged over the study period. In contrast to measurements in the botanical garden, slightly less mean solar radiation was observed at the urban site. The maximum value of 186 mV was found above the street at around 14:00.

Normally, radiation scheme is altered in the urban area. Typically, incoming sky radiation is decreased by about 10% and the average of sunshine hours per day is reduced to about 8 hours in summer (TEEB 2016). In the study at hand, averaged mean incoming solar radiation over the study period was decreased by 4.1 % in the urban environment. Maximum value was

3.2 % higher at the urban site than at the rural site, which might be due to multi-reflected radiation. Sunshine hours were not reduced, at both sites 15.5 hours incoming solar radiation were measured. As Pretzsch et al. (2015) explained, the amount of incoming solar radiation is dependent on the openness of the site. Generally, a decreased sky view factor was observed in streets, because of surrounding buildings, trees and other obstacles which reduce the openness of the site. Norton (2013) named streets width and buildings heights as very important parameter for heat risk determination. Wide architectural systems can get hotter at daytime but cool quicker at nighttime than narrow canyons. Narrow street canyons are no typical architecture for Bayreuth as houses are commonly not very high and streets are often wide. Also the density function of solar radiation values between the botanical garden and above the street showed no big differences. Also at the botanical garden a wide environment and the absence of obstacles prevented shading. Cooling differences can therefore not be attributed to the architectural situation.

### **5.2.1.3 Moisture**

Relative air humidity [%] was measured above the street, at both weather stations and in the botanical garden during the whole study period. As already discussed, moisture content is an important parameter for heating, as energy exchange can be done either by the release of latent or sensible heat. When moisture content is high, latent heat fluxes increase instead of sensible heat fluxes and therefore prevent urban heating.

At the vegetated sites as well as at the urban sites, relative humidity during the night was high and reached maximum values in the morning at around 7:00 and minimum values in the afternoon before sunset. Because solar radiation was not available and temperatures were lower at night, evaporation levels were lower. It accumulated to a maximum just before sunrise. During the day, incoming solar radiation led to uprising air masses, increased windspeed and therefore supported a quick removal of humidity, which was transpiring because of increased heat. Comparing all datasets, relative air humidity was lowest above the street during the day. Because of impervious surface materials, moisture was not able to penetrate the ground and evaporated quicker with rising temperatures, which lead to very low relative air humidity in the afternoon, when all available moisture was transpired and removed. A small

increase of about 2.5 percentage points occurred in the afternoon and was most likely due to increased windspeed in the afternoon (see section 4.2.1), which might have brought humidity from the waterbody nearby or from vegetated areas. Humidity values of the weather stations were very similar particularly during the night and in the morning. Both weather stations were placed in a small distance (see 3.1.4), so air mixing lead to similar humidity levels. During the day, humidity values of the parking site were even higher than above the street. The selected street was straight for about 700 m, which made it easier for winds to take up speed and remove air humidity. The environment of the weather stations was small scaled and heterogeneous, which decreased winds and increased air humidity. In the evening humidity above the street was rising quicker than at the weather stations. Averaged values were slightly higher at the greenspace (73.3 %) than at the parking site (72.7 %) because the greenery led to increased evapotranspiration and humidity at the site, as can be seen in the results of the botanical garden as well. The small increase of about 2.5 % in the afternoon at the greenspace might be due to increased windspeed or shading. By far the highest relative air humidity was measured in the botanical garden with an average of 80 %. Even at very hot temperatures the penetrated moisture was still present in the ground and was able to evaporate, which led to high air humidity. The averaged maximum value measured in the early morning of 101.3 %, was due to inaccuracy of the sensor of  $\pm 2$  %. It can be assumed, that the air at the botanical garden was saturated to about 100 %. At the botanical garden the ground enabled water to penetrate, so the water storage capacity was much greater than at the urban sites. Moreover, the botanical garden as a rural site was surrounded by a natural environment with a lot of vegetation, which increased air saturation. Again the slight rise in the afternoon was due to wind turbulences.

To conclude, the differences between the very high relative air humidity in the botanical garden during the night and the very low values measured above the street during the day were most striking. The density function supported those findings and showed lower humidity values more often above the street and maximum saturation in the botanical garden.

Comparison of the datasets of the botanical garden and the measurements above the street showed statistically significant differences.

#### 5.2.1.4 Ground temperature

One of the most important factors for the urban heat island effect is surface heating due to material choice. Spronken-Smith & Oke (1998) described how surface temperature is depending on the materials albedo, available shading and water during the day.

In the study at hand, object temperature was measured via infrared diode over the whole study period to gain a better insight into surface temperature pattern. The density function of all object temperature measurements over the whole study period found highest density at 20 °C. As can be seen in 4.1.1, averaged air temperature for the study months were 16.7 °C for June and 18.4 °C for July. Temperature pattern of surfaces generally follow air temperature pattern but are of greater magnitude, as already Norton (2013) described, so the result found was not surprising. Object temperatures below 20 °C was barely found. Also higher temperatures above 20 °C were measured less often. Density of really high temperatures (28 °C – 49 °C) was rare (<0.03), but existent at some hot afternoons. The comparison of the averaged surface temperature and averaged air temperature showed expected pattern over the day: minimum temperature was measured in the morning, when solar radiation was not yet leading to heating and maximum temperature was measured in the afternoon. Surface temperature was always higher than air temperature with maximum differences in the afternoon. Ca & Aseda (1996) observed largest differences between air and ground temperature at noon. A detailed comparison on the surface characteristics helps to fully understand the results: The ground at the study site consisted mostly of asphalt and stones made of concrete. Both surfaces had a low albedo, which means they stored and re-radiated heat to a higher extent (Rizwan et al. 2008). The albedo of surfaces is not only dependent on visible reflectivity, but also on reflectivity of infrared-waves, which comprises a large share of incoming solar radiation (Rosenfeld et al. 1995). When temperature differences between surface and air were small, incoming infrared radiation was almost balanced out by infrared radiation coming from the ground. In case of heated surfaces, where temperature differences between surface and air were large, infrared radiation from the ground was significantly larger and increased infrared-values were measured from the ground (Eliasson 1994). Oke (1987) as well described characteristics of different surface materials and found high thermal admittance of asphalt and stone. He focused on heat conductivity, specific heat, porosity and reflectivity and found very high values for concrete (Spronken-Smith & Oke 1999, Chang et al. 2007, Nakayama 2011, Ca & Aseda

1996). Ca & Aseda (1996) observed even greater infrared absorption for asphalt pavement than for soil surface or concrete pavements. They described a considerably greater heating for asphalt than for other materials. In the study at hand, concrete was mostly found in the north, while asphalt was found in the south of the trees. See 5.2.2.3 for North/South differentiating. Because of the described characteristics, open parking lots and street surfaces, which are covered by concrete or asphalt show very high surface temperatures (Coutts & Harris 2012). The increased storage capability leads to a delayed cooling in the evening, as can be seen in the results of the existing study. Also Sakakibara (1996) found urban streets to cool slower than parking lots because of geometrical reasons.

To sum up, high surface temperatures increase sensible heat fluxes and contribute to the urban heat island effect. Therefore, reducing surface temperatures in cities should be a central target for mitigation strategies (Ali-Toudert & Mayer 2006).

#### **5.2.1.5 Aerodynamics**

Some of the selected trees were equipped with cup anemometers to measure windspeed [m/sec] during the study period. Data taken at the study site were compared to windspeed measured at the official weather station of Bayreuth in the botanical garden. It has to be kept in mind, that measuring devices were not equal and haven't been tested against each other. The diurnal pattern in the botanical garden and above the street were generally the same, as windspeed was lowest at night and greatest during the day. This trend was expected as heating during the day led to uprising air masses, which in turn led to increased wind speed. But still, there were striking differences between the botanical garden and the urban site. Windspeed in the botanical garden was at any time greater than at the urban site. The results supported the consensus in literature, which states that wind speed in urban areas is generally lower than on the countryside because of increased resistance. In the botanical garden, with open grass fields as the dominating ground cover and no trees at the measuring site, only a low wind resistance was existent. Heated air masses were able to rise, which led to cooler temperatures through convection (Bowler et al. 2010). In the urban environment mixing of air masses was reduced and sudden temperature changes enhanced. Vertical air movements were able to increase in the urban area, but open sites like at the botanical garden were able

to allow circular flow, which enhanced horizontal interchange as well (TEEB 2016). Also the vegetation type could have affected air movement (Bonan 1997). Matzarakis (2001) already described the increased roughness of cities which leads to turbulences but can also function as an obstacle for wind currents. Also Goldbach & Kuttler (2013) presumed that wind speed in cities is decreased by about 20% while squalls increase. Also in the study at hand, wind might have been trapped by obstacles and under tree cover at the urban site. It might have been hindered from uprising and lead to reduced windspeed. The results of the study at hand showed as well, that wind speed was reduced in a dense urbanized environment. As Miller (2015) already described, wind and radiation affect convective heat transfer and therefore air temperature. Also throughout the study at hand, the influence of windspeed on temperature pattern was observed. No normal distribution was existent and datasets were significantly different.

## **5.2.2 Effects of urban trees**

### **5.2.2.1 Cooling effect**

Trees have their own microclimate (Miller 2015), which can reduce temperature at the local scale because of cooling through transpiration and shading. Tree planting was rated as the best measure to mitigate urban heat island effect (Rosenzweig et al. 2006). In the study at hand, cooling effect of urban trees was calculated as difference between temperature measurements in all selected trees and temperature measured above the street. Because results from Melbourne showed particular effectiveness at hot days (Coutts & Harris 2012), 24.06.2016 as a hot and sunny day was chosen for analyzing cooling effect. On average a cooling effect of 0.77 °C was observed. During the night from 19:10 until 5:00 the cooling effect was on average -0.45 °C, while it was on average 1.76 °C during the day (5:10 – 19:00). Other studies found averaged differences of 1.0 and 0.9 °C between tree influenced and tree uninfluenced study sites (Matzarakis 2001). Akabari et al (2001) simulated cooling effect of trees for a whole city and found temperature reductions of about 0.3 to 1 °C at 14:00 and maximum values of 3 °C in some parts of the city. One German study from Bernatzky (1982) illustrated, that the green belt around Frankfurt is lowering air temperature of up to 3 - 5 °C.

Cooling effect of urban trees was observed in relation to air temperature, surface temperature and windspeed at a day, where air temperature reached 37.7 °C. Windspeed was low at the chosen day (max. 1.6 m/sec), but still cooling effect fluctuates a lot with changing windspeed. Increased wind speed led to mixing of air masses, which decreased the difference between air temperature above the street and temperature measured in the trees. Greatest values were found in the morning with highest values around 3,8 °C, because photosynthesis activity was high. Around 14:00, when surface temperature was at its maximum of 49.1 °C, air temperature was 35.7 °C and windspeed was about 1.25 m/sec cooling effect of trees decreased and fluctuated between 0°C and 1,5 °C. Trees close their stomata when temperatures get too high to avoid great water losses. As a result, there was no cooling through evapotranspiration but shading. Additionally, increased windspeed made it difficult to measure exact values due to effective air mixing. Also the increase of cooling effect in the evening, despite elevated air temperature above the street was due to wind turbulences, as windspeed was at its maximum of 1.6 m/sec. Cooling effect dropped to its minimum at 19:10 of -0.98 °C and stayed negative until 5:00 in the morning. Norton (2013) and Oke (1999) described, how heat from ground surfaces might be trapped under the canopies during the night. Surfaces in the urban area emit energy during the night. As windspeed was decreased in tree canopies (see section 5.2.2.4), removal of warmer air masses was hindered and led to higher temperature measurements in canopies. Additionally, cooling effect was observed at different heights in the trees R1, R2, T1 and T2. In the course of the morning, cooling effect increased at all positions in the trees as photosynthesis activity increased and led to increased evapotranspiration. Because at the middle position incoming solar radiation was not as intense as at the highest position and heating due to reradiating surfaces was lower as at the lowest position, greatest cooling effect was documented here with an average temperature decrease of 0.47 °C over the day. Greatest cooling effect at the middle position was observed in the morning and in the late afternoon when heating was greatest at the other positions. Cooling effect was twice as great at the highest position than at the lowest position, which can surely be reasoned by increased surface temperature in the afternoon. After sunset, when cooling effect dropped at all positions, particularly at the lowest position cooling effect was even negative until the next morning because of heated ground surfaces. Not only height differences were observed, also species differences (see 4.2.3 and 5.2.3) and individual differences were present. The last figure in 4.2.2.1 shows, how averaged cooling effect was not only varying between species, but also

between individual trees. While both individuals of the species *T. cordata* had different peaks of cooling effect either in the morning or in the afternoon, totally differing cooling effects of the individuals of the species *R. pseudoacacia* were observed. Investigations showed, that R2 might have been a *R. pseudoacacia unifoliola*, with slightly different leaves and it was additionally suffering from a root fungus in year 2011, which might explain different results.

Generally, urban trees are one vegetation type which can be implemented in cities to cool the environment. They generally have the same functions as all vegetation types, but because of their height, 80% of the cooling effect is due to shading and evapotranspiration and has therefore the major effects on the urban climate (Shashua-Bar 2003).

### 5.2.2.2 Transpiration

Transpiration describes a vaporization process over the leaf surface through stomata, which increases air humidity. Transpiration leads to cooling of the urban environment because of the conversion of energy to latent heat rather than sensible heat. This process is particularly important on hot summer days (Pretzsch et al. 2015, Bowler et al. 2010).

Transpiration values have to be seen in comparison to incoming solar radiation, which determines temperature development and therefore also water holding capacity. This in turn affects vapor pressure deficit and correlates with leaf to air pressure difference. Leaf to air vapor pressure difference is an important transpiration factor, as it affects stomata conductance and therefore evapotranspiration. Results of the study of Mott & Parkhurst (1991) can be seen in figure 51.

In the study at hand averaged relative air humidity in tree canopies was compared to relative air humidity measured above the street and incoming solar radiation at a hot and sunny day.

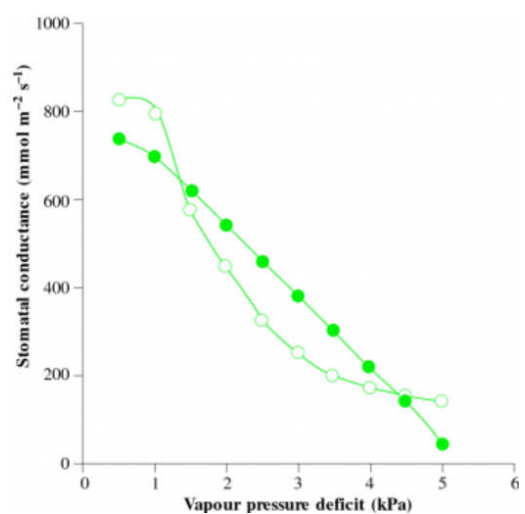


Figure 46: Stomata are affected by atmospheric vapor pressure deficit. As a result, stomata can prevent faster transpiration at low atmospheric humidity by closing. Patterns of response differ between species. The graph shows two common examples. Source: Mott & Parkhurst (1991).

Any differences found were mostly less than 5% and statistical testing showed no normal distributions and no dependencies between the two datasets. Humidity was changing contradictory to incoming solar radiation with some delay, because increased solar radiation in the afternoon led to temperature increase and eased quicker evaporation and removal of moisture after heating. This mechanism explains why lowest relative air humidity levels were measured after 14:00 (about 20%) while greatest solar radiation values (280 mV) were measured at 13:00. Highest humidity values in the tree as well as above the street were found in the early morning, when solar radiation was low. During the day, relative air humidity was always higher in tree canopies than above the street. The opposite was observed during the night. Plants use photosynthesis when light is available as their energy source. When opening their stomata, moisture evapotranspires (Eaton-Rye 2011). This process explains higher humidity levels in the tree canopies than above the street during the day. At night, stomata stay closed and evapotranspiration decreases. Additionally, the heated street surface prevented condensing during the night so relative air humidity above the street stays relatively high. Fluctuations could be due to small spatial air turbulences.

Additionally, relative air humidity was measured in the top of the tree and at the bottom of the crown during the study period and was compared to humidity measured above the street. Generally, the same daily course was observed and was already discussed above. Values measured at the top of the trees and above the street were very similar over the day due to effective air mixing. Before noon, air humidity above the street was slightly lower than in the top of the tree. With increasing solar radiation in the morning, transpiration increases and led to higher humidity values at position A. In the crown (position D) 2 % lower humidity values during the night are due to heat, which was emitted from energy storing surfaces below the tree canopy and affected the character of lower air layers. Particularly during the day, relative air humidity at position D was greater than at position A at any time with maximum differences of 4.3 %. As the crowns diameter was much bigger at the lower position, increased biomass led to greater humidity and was less influenced by winds. The slight rise at 17:00 was due to increased winds (see 4.2.1.5).

Light was already included in analysis as the most important factor determining the transpiration process. Moisture availability was also a very important abiotic factor which could have been observed with soil-moisture-experiments. Moisture availability is strongly dependent on

the site, which at least partly explains, why Pretzsch et al. (2015) found different transpiration values, which also resulted in differing cooling effects. The most important biotic factor is leaf area index (Wilde 2011, Norton 2013, Hunter Block et al. 2012). Species differences were discussed in section 5.2.3.

### **5.2.2.3 Ground temperature**

Lindberg & Grimmond (2011) already stated, that besides transpiration shading is the most important contribution to thermal comfort in cities during hot periods. Norton (2013) rated trees as the optimal solution to provide overhead shading. Therefore, shading was observed via infrared-diodes, which measured surface temperature in the southern and northern direction of the tree (position C & E, see 3.1.3) at a hot and sunny day with temperatures of up to 37.5 °C. As a very important influencing factor, background air temperature needed to be the basis for comparisons. In the study at hand, averaged surface temperature was compared to air temperature. Leuzinger (2010) already did a study of shaded and unshaded surface temperatures and described surface temperatures to be reduced by more than 50% when shaded. In the existent study, the difference at maximum temperature was 1.9 °C (northern direction: 38.3 °C, southern direction: 40.2 °C). Lindberg & Grimmond (2011) were also surprised by relatively high temperatures below vegetation canopies. They hypothesized that the relatively colder sky was blocked by tree canopies and therefore the share of longwave radiation coming from the vegetation rather than the sky increased and altered temperature pattern.

At night, when there was no solar radiation, temperatures were very similar in all three datasets. Lowest temperatures were always observed in the early morning, but southern surface temperature was already 0.5°C warmer than at the northern side and air temperature was cooler than any surface. This result might be due to different surface materials in the southern and the northern direction of the trees: while there was concrete in the north, an asphalt covered street was in the south of the trees. As described in section 2.4.4 concrete reflects four times more radiation than asphalt. Heat, which was stored in both materials but particularly in asphalt, was released at night and led to the observed results. Moreover, there was a water body in the northern direction, close to sub-group 2 (see section 3.1.4.1), which might

have cooled the environment particularly when there was less air mixing because of low wind-speed during the night. Also Leuzinger et al. (2010) found water bodies to be the coolest surfaces. Furthermore, illuminated surfaces in the south of the tree exceeded air temperature already at 10:30, while shaded ground in the north of the tree stayed cooler until 14:30. This delay of four hours might lead to increased wellbeing and to a relief of the cardiovascular system (see section 2.4). Also the averaged surface temperatures in the south and the north as a function of air temperature showed the same result: Surfaces in the northern direction of the tree heated up less with rising air temperatures than surfaces in the southern direction of the tree. Moreover, the maximum temperature was reached two hours later in the north than in the south. This very important result was due to shading of the trees. Surprisingly in the evening, surfaces cooled as quick as the air and no delay could be observed. Differences of the datasets of surface temperature in the south and in the north of the tree were statistically significant.

The degree of shading was determined by permeability of the leafs (Norton 2013). Roughly only 30% of incoming solar radiation can penetrate a leaf, but numbers vary with species choice. So foliage density and leaf area density of the tree species were influencing shading effect most (White et al. 2012). See 3.1.2, 4.2.3 and 5.2.3 for more species specific details. Other influencing factors such as geometric configuration of the site, tree characteristics and growth factors were not taken into account.

#### **5.2.2.4 Aerodynamics**

Four selected trees were equipped with cup anemometers to measure windspeed in m/sec over the study period. The averaged diurnal variation of windspeed measured in trees was drawn against the windspeed measured above the street. The same general windspeed pattern as in 4.2.1.5 and 5.2.1.4 was observed: windspeed was lowest during the night and greatest during the day. Again this pattern was due to heating during the day which led to uprising of air masses which in turn led to increased wind speed. Moreover, the windspeed was at any time greater above the street than in trees. Differences were greatest in the afternoon with on average 1.13 m/sec difference and lowest at night with 0.23 m/sec difference. Oke (1982)

found present vegetation to be one influence to wind pattern of the region because of increased resistance. Because of less air mixing temperature differences tend to be greater. Bonan (1997) showed how vegetation type can influence air movement. Trees for example can trap heat under their crowns as it might be hindered from uprising. Less wind intensity can be observed as a result, like in the study at hand.

### 5.2.3 Species differences

Results showed, that services did not only differ between species, but also strongly depend on each individual. In the study at hand, cooling effect of R1 and R2 was very different. R1 showed strong variations, while mean cooling effect of R2 was lower but more constant. Nevertheless, median difference was small with 0.25 °C. Consultation with the gardening department showed, that R2 might have been a *R. pseudoacacia unifoliola*, with a slightly different leaf size. Additionally, it suffered from a root fungus in year 2011. Pretzsch et al. (2015) described *R. pseudoacacia* as alien species, which is not particularly susceptible to common diseases in Germany. Nevertheless, data from R2 was included in analysis, as illness is a natural factor. Cooling effect of both *Tilia cordata* individuals was very similar and on average greater than effects of *R. pseudoacacia*.

Also results of the averaged cooling effect of the whole period showed slightly greater values of *T. cordata* during the day with a maximum cooling effect of 1.14 °C and maximum differences between the species of 0.17 °C. Mean cooling effect over the study period was 0.47 °C in case of *T. cordata*, while it was 0.42 °C in case of *R. pseudoacacia*. Pretzsch et al. (2015) found opposed results with a slightly greater cooling effect of *R. pseudoacacia*. He named the chosen study site as main influencing factor. Living conditions are harsh in the urban environment but Aas (2016) and Pretzsch et al. (2015) described both species as very tolerant. *T. cordata* does require some warmth, but does not need much nutrients and humidity and can grow on many different soils. *R. pseudoacacia* can also grow on almost any soils, and is only limited by low soil aeration and waterlogging (Wojda et al. 2015, Sitzia et al. 2016). Main difference between the two selected species is light dependency: while *T. cordata* is shade tolerant, *R. pseudoacacia* is light dependent. But as the study site was very open (see 3.1.4), lack

of solar radiation was no issue. Differing results might be to species differences and different leaf sizes or the root fungus of R2. No cooling effect was observed during the night because of missing photosynthesis and no shading. Particularly *R. pseudoacacia* showed even a negative cooling effect in the early evening, which was surprising. Negative cooling effect during the night was due to surfaces materials: stored heat was emitted and trapped under the canopy which led to increased temperatures. *T. cordata* is very dense growing, which on the one hand leads to a high light emitting efficiency and enables growing in relatively shaded areas, but on the other hand should also result in higher temperatures during the night. Further research is necessary.

Both species showed greatest cooling effect before afternoon with values of 0.8 °C – 1.1 °C, when maximum air temperature above the street did not yet reach the averaged maximum temperature of 24.1 °C because photosynthesis works best at lower temperature as water loss is smaller (Eaton-Rye 2011). Fluctuations were due to wind turbulences. No normal distribution was existent and differences of the datasets were only statistically significant, when data taken during the night was excluded.

Cooling effect of trees is particularly important at days of increased temperatures. The effect of both species is therefore plotted for a hot and sunny day (June 24<sup>th</sup>). Maximum temperature above the street was 37,7 °C. Also at the hot day, *T. cordata* showed a slightly greater cooling effect during the day than *R. pseudoacacia*, even though *R. pseudoacacia*, as a light dependent and drought resistant tree should have had best weather conditions. Maximum difference was again 0.17 °C, but generally cooling effect of the two species was more in accordance. Maximum cooling effect of *T. cordata* was 1.21 °C. Both species showed greatest cooling effect in the morning, when temperature above the street was below 30 °C, because stomata are closed when temperatures are too high to prevent increased water loss. Surprisingly, differences between the two species became more distinct, when temperature above the street exceeded 36 °C even though *R. pseudoacacia* was expected to perform better at warmer temperatures. Also Pretzsch et al. (2015) predicted further expansion of *R. pseudoacacia* with climate change. But in the study at hand, cooling effect was decreasing in both cases. Fluctuations were due to wind turbulences. Differences between the datasets were statistically not significant.

Furthermore, relative air humidity was documented in both tree species over the whole period. Both species showed the same trend over the day, but measurements in *T. cordata* were almost constantly 0.5% greater than in *R. pseudoacacia*. The result might be due to dense growing of *T. cordata*, which in turn might have led to an enclosed microclimate with increased humidity. On average mean humidity difference was + 1.6 % in *T. cordata* and + 1.1 % in *R. pseudoacacia*. Increased humidity was due to transpiration in the course of photosynthesis. Maximum differences were 4.8 % for *T. cordata* and 4.1 % for *R. pseudoacacia*. Differences between the datasets were statistically significant.

Additionally, incoming solar radiation was measured in the tree canopies of each species, which has effects on shading. Differences to solar radiation above the street were analyzed. With rising incoming radiation in the morning above the street, differences to solar radiation measured in the tree canopy increased in both species because of shading leaves. In the morning radiation differences in the canopy of *R. pseudoacacia* were slightly lower because *T. cordata* grows very dense and solar penetration was smaller. After solar radiation peak has been overcome, differences between the species decreased. Testing for normal distribution was negative, but differences between the datasets of the species were statistically significant. Measuring inaccuracies in *T. cordata* might be possible because honeydew was plastering the photo sensors, see also 5.4. It was already described as a “disservice” by Eaton et al. (2016).

#### **5.2.4 Age differences**

It was assumed, that cooling effect changes with size and age. Cailliau (2016) modelled age and crown volume [m<sup>3</sup>] of all selected trees, so averaged cooling effect of *T. cordata* was analyzed as a function of modelled data. Contradictory to assumptions, age and crown volume was not always correlating. Different growing pattern are a result of natural variation, which were also affecting cooling effects.

Nevertheless, a tendency of increased cooling effect with greater age was observed. Cooling effect of a 50-year-old tree was 0.28 °C greater than a 20-year-old tree. Naturally, older trees are of greater size and produce more biomass than younger ones. Therefore, the same tendency was observed, when cooling effect was drawn against crown volume. A tree with a

crown volume of 500 m<sup>3</sup> had a greater cooling effect of on average 0.3 °C than a tree with a crown volume of 100 m<sup>3</sup>. In the study at hand it was assumed, that cooling effect was mainly due to transpiration and shading. Therefore, those two factors were as well analyzed as a function of age and crown volume. Again the same tendencies were observed in case of measurements of relative air humidity [%] and solar radiation [mV] in contrast to conditions above the street. Relative air humidity difference was 0.9 % greater in a 50-year-old tree than in a 20-year-old tree. A relative air humidity difference of 1% was observed between crown volumes of 100 m<sup>3</sup> and 500 m<sup>3</sup>. Solar radiation in the canopy of a 50-year-old tree was 8 mV lower than in the canopy of a 20-year-old tree. A difference of only 7 mV was observed, when radiation differences of a 100 m<sup>3</sup> canopy were compared to differences of a canopy of 500 m<sup>3</sup>. In comparison to different cooling effects and different relative air humidity in trees of different age and size, differences of solar radiation values were small. Leuzinger (2010) found only 30 % of incoming solar radiation was able to penetrate a leaf. Penetrating solar radiation was therefore negligible small after only a few leaf layers. Microclimate in canopies of older trees with a greater crown size might have been more humid and shaded because of more photosynthetic active biomass. Increased biomass functioned as a greater obstacle and hindered winds to remove moistened cooled air.

The experimental group was small with n=10, so results have to be understood as a tendency rather than definite numbers. Moreover, results are only valid for the selected trees. To transfer conclusions on other tree populations entails uncertainties.

### **5.3 Conclusion**

After the urban climate was investigated to have a basis for comparison, the assumption weather or not urban trees significantly reduce the heat stress on streets was tested. Focusing on *T. cordata* and *R. pseudoacacia*, a cooling effect of on average 0.77 °C was observed at a hot and sunny day, while cooling effect was on average 0.45 °C over the study period. Because of photosynthetic activity, cooling effect was on average 1.76 °C on a hot and sunny day, mainly due to transpiration and shading. As both don't have played a role during night, a negative cooling effect was observed, which might have been intensified due to reradiated heat from surfaces. Greatest cooling effect was found in the morning of a hot and sunny day, when

temperature in the canopies was 3,8 °C lower than above the street. The hypothesis, that urban trees significantly reduce heat stress on streets can be affirmed. Therefore, the plantation of urban trees, particularly on the bigger scale would have a positive effect on the urban climate and dwellers would benefit from reduced heat. It is therefore important to confirm the results at hand by conducting a study with a greater experimental group. The cooling effect of urban trees was significantly reduced during the night because reradiated heat from artificial surfaces was not removed. Future studies, which focus on this discrepancy and study the different effects of dense and penetrable canopy structures are necessary.

Furthermore, it was assumed, that the species *T. cordata* and *R. pseudoacacia* have different cooling effects on streets. Both are commonly used, but demands differ, as *T. cordata* is tolerating shade, while *R. pseudoacacia* is light dependent. Averaged cooling effect of *T. cordata* was slightly greater during the day with maximum differences between the species of 0.17 °C. Differences became more distinct, when temperature above the street exceeded 36 °C. The hypothesis, that the species *T. cordata* and *R. pseudoacacia* have different cooling effects on streets can again be affirmed. Nevertheless, differences were small and other factors such as growing patterns, visual appearance and maintenance might play a major role. Results should therefore be affirmed by future studies and other species with particularly small or large leaves should be included.

Moreover, it was assumed, that cooling effect changes with size and the age. In fact, increased cooling effect with greater age and size was observed. Cooling effect of a 50-year-old tree was 0.28 °C greater than a 20-year-old tree and a tree with a crown volume of 500 m<sup>3</sup> had a greater cooling effect of on average 0.3 °C than a tree with a crown volume of 100 m<sup>3</sup>. The hypothesis, that cooling effect changes with size and the age can again be affirmed. It is therefore necessary to rather maintain older trees than plant younger ones. As older trees are often removed because of security reasons, research should focus on different maintenance techniques such as stabilization and disease control.

#### 5.4 Sources for inaccuracies

Even though efforts were made to exclude any source of inaccuracy, it was not possible to exclude all. Moreover, many factors influence the results but are not susceptible.

Climate of the season and at the site is the main influencing factor for any climatic measurements. The period, which was analyzed in the study at hand was not particularly hot and dry, which would have shown the most interesting results.

For the study at hand, only a small experimental group was selected, which could have led to a great source of inaccuracy. The existent study gave a small insight into urban climate of Bayreuth and the cooling effect of the selected urban trees. Further research and experiments are necessary to produce reliable data but would have gone beyond the scope of a master's thesis. Furthermore, as experiments were conducted in the field, the selected trees were exposed to many influences, which were not susceptible. The waterside and the greenspace as potentially cooling factors are two examples. But also the architecture of the site determined the results. The chosen site was no typical street canyon as it was described in literature. Instead it was very open and heterogeneous. Architecture could have affected wind turbulences and therefore also heating pattern.

The devices used were self-constructed and were tested before using. Nevertheless, the used sensors measured with some inaccuracy, which are also explained in 3.2.1. Tests were made, in which temperature measurements of the self-constructed devices were compared to temperature measurements of the weather station of Bayreuth. Results can be seen in figure 52. An increasing temperature difference was observed with rising radiation values. Temperature measurements of the self-constructed devices were on average 0 – 1.2 °C greater. But inaccuracies of -1.5 – 4.8 °C were also existent. Considering the small temperature differences, which were discussed in the thesis, those inaccuracies are not negligible. Besides those inaccuracies, data of some devices is sometimes incomplete. NA's were excluded in all cases but could have led to uneven weighting.

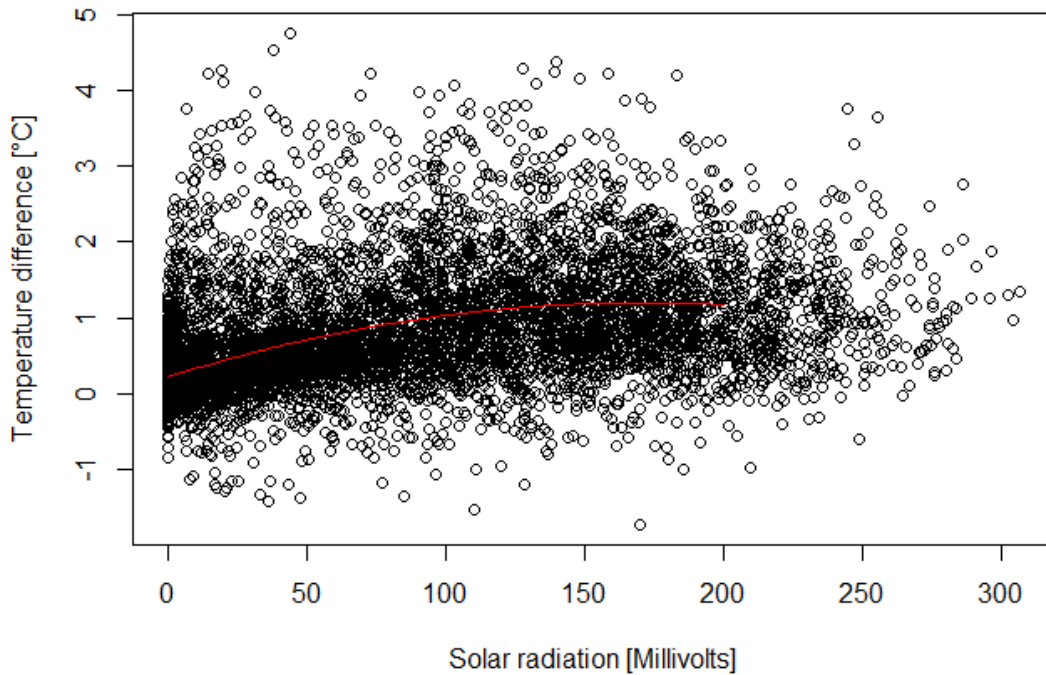


Figure 47: Temperature difference of the measurements of the used devices ( $n=1$ ) in comparison to temperature measurements of the weather station of Bayreuth ( $n=1$ ) as a function of incoming solar radiation.

Positions of the devices are explained in 3.1.3 and further described in the appendix A. It can be observed, that positions were not exactly at the same height which was partly due to the fact that trees are not uniformly grown. Also it was sometimes not possible to put devices at the exact cardinal direction. Moreover, some were slightly tilted around the branch during the study period of two months, which could have led to some inaccurate radiation measurements.

*Robinia pseudoacacia* and *Tilia cordata* were used for the study at hand. Results showed very different results for each individual. Particularly R1 and R2 differed substantially. In the summer months slightly different leaf sizes and shapes were observed. Further research showed, that R1 might be a *R. pseudoacacia unifoliola*. Leaves were slightly bigger and the trees crown grew more densely. Other reasons might be the root fungus at R2 and the edge effect at R1. *T. cordata* on the other hand was spread over the whole side and was therefore affected by many different factors. (e.g. T10 might have been influenced by a greenspace). Furthermore, individuals were of different age (see 4.1.4), but were treated evenly in most cases. Photodiodes in *T. cordata* were plastered with honeydew, which probably led to smaller radiation values and some inaccuracies.

The most important dataset was measured above the street, as it was used for most comparisons. In almost all cases, S1 provided better data because S2 was shaded in the afternoon.

Also the weather station at the parking site did not show expected values. Data was still used but problems were always mentioned. Results were probably influenced by shade and heterogeneity.

To conclude: the study at hand did only give a small insight into the urban climate of Bayreuth and the cooling effect of *T. cordata* and *R. pseudoacacia*. Further research is definitely necessary to validate the results made in the study at hand.

## 6. List of references

Aas G. (2016): Winterlinde: Verwandtschaft, Morphologie und Ökologie.

Ahmed K. S.: Comfort in urban spaces: defining the boundaries of outdoor thermal comfort for the tropical urban environments 2003.

Akbari H., Pomerantz M., Taha H. (2001): Cool surfaces and shade trees to reduce energy use and improve air quality in urban areas. In: *Solar Energy* 70 (3), S. 295–310. DOI: 10.1016/S0038-092X(00)00089-X.

Ali-Toudert F., Mayer H. (2007): Effects of asymmetry, galleries, overhanging façades and vegetation on thermal comfort in urban street canyons. In: *Solar Energy* 81 (6), S. 742–754. DOI: 10.1016/j.solener.2006.10.007.

Arnfield A. J. (1990): Street design and urban canyon solar access. In: *Energy and Buildings* 14 (2), S. 117–131. DOI: 10.1016/0378-7788(90)90031-D.

Asaeda T., Ca V. T. (2000): Characteristics of permeable pavement during hot summer weather and impact on the thermal environment. In: *Building and Environment* 35 (4), S. 363–375. DOI: 10.1016/S0360-1323(99)00020-7.

Asaeda T., Ca V. T., Wake A. (1996): Heat storage of pavement and its effect on the lower atmosphere. In: *Atmospheric Environment* 30 (3), S. 413–427. DOI: 10.1016/1352-2310(94)00140-5.

Bärring L., Mattsson J. O., Lindqvist S. (1985): Canyon geometry, street temperatures and urban heat island in malmö, sweden. In: *J. Climatol.* 5 (4), S. 433–444. DOI: 10.1002/joc.3370050410.

Beckroege R. (1984): Klimatische Phaenomene. In: Stadtklima und Luftreinhaltung. In: *Handbuch VDI. Springer.*

Benedict, Ma. & McMahon ET.: Green infrastructure: Smart conservation for the 21st century. *Renewable Resources Journal* 2002 (20), S. 12–18.

Bernatzky A.: The contribution of trees and green spaces to a town climate. In: *Journal of Energy and Buildings* 1982 (5), S. 1–10.

Block A. H., Livesley S. J., Williams N. S. (2012): Responding to the urban heat island: a review of the potential of green infrastructure. In: *Melbourne: Victorian Centre for Climate Change Adaptation (VCCCAR).*

Bocquier P. (2005): World Urbanization Prospects. In: *DemRes* 12, S. 197–236. DOI: 10.4054/Dem-Res.2005.12.9.

Bolund P., Hunhammar S. (1999): Ecosystem services in urban areas. In: *Ecological Economics* 29 (2), S. 293–301. DOI: 10.1016/S0921-8009(99)00013-0.

Bonan, Gordon B. (1997): Effects of Land Use on the Climate of the United States. In: *Climatic Change* 37 (3), S. 449–486. DOI: 10.1023/A:1005305708775.

Bowler D. E., Buyung-Ali L., Knight T. M., Pullin A. S. (2010): Urban greening to cool towns and cities. A systematic review of the empirical evidence. In: *Landscape and Urban Planning* 97 (3), S. 147–155. DOI: 10.1016/j.landurbplan.2010.05.006.

Ca V.T., Aseada T., Abu E.M. (1998): Reduction in air conditioning energy caused by a near by park. In: *Energy and Buildings* (29), S. 83–92.

Cailliau, C.: Bayreuth's Next Top Tree – Comparing Four Common City Tree Species under Climate Change 2016.

Campana M.: Die Linde. *Tilia platyphyllos*, *Tilia cordata*.

- Chang C., Li M., Chang S. (2007): A preliminary study on the local cool-island intensity of Taipei city parks. In: *Landscape and Urban Planning* 80 (4), S. 386–395. DOI: 10.1016/j.landurbplan.2006.09.005.
- Corburn J. (2009): Cities, Climate Change and Urban Heat Island Mitigation. Localising Global Environmental Science. In: *Urban Studies* 46 (2), S. 413–427. DOI: 10.1177/0042098008099361.
- Coumou D., Robinson A. (2013): Historic and future increase in the global land area affected by monthly heat extremes. In: *Environ. Res. Lett.* 8 (3), S. 34018. DOI: 10.1088/1748-9326/8/3/034018.
- Coutts A. M., Beringer J., Tapper N. J. (2007): Impact of Increasing Urban Density on Local Climate. Spatial and Temporal Variations in the Surface Energy Balance in Melbourne, Australia. In: *J. Appl. Meteor. Climatol.* 46 (4), S. 477–493. DOI: 10.1175/JAM2462.1.
- Coutts A., Harris R. (2012): Urban heat island report: a multi-scale assessment on urban heating in Melbourne during an extreme heat event: policy approaches for adaptation. In: *Victorian Centre for Climate Change Adaptation Research*.
- Davis A. Y., Pijanowski B. C., Robinson K. D., Kidwell, P. B. (2010): Estimating parking lot footprints in the Upper Great Lakes Region of the USA. In: *Landscape and Urban Planning* 96 (2), S. 68–77. DOI: 10.1016/j.landurbplan.2010.02.004.
- Duckworth F. S., Sandberg J. S. (1954): The effect of cities upon horizontal and vertical temperature gradients. In: *Amer. Meteor. Soc.* (35), S. 198–207.
- Eaton, E., G. Caudullo, and D. de Rigo (2016): *Tilia cordata*, *Tilia platyphyllos* and other limes in Europe: distribution, habitat, usage and threats. In: *European atlas of forest tree species. Publ. Off. EU, Luxembourg, pp. e010ec5*.
- Eaton-Rye, J. J., Tripathy, B. C., & Sharkey, T. D. (2011): *Photosynthesis: plastid biology, energy conversion and carbon assimilation* (Vol. 34). Springer Science & Business Media.
- Eliasson I.: Urban nocturnal temperatures, Street geometry and land use 1994.
- Fenner D., Meier F., Scherer D., Polze A. (2014): Spatial and temporal air temperature variability in Berlin, Germany, during the years 2001–2010. In: *Urban Climate* 10, S. 308–331. DOI: 10.1016/j.uclim.2014.02.004.
- Fezer F. (1995): Das Klima der Städte. In: *Gotha, Justus Perthes Verlag*.
- Forsa - Gesellschaft für Sozialforschung und Statistische Analysen MBH (2014): Zufriedenheit mit urbanem Grün in deutschen Großstädten. Download. Online verfügbar unter [http://taspo.de/uploads/media/forsa-Umfrage\\_2014.pdf](http://taspo.de/uploads/media/forsa-Umfrage_2014.pdf), zuletzt geprüft am 27.08.2016.
- Fouillet A., Rey G., Laurent F., Pavillon G., Bellec S., Ghihenneuc-Jouyaux C., Hémon D.: Excess mortality related to the August 2003 heat wave in France. In: *Int Arch Occup Environ Health*. 2006.
- Gabriel K. M. A., Endlicher W. R. (2011): Urban and rural mortality rates during heat waves in Berlin and Brandenburg, Germany. In: *Environmental pollution (Barking, Essex : 1987)* 159 (8-9), S. 2044–2050. DOI: 10.1016/j.envpol.2011.01.016.
- Gallo K. P., McNab A. L., Karl T. R., Brown J. F., Hood J. J., Tarpley J. D. (1993): The use of a vegetation index for assessment of the urban heat island effect. In: *International Journal of Remote Sensing* 14 (11), S. 2223–2230. DOI: 10.1080/01431169308954031.
- Gill S.E, Handley J.F, Ennos A.R, Pauleit S. (2007): Adapting Cities for Climate Change. The Role of the Green Infrastructure. In: *built environ* 33 (1), S. 115–133. DOI: 10.2148/benv.33.1.115.
- Goldbach A., Kuttler W. (2013): Quantification of turbulent heat fluxes for adaptation strategies within urban planning. In: *Int. J. Climatol.* 33 (1), S. 143–159. DOI: 10.1002/joc.3437.

- Gómez-Muñoz V. M., Porta-Gándara M. A., Fernández, J. L. (2010): Effect of tree shades in urban planning in hot-arid climatic regions. In: *Landscape and Urban Planning* 94 (3-4), S. 149–157. DOI: 10.1016/j.landurbplan.2009.09.002.
- Gosling S. N., Lowe J. A., McGregor, G. R., Pelling M., Malamud B. D. (2009): Associations between elevated atmospheric temperature and human mortality. A critical review of the literature. In: *Climatic Change* 92 (3-4), S. 299–341. DOI: 10.1007/s10584-008-9441-x.
- Grimmond C. S. B., et al. (2002): Local-scale surface flux measurements at a downtown site in Marseille during the escompte field campaign.
- Grimmond C. S. B., Souch C., Hubble M. (1996): Influence of tree cover on summertime surface energy balance fluxes, San Gabriel Valley, Los Angeles. In: *Climate Research* (6), S. 45–57.
- Hamdi R., Schayes G. (2008): Sensitivity study of the urban heat island intensity to urban characteristics. In: *Int. J. Climatol.* 28 (7), S. 973–982. DOI: 10.1002/joc.1598.
- Helbig A., Baumüller J., Kerschgens M. J. (Hg.) (1999): *Stadtklima und Luftreinhaltung*. Berlin, Heidelberg: Springer Berlin Heidelberg.
- Heudorf U., Meyer C. (2005): Health effects of extreme heat--an example of the heat wave and mortality in Frankfurt am Main in August 2003. In: *Gesundheitswesen (Bundesverband der Ärzte des Öffentlichen Gesundheitsdienstes (Germany))* 67 (5), S. 369–374. DOI: 10.1055/s-2004-813924.
- Höppe P.: The physiological equivalent temperature--a universal index for the biometeorological assessment of the thermal environment. In: *Int. J. Biometeorol.* (43), S. 71–75.
- Intergovernmental panel on climate change (IPCC). *Climate Change 2013, The Physical Science Basis, Summary for Policymakers* (2013).
- Jehn M., Donaldson G., Kiran B., Liebers U., Mueller K., Scherer D., Endlicher W., Witt C. (2013): Telemonitoring reduces exacerbation of COPD in the context of climate change--a randomized controlled trial. In: *Environmental health : a global access science source* 12, S. 99. DOI: 10.1186/1476-069X-12-99.
- Jendritzky G., Grätz A. (1999): Das Bioklima des Menschen in der Stadt. In: Helbig A., Baumüller J., Kerschgens M. J. (Hg.): *Stadtklima und Luftreinhaltung*. Berlin, Heidelberg: Springer Berlin Heidelberg, S. 126–158.
- Jenerette G.D., Sharon L., Brazel A., Jones N., Larsen L., Stefanov W. L. (2007): Regional relationships between surface temperature, vegetation, and human settlement in a rapidly urbanizing ecosystem. In: *Landscape Ecol* 22 (3), S. 353–365. DOI: 10.1007/s10980-006-9032-z.
- Jim C. Y. (2000): The urban forestry programme in the heavily built-up milieu of Hong Kong. In: *Cities* 17 (4), S. 271–283. DOI: 10.1016/S0264-2751(00)00023-8.
- Johansson E. (2006): Influence of urban geometry on outdoor thermal comfort in a hot dry climate. A study in Fez, Morocco. In: *Building and Environment* 41 (10), S. 1326–1338. DOI: 10.1016/j.buildenv.2005.05.022.
- Johnson G. T., Oke T. R., Lyons T. J., Steyn D. G., Watson I. D., Voogt J. A. (1991): Simulation of surface urban heat islands under ? IDEAL? conditions at night part 1: Theory and tests against field data. In: *Boundary-Layer Meteorol* 56 (3), S. 275–294. DOI: 10.1007/BF00120424.
- Kjelgren R. K., James R. C.: *Microclimates and tree growth in three urban spaces* 1992.
- Kjelgren R., Montague T. (1998): Urban tree transpiration over turf and asphalt surfaces. In: *Atmos. Environ.* (32), S. 35–41.
- Kovats R. S., Hajat S. (2008): Heat stress and public health: a critical review. In: *Annual review of public health* 29, S. 41–55. DOI: 10.1146/annurev.publhealth.29.020907.090843.

- Lambers H., Chapin F.S., Pons T. L. (2008): Photosynthesis. In: Hans Lambers, F. Stuart Chapin und Thijs L. Pons (Hg.): *Plant Physiological Ecology*. New York, NY: Springer New York, S. 11–99.
- Lambers, Hans; Chapin, F. Stuart; Pons, Thijs L. (Hg.) (2008): *Plant Physiological Ecology*. New York, NY: Springer New York.
- Landsberg H. E. (1981): *The urban climate*. Vol. 28: Academic press.
- Lawrence Livermore Laboratory (Hg.) (2006): Hilft Bäume pflanzen gegen den Klimawandel?
- Leuzinger S., Vogt R., Körner C. (2010): Tree surface temperature in an urban environment. In: *Agricultural and Forest Meteorology* 150 (1), S. 56–62. DOI: 10.1016/j.agrformet.2009.08.006.
- Lin X., Hubbard K. G., Meyer G. E.: Airflow characteristics of commonly used temperature radiation shields. 2001 (18), S. 329–339.
- Lindberg F., Grimmond C. S. B. (2011): Nature of vegetation and building morphology characteristics across a city. Influence on shadow patterns and mean radiant temperatures in London. In: *Urban Ecosyst* 14 (4), S. 617–634. DOI: 10.1007/s11252-011-0184-5.
- Lindberg, Fredrik; Grimmond, C. S. B. (2011): The influence of vegetation and building morphology on shadow patterns and mean radiant temperatures in urban areas. Model development and evaluation. In: *Theor Appl Climatol* 105 (3-4), S. 311–323. DOI: 10.1007/s00704-010-0382-8.
- Lottrup L., Grahn P., Stigsdotter U. K. (2013): Workplace greenery and perceived level of stress. Benefits of access to a green outdoor environment at the workplace. In: *Landscape and Urban Planning* 110, S. 5–11. DOI: 10.1016/j.landurbplan.2012.09.002.
- Lüers J., Soldner M., Olesch J., Foken T. (2014): 160 Jahre Bayreuther Klimazeitreihe - Homogenisierung der Bayreuther Lufttemperatur- und Niederschlagsdaten.
- Luvall J. C., Holbo H. R. (1989): Measurements of short-term thermal responses of coniferous forest canopies using thermal scanner data. In: *Remote Sensing of Environment* 27 (1), S. 1–10. DOI: 10.1016/0034-4257(89)90032-1.
- Matzarakis A. (2001): Climate and bioclimate information for tourism in Greece. Proceedings of the first international workshop on climate, tourism and recreation.
- Matzarakis, A. (2001): Klimawandel und Städte - Stadtklimatischer Einfluss von Bäumen.
- McCarthy H. R., Pataki D. E. (2010): Drivers of variability in water use of native and non-native urban trees in the greater Los Angeles area. In: *Urban Ecosyst* 13 (4), S. 393–414. DOI: 10.1007/s11252-010-0127-6.
- McPherson G., Simpson J. R., Peper P. J., Maco S., Xiao Q. (2005): Municipal Forest Benefits and Costs in Five US Cities. In: *Journal of Forestry* (8), S. 411–416.
- McPherson, G. E.; Nowak, David, J.; Rowntree, R. A.: Chicago's urban forest ecosystem: results of the Chicago Urban Forest Climate Project 1994.
- Meehl G. A., Tebaldi C. (2004): More intense, more frequent, and longer lasting heat waves in the 21st century. In: *Science (New York, N.Y.)* 305 (5686), S. 994–997. DOI: 10.1126/science.1098704.
- Michelozzi P., Accetta G., Sario M., D'Ippoliti D., Marino C., Baccini M., Biggeri A., Anderson H. R., Katsouyanni K., Ballester F., Bisanti L., Cadum E., Forsberg B., Forastiere F., Goodman P. G., Hojs, A. (2009): High temperature and hospitalizations for cardiovascular and respiratory causes in 12 European cities. In: *American journal of respiratory and critical care medicine* 179 (5), S. 383–389. DOI: 10.1164/rccm.200802-217OC.
- Miller R. A. (2015): The impact of microclimate variation on budburst phenology within a mature Douglas-fir tree (*Pseudotsuga menziesii*).

- Miller, R. A.; Thomas, C.: The impact of microclimatic variation on budburst phenology within a mature Douglas-fir-tree 2015.
- Nakayama T., Fujita T. (2010): Cooling effect of water-holding pavements made of new materials on water and heat budgets in urban areas. In: *Landscape and Urban Planning* 96 (2), S. 57–67. DOI: 10.1016/j.landurbplan.2010.02.003.
- Nakayama, Tadanobu; Hashimoto, Shizuka (2011): Analysis of the ability of water resources to reduce the urban heat island in the Tokyo megalopolis. In: *Environmental pollution (Barking, Essex : 1987)* 159 (8-9), S. 2164–2173. DOI: 10.1016/j.envpol.2010.11.016.
- Naturkapital Deutschland – TEEB DE: Ökosystemleistungen in der Stadt. Gesundheit schützen und Lebensqualität erhöhen. 2016.
- Norton B. et al.: Decision Principles for the selection and placement of Green Infrastructure - Technical Report 2013.
- Oke J. B. (1974): Absolute Spectral Energy Distributions for White Dwarfs. In: *Astrophysical Journal Supplement* (vol. 27), S. 21.
- Oke, T. R. (1973): City size and the urban heat island. In: *Atmospheric Environment (1967)* 7 (8), S. 769–779. DOI: 10.1016/0004-6981(73)90140-6.
- Oke, T. R. (1979): Advectionally-assisted evapotranspiration from irrigated urban vegetation. In: *Boundary-Layer Meteorol* 17 (2), S. 167–173. DOI: 10.1007/BF00117976.
- Oke, T. R. (1981): Canyon geometry and the nocturnal urban heat island. Comparison of scale model and field observations. In: *J. Climatol.* 1 (3), S. 237–254. DOI: 10.1002/joc.3370010304.
- Oke, T. R. (1982): The energetic basis of the urban heat island. In: *Q.J Royal Met. Soc.* 108 (455), S. 1–24. DOI: 10.1002/qj.49710845502.
- Oke, T. R.: City size and the urban heat island. In: *Atmos. Environ.* 1976 (7), S. 769–779.
- Oke, T. R.; Cleugh, H. A.: Urban heat storage derived as energy balance residuals 1987.
- Oke, T. R.; Crowther, J. M.; McNaughton, K. G.; Monteith, J. L.; Gardiner, B. (1989): The Micrometeorology of the Urban Forest [and Discussion]. In: *Philosophical Transactions of the Royal Society B: Biological Sciences* 324 (1223), S. 335–349. DOI: 10.1098/rstb.1989.0051.
- Oke, T. R.; Johnson, G. T.; Steyn, D. G.; Watson, I. D. (1991): Simulation of surface urban heat islands under ? Ideal? conditions at night part 2: Diagnosis of causation. In: *Boundary-Layer Meteorol* 56 (4), S. 339–358. DOI: 10.1007/BF00119211.
- O'Neill M. S., Ebi K. L. (2009): Temperature extremes and health: impacts of climate variability and change in the United States. In: *Journal of occupational and environmental medicine / American College of Occupational and Environmental Medicine* 51 (1), S. 13–25. DOI: 10.1097/JOM.0b013e318173e122.
- Pandit R., Polyakov M., Tapsuwan S., Moran T. (2013): The effect of street trees on property value in Perth, Western Australia. In: *Landscape and Urban Planning* 110, S. 134–142. DOI: 10.1016/j.landurbplan.2012.11.001.
- Pataki D., McCarthy H. R., Litvak E., Pincetl S. (2011): Transpiration of urban forests in the Los Angeles metropolitan area. In: *Ecological Applications* 21 (3), S. 661–677. DOI: 10.1890/09-1717.1.
- Pauleit S., Jones N., Garcia-Martin G., Garcia-Valdecantos J. L., Rivière L. M., Vidal-Beaudet L., Bodson M., Randrup T. B. (2002): Tree establishment practice in towns and cities – Results from a European survey. In: *Urban Forestry & Urban Greening* 1 (2), S. 83–96. DOI: 10.1078/1618-8667-00009.
- Pretzsch H., Pauleit S., Rötzer T., Moser A. (2015): Leitfaden für Kommunen- Stadtbäume im Klimawandel: Wuchsverhalten, Umweltleistungen und Perspektiven.

- Pretzsch, Hans; Biber, Peter; Uhl, Enno; Dahlhausen, Jens; Rötzer, Thomas; Caldentey, Juan et al. (2015): Crown size and growing space requirement of common tree species in urban centres, parks, and forests. In: *Urban Forestry & Urban Greening* 14 (3), S. 466–479. DOI: 10.1016/j.ufug.2015.04.006.
- Richardson S. J.; Brock F. V.; Semmer, S. R.; Jirak C. (1999): Minimizing Errors Associated with Multiplate Radiation Shields. In: *Journal of Atmospheric and Oceanic Technology* 16 (11), S. 1862–1872. DOI: 10.1175/1520-0426(1999)016<1862:MEAWMR>2.0.CO;2.
- Rizwan A. M., Dennis L. Y.C., Liu C. (2008): A review on the generation, determination and mitigation of Urban Heat Island. In: *Journal of Environmental Sciences* 20 (1), S. 120–128. DOI: 10.1016/S1001-0742(08)60019-4.
- Robine J., Cheung S., Le Roy S., van Oyen H., Griffiths C., Michel J., Herrmann F. R. (2008): Death toll exceeded 70,000 in Europe during the summer of 2003. In: *Comptes rendus biologies* 331 (2), S. 171–178. DOI: 10.1016/j.crvi.2007.12.001.
- Roetzer T., Wittenzeller M., Haeckel H., Nekovar J. (2000): Phenology in central Europe - differences and trends of spring phenophases in urban and rural areas. In: *International Journal of Biometeorology* 44 (2), S. 60–66. DOI: 10.1007/s004840000062.
- Roloff A., Goede M., Weiß H. (2004): Tharandter Baumdiagnose—ein integriertes Verfahren zur Beurteilung von Problembäumen im Stadt-und Straßenbereich. AFZ-Der Wald, 2004, 2. Jg., S. 52-55.
- Rosenfeld A. H., Akbari H., Bretz S., Fishman B. L., Kurn D. M., Sailor D., Taha H. (1995): Mitigation of urban heat islands: materials, utility programs, updates, S. 255–265.
- Saaroni H., Ben-Dor E., Bitan A., Potchter O. (2000): Spatial distribution and microscale characteristics of the urban heat island in Tel-Aviv, Israel. In: *Landscape and Urban Planning* 48 (1-2), S. 1–18. DOI: 10.1016/S0169-2046(99)00075-4.
- Sakakibara Y.: A numerical study of the effect of urban geometry upon the surface energy budget. In: *Atmos. Environ.* 1996 (30), S. 487–496.
- Schar C., Jendritzky G. (2004): Climate change: hot news from summer 2003. In: *Nature* 432 (7017), S. 559–560. DOI: 10.1038/432559a.
- Schmid H. P., Oke T. R. (1990): A model to estimate the source area contributing to turbulent exchange in the surface layer over patchy terrain. In: *Q.J Royal Met. Soc.* 116 (494), S. 965–988. DOI: 10.1002/qj.49711649409.
- Shashua-Bar L., Hoffman M. E. (2002): The Green CTTC model for predicting the air temperature in small urban wooded sites. In: *Building and Environment* 37 (12), S. 1279–1288. DOI: 10.1016/S0360-1323(01)00120-2.
- Shashua-Bar, Limor; Hoffman, Milo E. (2003): Geometry and orientation aspects in passive cooling of canyon streets with trees. In: *Energy and Buildings* 35 (1), S. 61–68. DOI: 10.1016/S0378-7788(02)00080-4.
- Shashua-Bar, Limor; Hoffman, Milo E.: Vegetation as a climatic component in the design of an urban street An empirical model for predicting the cooling effect of urban green areas with trees 1999.
- Shashua-Bar, Limor; Pearlmutter, David; Erell, Evyatar (2009): The cooling efficiency of urban landscape strategies in a hot dry climate. In: *Landscape and Urban Planning* 92 (3-4), S. 179–186. DOI: 10.1016/j.landurbplan.2009.04.005.
- Sitzia T., Cierjacks A., de Rigo D., Caudullo G. (2016): Robinia pseudoacacia in Europe: distribution, habitat, usage and threats.
- Spronken-Smith R. A., Oke T. R. (1998): The thermal regime of urban parks in two cities with different summer climates. In: *International Journal of Remote Sensing* 19 (11), S. 2085–2104. DOI: 10.1080/014311698214884.

- Spronken-Smith R. A., Oke T. R. (1999): Scale Modelling of Nocturnal Cooling in Urban Parks. In: *Boundary-Layer Meteorology* 93 (2), S. 287–312. DOI: 10.1023/A:1002001408973.
- Stone B., Rodgers M. O. (2001): Urban Form and Thermal Efficiency. How the Design of Cities Influences the Urban Heat Island Effect. In: *Journal of the American Planning Association* 67 (2), S. 186–198. DOI: 10.1080/01944360108976228.
- Stott P. A., Stone D. A., Allen M. R. (2004): Human contribution to the European heatwave of 2003. In: *Nature* 432 (7017), S. 610–614. DOI: 10.1038/nature03089.
- Swaid H., Hoffman M. E. (1990): Climatic impacts of urban design features for high- and mid-latitude cities. In: *Energy and Buildings* 14 (4), S. 325–336. DOI: 10.1016/0378-7788(90)90095-Z.
- Taesler R., Karlsson S.: Power law estimates of the urban wind profile 1981.
- Taha H. (1997): Urban climates and heat islands. Albedo, evapotranspiration, and anthropogenic heat. In: *Energy and Buildings* 25 (2), S. 99–103. DOI: 10.1016/S0378-7788(96)00999-1.
- Thomas C. K., Smoot A. R. (2013): An Effective, Economic, Aspirated Radiation Shield for Air Temperature Observations and Its Spatial Gradients. In: *J. Atmos. Oceanic Technol.* 30 (3), S. 526–537. DOI: 10.1175/JTECH-D-12-00044.1.
- Thoreau Rory T., Coops N. C., Voogt J. A., Meitner, M. J. (2011): Tree structure influences on rooftop-received solar radiation. In: *Landscape and Urban Planning* 102 (2), S. 73–81. DOI: 10.1016/j.landurbplan.2011.03.011.
- Tilia cordata, Tilia platyphyllos and other limes in Europe: distribution, habitat, usage and threats (2016) E. Eaton, G. Caudullo, D. de Rigo.
- Unger J.: Intra-urban relationship between surface geometry and urban heat island: review and new approach. In: *Climate Research* 2004 (27), S. 253–264.
- van Renterghem T., Botteldooren D. (2009): Reducing the acoustical façade load from road traffic with green roofs. In: *Building and Environment* 44 (5), S. 1081–1087. DOI: 10.1016/j.buildenv.2008.07.013.
- White E., Coutts A., Tapper N., Beringer J. (2012): Urban microclimate & street trees: understanding the effects of street trees on human thermal comfort.
- Whitford V. (2001): City form and natural processes as indicators for the ecological performance of urban areas and their application to Merseyside, UK. In: *Landscape and Urban Planning* 57 (2), S. 91–103. DOI: 10.1016/S0169-2046(01)00192-X.
- Wilde M. (2011): Bäume und ihre Wohlfahrtswirkungen im städtischen Siedlungsraum. Warum wir sorgsamer mit unseren Bäumen umgehen sollten.
- Wojda T., Klisz M., Jastrzębowski S., Mionskowski M., Szyg-Borowska I., Szczygieł K. (2015): The Geographical Distribution Of The Black Locust (Robinia Pseudoacacia L.) In Poland And Its Role On Non-Forest Land. In: *Papers on Global Change IGBP* 22 (1). DOI: 10.1515/igbp-2015-0018.
- Wojtkiewicz W., Heiland S. (2012): Landschaftsverständnisse in der Landschaftsplanung. Eine semantische Analyse der Verwendung des Wortes „Landschaft“ in kommunalen Landschaftsplänen. In: *Raumforsch Raumordn* 70 (2), S. 133–145. DOI: 10.1007/s13147-011-0138-7.

## 7. Appendix

### Appendix A)

Devices were put in all selected trees. R1, R2, T1 and T2 were equipped with five devices at position A, B, C, D & E. Data at T3 – T10 was taken at position C, D & E. Position were documented with the aid of a Leica disto device. Positions can be seen in the table below:

*Table 13: Positions of all devices, measured with Leica disto.*

Tree individual	Tree Height [m]	Position [m]				
		A	B	C	D	E
R1	16.5	13.6	10.7	6.6	6.9	8.2
R2	13.8	11.4	8.7	6.9	6	7.7
T1	12.5	12	9.1	5.2	8.4	8.1
T2	10.5	9.6	7.6	5	4.7	4.7
T3	7.7	/	/	4.5	3.5	3.3
T4	9.3	/	/	4	3.7	4
T5	10.4	/	/	5.1	3.7	4.1
T6	10.5	/	/	4.7	5	5.1
T7	10.8	/	/	4	4.2	4.8
T8	9.6	/	/	4.2	3.5	4
T9	11.4	/	/	6.4	4.5	5.6
T10	8.6	/	/	4.5	4.7	4.6

Devices position is depending on the trees height. On average devices at position A were located in a height of 11.8 m. Position B was on average at a height of 9.03 m. Position C, D & E were at similar heights as only the cardinal direction differed. Average heights: Position C: 5.1 m, Position D: 4.9 m, Position E: 5.4 m.

## Appendix B)

Five different materials were tested as potentially improvement of the radiation shield. Tested were a radiation shield without modification, a chrome-tube, which was blackened from inside and three aluminium-tubes, of which one was blackened from inside and two were non-colored but of different size.

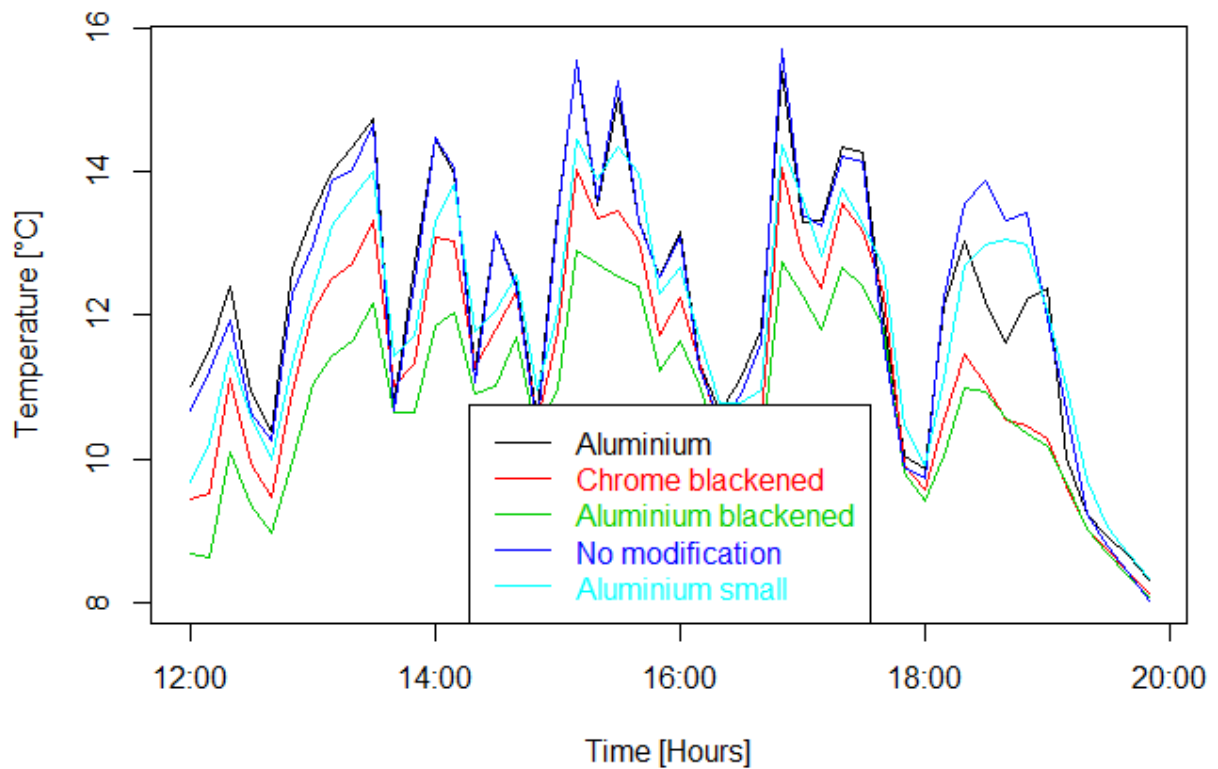


Figure 48: Testing with different adjustments of radiation protection (n=5). Green line shows result for the radiation protection with an aluminium-tube. Less temperature fluctuations can be seen.

The testing showed less fluctuations for a blackened aluminium-tube. It was used for all devices.

### Appendix C)

Incoming solar radiation measured at the urban and at the rural site was furthermore analyzed using a density function. The result can be seen in the figure below:

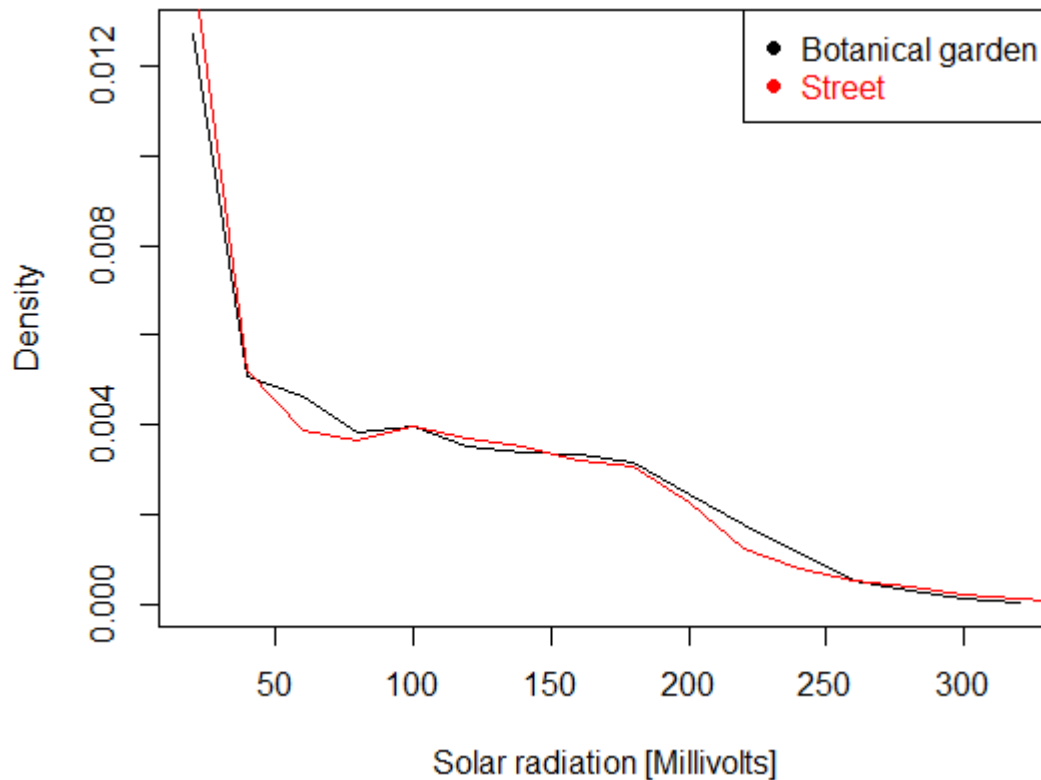


Figure 49: Density function of incoming solar radiation in mV measured in the botanical garden (rural area, n=1) and above the street (n=1) during the study period of 61 days.

Data of incoming solar radiation of the study period from 29.05.2016 to 29.07.2016 was used for analysis. Density function showed no great differences of solar radiation measured above the street and at the rural site.

#### Appendix D)

Object temperature was measured via an infrared diode over the whole study period at the urban site. Infrared-diodes were located at the south- and north-facing branch of every selected tree (position C and E, cf. 3.1.3) as well as above the street.

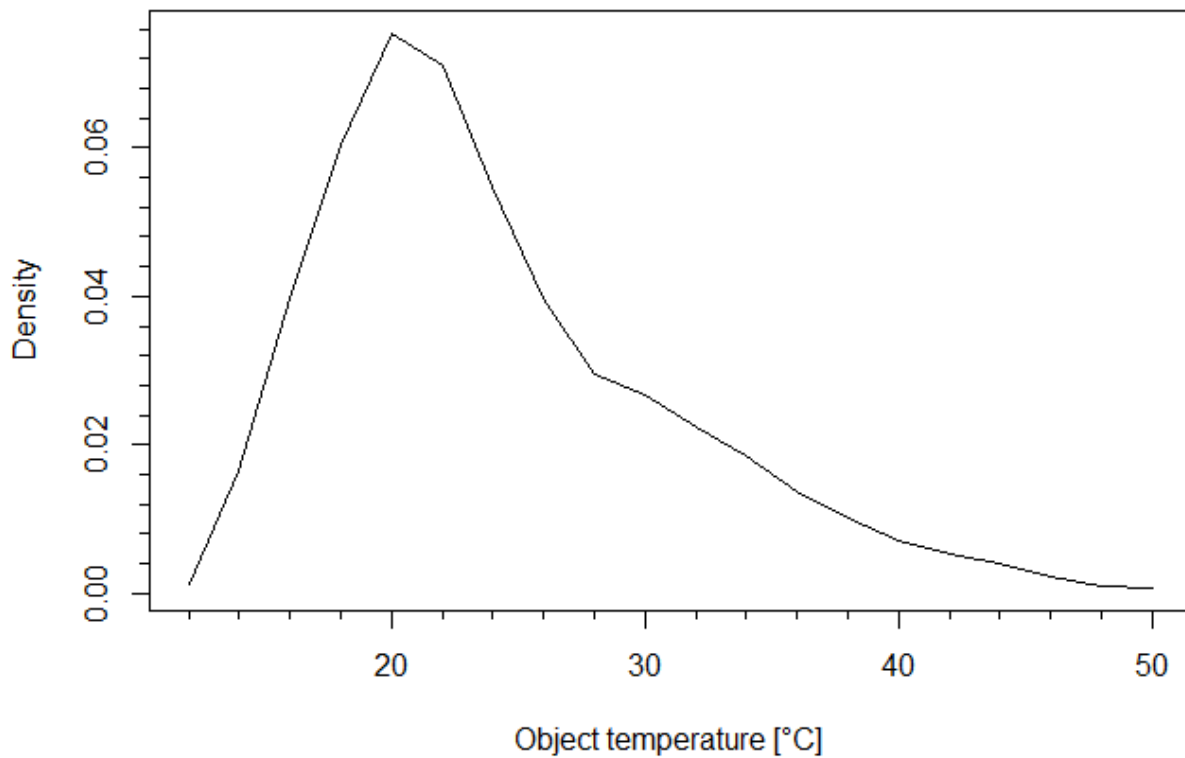


Figure 50: Density function of object temperature [°C] (n=25) over the whole study period (29.05.2016 - 29.07.2016).

The highest density was found at 20 °C with almost 8 %. Object temperatures below 20 °C were rare with 12 °C as the lowest measured temperature. Also, temperatures over 20 °C were measured less often. Density decreased quickly to 28 °C. The occurrence of really high temperatures (28 °C – 49 °C) was rare (< 0.03), but existent.

## Appendix E)

The averaged cooling effect over the study period of subgroup 1 was analyzed for each individual. In the figure below, the averaged cooling effect was plotted together with the averaged air temperature above the street:

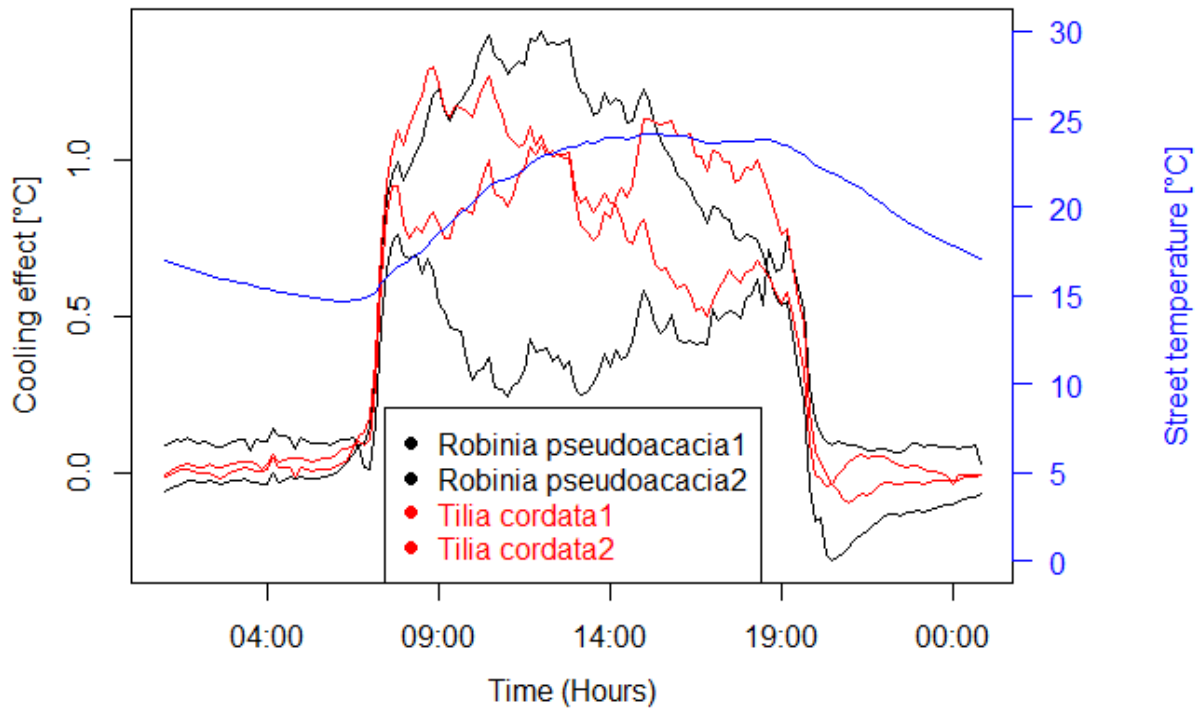


Figure 51: Cooling effect of T1 (n=5), T2 (n=5), R1(n=5) & R2 (n=5) averaged over the study period of 61 days.

All four individuals of subgroup 1 showed no cooling effect during the night from 19:00 to 07:00. After 7:00, the cooling effect of all individuals rose quickly to at least 0.75 °C. In the afternoon, the cooling effect differed substantially between the individuals and fluctuated a lot. R1 showed the greatest cooling effect with 1.4 °C at 12:00, while the least cooling effect was documented at R2 at 11:00 with 0.24 °C. Cooling effect of *T. cordata* was also varying: While cooling effect of T2 was greatest in the morning, cooling effect of T1 was greatest at 15:00.

## Appendix F)

Greatest cooling effect was observed during the day. To analyze this part more in detail, averaged cooling effect of both species from 10:00 to 18:00 over the whole period was plotted against air temperature measured above the street:

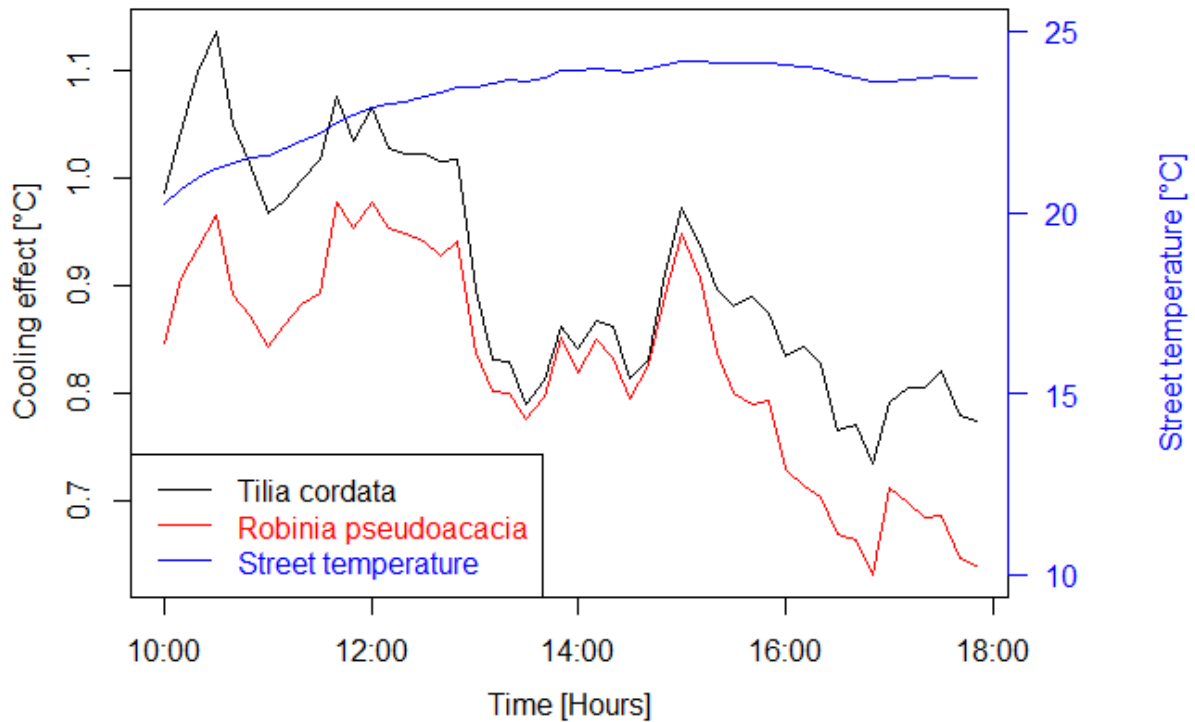


Figure 52: Averaged cooling effect of both species ( $n=10$  each) from 10:00 to 18:00 and air temperature measured above the street ( $n=1$ ).

With rising air temperature in the afternoon, cooling effect of both species decreased by about 0.35 °C. Cooling effect of *T. cordata* was greater at any time. Differences of the cooling effects of the species were small, with a maximum of 0.17 °C. Cooling effect was fluctuating in both cases.

Result of the Wilcoxon-Mann-Whitney rank sum test: The P-value was 0.00124 ( $W=1588$ ), therefore  $<0.05$ .  $H_0$  was rejected for  $\alpha = 0.05$  and difference was statistically significant.

## Appendix G)

Cooling effect is most important at hot and sunny days. Therefore, averaged cooling effect of both species from 10:00 to 18:00 was analyzed in detail. Averaged cooling effect of both species was plotted against air temperature measured above the street:

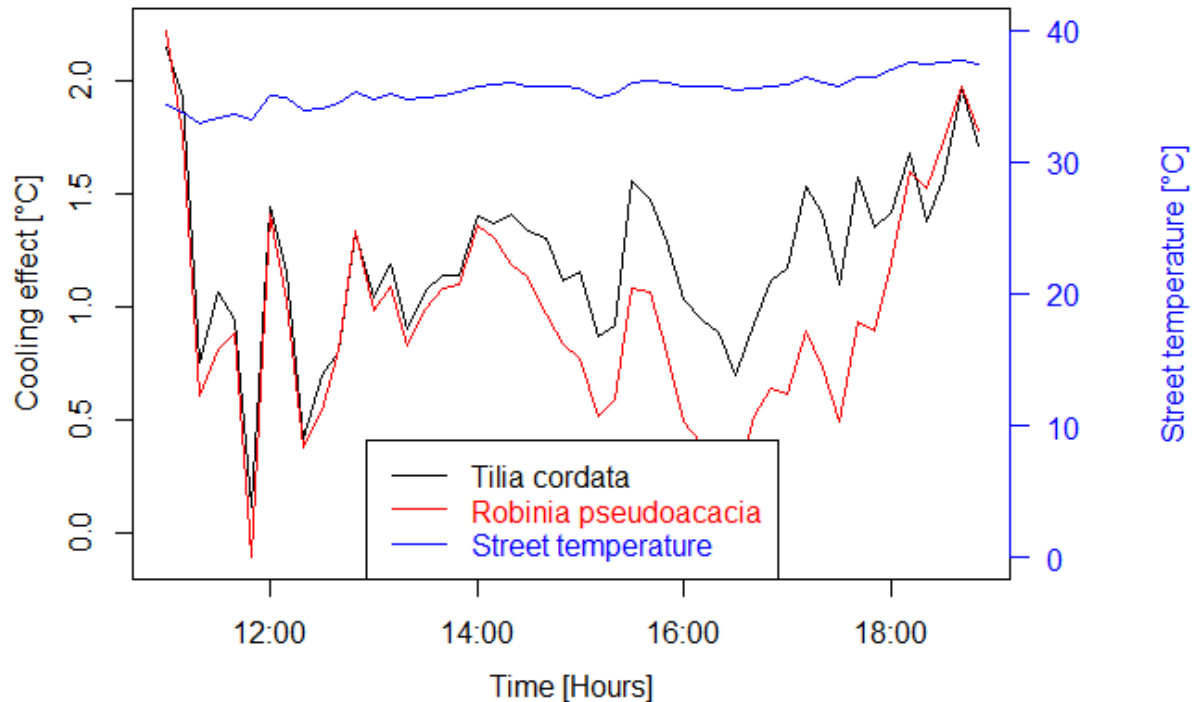


Figure 53: Averaged cooling effect of both species ( $n=10$  each) and air temperature measured above the street ( $n=1$ ) at an exemplary hot and cloud free day from 10:00 to 18:00.

At this particular day, air temperature above the street was rising slightly, even after 18:00. Cooling effect was fluctuating a lot, even though temperature above the street was rising stable. No decreasing or increasing cooling tendency was documented. The effect of *T. cordata* was again greater at any time with a mean of 1.21 °C. Mean cooling effect of *R. pseudoacacia* was 0.96 °C. Differences were small, with a maximum of 0.17 °C.

Results of the Wilcoxon-Mann-Whitney rank sum test: The P-value was 0.0022 ( $W=1566$ ) and therefore  $< 0.05$ .  $H_0$  was rejected for  $\alpha = 0.05$  and difference was deemed statistically significant.

## Appendix H)

Comparing field measurements to modelled data

For direct comparisons, kWh/year needed to be compared to °C/day. It was possible to convert modelling unit kWh to °C/m<sup>3</sup> per day. Attempts can be seen in the following:

Table 14: Cooling effect by Mack (2016) and Cailliau (2016).

Cooling effect by Mack (2016)	Cooling effect by Cailliau (2016)
0.47 °C/day	8748 kWh/year

- 1) Converting kWh into kJ:

$$8748 \text{ kWh} * 3.6 = 31493 \text{ kJ}$$

- 2) Offsetting with specific heat capacity of air:

$$\frac{31493 \text{ kJ}}{1.03 \frac{\text{kJ}}{\text{kg} \cdot ^\circ\text{C}}} = 30576 \frac{\text{kg}}{^\circ\text{C}}$$

- 3) Dividing with air density:

$$\frac{30576 \frac{\text{kg}}{^\circ\text{C}}}{1.204 \frac{\text{kg}}{\text{m}^3}} = 25395 \frac{^\circ\text{C}}{\text{m}^3}$$

- 4) For one day:

$$\frac{25395 \frac{^\circ\text{C}}{\text{m}^3}}{365} = 69.58 \frac{^\circ\text{C}}{\text{m}^3}$$

Data can hardly be compared due to different temporal and spatial scales. Further research is necessary.

### **Statutory Declaration**

I declare that I have developed and written the enclosed Master Thesis completely by myself, and have not used sources or means without declaration in the text. Any thoughts from others or literal quotations are clearly marked. The Master Thesis was not used in the same or in a similar version to achieve an academic grading or is being published elsewhere.

.....

Date

.....

Signature

## Acknowledgement

I would like to express my gratitude to Astrid Moser and my supervisor Prof. Cyrus Samimi not only for the great support, useful comments and engagement through the process of this master thesis but also for having a very friendly and personal atmosphere.

Furthermore, I would like to thank Stefan Holzheu and Gerhard Müller for introducing me to the world of technical development and enabling this big project in a very short time. Also, I like to thank Arnd Sesselmann of Bayreuth's gardening department for his interest, his engagement and his support, which was essential for the study. I like to thank Hermann Hauffe and all employees of the District Office of Bayreuth, who gave me the permission to conduct the study on their ground without hesitation and who were always open minded and supportive. I am very thankful for all the support I got from Stefan Holzheu and Katja Reinhard to overcome initial difficulties with the program R.

Last, but not least I would like to thank Fabian Groß, my family and all my friends, who have supported me throughout the entire process, who have listened to every problem, helped to solve it and never got tired.

Thank you.